

ENGINEERING RESEARCH INSTITUTE  
THE UNIVERSITY OF MICHIGAN  
ANN ARBOR

Technical Report

AN INVESTIGATION IN THE ZONE THEORY  
OF THE ENERGY OF ELECTRONS IN METALS

George B. Spence  
Author

Ernst Katz  
Project Supervisor

Project 2158

U. S. AIR FORCE  
AIR RESEARCH AND DEVELOPMENT COMMAND  
CONTRACT NO. AF 18(600)-750  
E.O. NO. 670-729-BR-1, PROJECT NO. R-355-40-10

August 1956

This report has also been submitted as a dissertation in partial fulfillment of the requirements for the degree of Doctor of Philosophy in The University of Michigan, 1956.

## TABLE OF CONTENTS

	Page
LIST OF TABLES	v
LIST OF ILLUSTRATIONS	vi
ABSTRACT	viii
OBJECTIVE	x
CHAPTER I. INTRODUCTION	1
CHAPTER II. DEFINITIONS AND PROPERTIES OF ZONES	5
2.1. PHYSICAL REASON FOR ZONES	5
2.2. BRILLOUIN ZONES	9
2.3. OTHER EXTENDED ZONE SCHEMES	10
2.4. JONES ZONES	11
CHAPTER III. GENERAL PROPERTIES OF ELECTRON ENERGIES IN JONES ZONES	14
3.1. DIRECTIONAL, SYMMETRY, AND ACCIDENTAL DEGENERACIES	14
3.2. SHAPE DEGENERACIES	15
3.3. POSSIBLE OMISSION OF CERTAIN PLANES FORMING ZONE BOUNDARIES	20
CHAPTER IV. ONE-DIMENSIONAL PROBLEMS WITH COSINE POTENTIALS	24
4.1. ONE-DIMENSIONAL EQUATION AND DIMENSIONLESS VARIABLES	24
4.2. ANALYTICAL SOLUTIONS	25
4.3. NUMERICAL PROBLEMS	27
CHAPTER V. THE (20) JONES ZONE WITH COSINE POTENTIALS	33
5.1. ENERGY CONTOURS	34
5.2. NEARLY-FREE-ELECTRON APPROXIMATION	41
5.3. DENSITY OF STATES	43

## TABLE OF CONTENTS (Concl.)

	Page
CHAPTER VI. THE (200) JONES ZONE WITH COSINE POTENTIALS	47
6.1. ENERGY SURFACES	47
6.2. DENSITY OF STATES	49
6.3. JONES'S APPROXIMATION TO THE DENSITY OF STATES	54
CHAPTER VII. TOTAL ELECTRON ENERGY AND THE HUME-ROTHERY RULES	58
7.1. CONTINUITY PROPERTIES OF THE TOTAL ENERGY OF THE ELECTRONS	59
7.2. TOTAL ELECTRON ENERGY FOR THE (200) JONES ZONE	60
7.3. REMARKS ON THE INTERPRETATION OF THE HUME-ROTHERY RULES	63
CHAPTER VIII. SUMMARY OF RESULTS	67
APPENDIX A. SOME BRILLOUIN ZONES OF THE CUBIC LATTICES	74
APPENDIX B. WHITTAKER-INCE SOLUTION OF HILL'S EQUATION	89
B.1. THE $\kappa$ -EXPANSION	90
B.2. THE $\sigma$ $1/4$ -EXPANSION	92
B.3. THE $\sigma$ $1$ -EXPANSION	99
B.4. COMPARISON WITH THE RESULTS OF INCE	105
APPENDIX C. ANALYSIS OF SEVERAL JONES ZONES	107
C.1. THE HEXAGONAL CLOSE-PACKED STRUCTURE	107
C.2. THE $\gamma$ -BRASS STRUCTURE	109
C.3. THE $\beta$ -MANGANESE STRUCTURE	110
BIBLIOGRAPHY	112



## LIST OF TABLES

Table		Page
5.1	Critical Points of the Energy	45
6.1	Form of the Density of States Near the Critical Energies	50
6.2	Effective Masses of Critical Points of the Energy, Perturbed Problem	54
A.1	Data on Certain Brillouin Zones	76
B.1	Nonzero Coefficients in the Expansions (B.5)	93
B.2	Nonzero Coefficients in the Expansions (B.9) and (B.12)	97
B.3	Nonzero Coefficients in the Expansions (B.14), (B.17), and (B.12)	102

## LIST OF ILLUSTRATIONS

Figure	Page
3.1 The (20) Jones zone.	18
3.2 The (30)(31) Jones zone.	18
3.3 The (50)(43) Jones zone.	19
3.4 Form of secular determinant.	22
4.1 Electron energies by different expansions.	29
4.2 Composite energy curve for perturbed problem and energy of free electron.	30
4.3 Composite energy curve for unperturbed problem.	32
5.1 Brillouin zones, square reciprocal lattice.	34
5.2 Energy contours for the unperturbed problem.	35
5.3 Seitz zones for the unperturbed problem.	36
5.4 Alternative method of plotting the energy for the unperturbed problem.	38
5.5 Energy contours for the perturbed problem.	41
5.6 Density of states, two-dimensional problems.	46
6.1 Critical energies and a critical energy surface for the unperturbed problem.	48
6.2 Critical energies for the perturbed problem.	49
6.3 Density of states for the unperturbed problem and for free electrons in the (200) zone.	51
6.4 Density of states for the perturbed problem.	53
6.5 Density of states by Jones's approximation for the unperturbed problem.	56

## LIST OF ILLUSTRATIONS (Concl.)

Figure		Page
7.1	Total electron energy and number of electrons per unit cell as a function of energy.	61
7.2	Total electron energy per unit cell as a function of the number of electrons per unit cell.	62
7.3	Difference between the total energy $U$ for the unperturbed problem and the energy $U_F$ of free electrons with the same effective mass at the center of the zone.	63
7.4	Typical graphical determinations of the phase boundaries according to equilibrium condition (7.10).	65
A.1	Brillouin zones, face-centered cubic reciprocal lattice.	77
A.2	Brillouin zones, face-centered cubic reciprocal lattice.	78
A.3	Brillouin zones, face-centered cubic reciprocal lattice.	79
A.4	Brillouin zones, face-centered cubic reciprocal lattice.	80
A.5	Brillouin zones, body-centered cubic reciprocal lattice.	81
A.6	Brillouin zones, body-centered cubic reciprocal lattice.	82
A.7	Brillouin zone, body-centered cubic reciprocal lattice.	83
A.8	Brillouin zone, body-centered cubic reciprocal lattice.	84
A.9	Brillouin zone, body-centered cubic reciprocal lattice.	85
A.10	Brillouin zone, body-centered cubic reciprocal lattice.	86
A.11	Brillouin zones, simple cubic reciprocal lattice.	87
A.12	Brillouin zones, body-centered cubic reciprocal lattice.	87
A.13	Brillouin zones, face-centered cubic reciprocal lattice.	88
C.1	The Jones zone of the hexagonal close-packed structure.	108
C.2	The second Brillouin zone of the hexagonal close-packed structure.	108
C.3	The Jones zone of the $\gamma$ -brass structure.	109

## ABSTRACT

This work is a theoretical investigation of certain general problems which occur in using the zone theory of the electron energy bands to determine the phase boundaries of those alloys agreeing with the Hume-Rothery electron concentration rules. There are four main objectives of the work.

The first objective pertains to the possible existence of an energy gap at an electron concentration corresponding to the volume of the zone, often called the Brillouin zone, of an alloy structure. It is shown that an energy gap cannot exist for some zones because of what is here called a shape degeneracy. Shape degeneracies exist in those zones which cannot be constructed from an integral number of mappings of the unit cell of the reciprocal lattice of the alloy structure. A "mapping" of the unit cell is the division of the unit cell into sections, if necessary, and the translation of each section by a reciprocal lattice vector. Shape degeneracies exist, for example, in the zones of the  $\gamma$ -brass and  $\beta$ -manganese structures.

The second objective is to obtain qualitative information about the energy surfaces in large zones by the correct use of the nearly-free-electron approximation. The main result here is that the electron energy surfaces in some large zones, for example, the  $\gamma$ -brass zone, are not qualitatively similar to the simple surfaces in the first zone of the conduction electrons of the noble metals.

Because of the existence of shape degeneracies and the necessarily complicated nature of the energy surfaces in certain large zones, the volume of these zones cannot, as has been assumed up to now, be used to predict precisely the location of energy gaps or low dips in the density of states.

The third objective is to solve accurately two simple numerical problems. The two- and three-dimensional problems are constructed from two one-dimensional Schrödinger equations with potentials of one and two cosine terms, respectively. The two-dimensional energy contours illustrate some of the complexities of the electron energies which occur in large zones. Accurate density-of-states functions  $N(E)$  for the three-dimensional problems illustrate the type of structure which can occur in these functions and also show the effect on these functions of Brillouin zone planes, corresponding to weak cosine terms, which cut inside the large zone.

The fourth objective is to gain a better qualitative interpretation of the Hume-Rothery rules. The usual approximation is made that the change in the thermodynamic free energy with electron concentration  $n$  is due only to the change in the total conduction electron energy  $U(n)$ . It is shown that for typical phase boundary problems  $U_1(n)$  for phase one, instead of increasing relative to  $U_2(n)$  as the zone is filled beyond the peak in  $N_1(E)$ , continues to decrease relative to  $U_2(n)$  until that energy is reached at which the total numbers of electrons are equal in the two phases. This shows that the positions of the phase boundaries cannot be accurately predicted theoretically from the electron concentration corresponding to the peak in the density of states.

Other results of this investigation suggest that  $N(E)$  and  $U(n)$  are determined primarily by the geometrical shape of the zone and hence should be about the same for different alloys with the same structure. It follows from this that the same phases of the different alloy systems should occur at the same electron concentrations.

## OBJECTIVE

A theoretical study of Brillouin zones, with special regard to the question of the appearance of energy gaps, is undertaken. It has a bearing on the Jones--Hume-Rothery theory of the physical properties of binary substitutional alloys.

CHAPTER I  
INTRODUCTION

This investigation belongs to what is usually called Brillouin zone theory or the zone theory of energy bands. More specifically, it is an attempt to understand certain general problems which arise in using this theory to determine the positions of the phase boundaries of certain alloys of copper, silver, and gold, or more generally of those alloys agreeing with the Hume-Rothery electron concentration rules. The results are of interest for other problems in alloy theory which depend primarily on the energy of the conduction electrons; but only the phase boundary problem will be explicitly considered.

In order to see the origin of the problems treated here, a brief sketch of the history of zone theory will be given. In the years from 1928 to 1933 the nearly-free-electron approximation for calculating the energies of the conduction electrons in perfect crystals was developed (references are given in Seitz's book).<sup>1</sup> In this work zone theory was developed as the natural way in which to display the electron energies as calculated by the nearly-free-electron approximation. By 1934 the inadequacy of this method for the exact calculation of electron energies had been established. However, in that same year Jones<sup>2</sup> used the nearly-free-electron approximation and zone theory to make a qualitative interpretation of the Hume-Rothery rules, the large diamagnetism, and the Hall coefficient of the  $\gamma$  phase of brass. In 1936 this work was extended in the book by Mott and Jones<sup>3</sup> and in 1937 made semi-quantitative in a partially empirical calculation by Jones<sup>4</sup> of the  $\alpha\beta$  phase boundaries of brass. This work by Jones is cited

in the current literature<sup>5</sup> as the basis for the theoretical interpretation of the empirically determined Hume-Rothery rules.

The main results of the nearly-free-electron approximation are discussed later in this work as they are needed. Here, it is sufficient to note two results: (1) except for edge effects, at each Brillouin zone boundary plane the energy changes discontinuously by an amount equal to twice the corresponding Fourier coefficient of the crystal potential and (2) this Fourier coefficient is approximately proportional to the geometrical structure factor of x-ray work and hence to the square root of the intensity of the x-rays reflected from the corresponding crystal lattice planes. These results are applied to the phase boundary problem in the following way. The lattice planes with the strongest x-ray lines are determined at the time of the identification of the structure of the alloy phase. The Brillouin zone boundary planes, corresponding to the lattice planes with strongest x-ray lines, mark out a zone in reciprocal or wave-vector space. According to the nearly-free-electron approximation, there should be a large increase in the energy across the faces of this zone and, hence, an energy gap in the density of states (the number of electron energy levels per unit energy range per unit volume of crystal) at that number of energy levels contained within the zone. Jones's work shows the importance of this energy gap in the interpretation of the physical properties mentioned above.

A careful examination of this line of reasoning reveals several unsatisfactory features, besides the lack of quantitative accuracy. In the remainder of this chapter the main problems are discussed which will be treated by more general methods in this investigation.

In the discussion given above the physical significance of the



zones was derived from a result of the nearly-free-electron approximation. One of the main purposes of this study is to investigate zone theory (that is, the theory of the electron energies in zones larger than the first or reduced zone) by general methods instead of by the nearly-free-electron approximation. As a starting point for this work, a chapter is included reviewing the physical reason for zones and giving definitions of Brillouin and other types of zones. The primary question is whether an energy gap can exist for a zone of prescribed geometrical shape. The factors which can prohibit an energy gap from existing are discussed and in particular a necessary condition on the geometrical shape of the zone is derived for the existence of an energy gap. Several zones of practical importance are examined with respect to this condition.

As for using the nearly-free-electron approximation, the point of view taken in this study is that, if applied correctly, it is a simple, useful tool for investigating the qualitative features of the electron energies. It may also be useful as an interpolation scheme for semi-quantitative work, provided the energies at points of the zone of high symmetry are otherwise accurately known; but this has not been definitely established. A second purpose of this study is to investigate two problems occurring in the qualitative application of the nearly-free-electron approximation to large zones. The first problem is that the existence of zones for which an energy gap can never exist contradicts the prediction by the nearly-free-electron approximation of a gap. The reason why this method does not actually predict a gap in such cases is shown by examples. The second problem concerns applications of the nearly-free-electron approximation to large zones in which all Brillouin zone boundary planes are neglected except those forming the faces of the zone. It will be shown that in some cases this does not, as heretofore supposed,

give the correct qualitative shape of the energy surfaces.

The final main topic investigated is the general shape of the function giving the total energy of the conduction electrons per unit volume of crystal as a function of the number of electrons per unit volume. By establishing the general continuity properties of this function and its derivatives, it is believed that a better understanding of the theoretical interpretation of the Hume-Rothery rules is obtained.

The theoretical results of this study are illustrated by simple two- and three-dimensional examples. Problems pertaining to the nature of the energy surfaces are constructed from two one-dimensional numerical problems. The first of these problems is based on a Schrödinger equation with a cosine potential (Mathieu's equation) and the second on an equation with a potential of two cosine terms (a special case of Hill's equation). For the three-dimensional problems accurate density-of-states functions are computed to illustrate the complexities which can occur in the shapes of these functions. Total electron energy functions are also given. A study of the shapes of these functions is of interest for the phase boundary problem.

## CHAPTER II

### DEFINITIONS AND PROPERTIES OF ZONES

The need for a modern and complete survey of the fundamentals of zone theory has recently been fulfilled by the appearance of an article entitled "Methods of the One-Electron Theory of Solids" by Reitz.<sup>6</sup> The first part of this article contains a discussion of the general problem of calculating the energy of electrons in solids and a development of the important concepts and results of zone theory. References to the literature in this field are also given. This article serves as an adequate introduction to the present chapter, except where otherwise indicated. Consequently, in this chapter only enough of the general theory will be given to establish the basic concepts and terminology used throughout the rest of this work.

#### 2.1. PHYSICAL REASON FOR ZONES

In order to calculate the energies of the electrons in a metal, a large number of approximations have to be made. It is outside the purpose of this study to discuss the validity of these approximations, but it is generally assumed that a qualitative understanding of the behavior of the electronic properties of metals can be obtained by studying the following idealized model. The structure of the metal is approximated by a perfect infinite crystal with basic translation vectors  $\vec{a}_1, \vec{a}_2, \vec{a}_3$ . The crystal can be considered as constructed of unit cells located at the points of the space lattice specified by the direct lattice vectors

$$\vec{A}_n = n_1\vec{a}_1 + n_2\vec{a}_2 + n_3\vec{a}_3 . \quad (2.1)$$

Each electron is assumed to move in a potential  $V(\vec{r})$  which has the symmetry of the space group of the metal. The possible energy levels of the electron

are approximated by the eigenvalues of the one-electron Schrödinger equation

$$(-\hbar^2/2m)\Delta\psi(\vec{r}) + V(\vec{r})\psi(\vec{r}) = E\psi(\vec{r}) . \quad (2.2)$$

Bloch has shown that a consequence of the translational symmetry of the potential is that electron wave functions can always be found which transform under a lattice translation as

$$\psi(\vec{r} + \vec{A}_n) = \exp[2\pi i(k_1n_1 + k_2n_2 + k_3n_3)]\psi(\vec{r}) , \quad (2.3)$$

where  $k_1, k_2, k_3$  are constants which must be real for a stationary state of an infinite lattice. This result can be put in a more convenient form by introducing the concept of the reciprocal space lattice with basic translation vectors  $\vec{b}_1, \vec{b}_2, \vec{b}_3$  defined implicitly by  $\vec{a}_i \cdot \vec{b}_j = \delta_{ij}$ . The reciprocal lattice vectors will be denoted by

$$\vec{B}_n = n_1\vec{b}_1 + n_2\vec{b}_2 + n_3\vec{b}_3 . \quad (2.4)$$

If the wave vector of the electron is defined as

$$\vec{k} = k_1\vec{b}_1 + k_2\vec{b}_2 + k_3\vec{b}_3 , \quad (2.5)$$

then the translational transformation properties can be written

$$\psi(\vec{r} + \vec{A}_n) = \exp(2\pi i\vec{k} \cdot \vec{A}_n)\psi(\vec{r}) . \quad (2.6)$$

It follows from this that  $\psi$  can be put in the functional form

$$\psi(\vec{r}) = \exp(2\pi i\vec{k} \cdot \vec{r}) u(\vec{r}) , \quad (2.7)$$

where

$$u(\vec{r} + \vec{A}_n) = u(\vec{r}) . \quad (2.8)$$

The wave vector  $\vec{k}$  is not unique, because the same function can be written

$$\psi(\vec{r}) = \exp[2\pi i(\vec{k} + \vec{B}_n) \cdot \vec{r}] u'(\vec{r}) , \quad (2.9)$$

where

$$u'(\vec{r}) = \exp(-2\pi i\vec{B}_n \cdot \vec{r}) u(\vec{r}) \quad (2.10)$$

is again a function with the periodicity of the direct lattice. This means that if  $\vec{k}$  is used as a set of three quantum numbers, then all physically

different states can be described by the set of  $\vec{k}$  vectors whose end points fill any fundamental region of reciprocal space. A region will be called a fundamental region if it has the following properties.

- 1) For every interior point  $\vec{k}$  in the region the point  $\vec{k} + \vec{B}_n$  lies outside of the region for all reciprocal lattice vectors  $\vec{B}_n$ .
- 2) For every boundary point  $\vec{k}$  of the region there is at least one other boundary point  $\vec{k}'$ , called a conjugate point, such that  $\vec{k}' = \vec{k} + \vec{B}_n$  for some reciprocal lattice vector  $\vec{B}_n$ .

Two procedures have proved useful in choosing the fundamental region or regions to be used. The first is called the reduced zone scheme. In this scheme only one fundamental region, called the reduced zone, is used. Consequently, there will be an infinite number of different wave functions with the same  $\vec{k}$  vector. These must be distinguished by an additional quantum number  $n$ . Thus, a wave function and its corresponding energy eigenvalue are denoted by

$$\psi_{n\vec{k}}(\vec{r}) = \exp(2\pi i \vec{k} \cdot \vec{r}) u_{n\vec{k}}(\vec{r}) \quad \text{and} \quad E_n(\vec{k}), \quad (2.11)$$

respectively. Functions and energies with the same  $n$  are said to belong to the same band. The energy is a multivalued function of  $\vec{k}$  in the reduced zone. It can be proven<sup>7</sup> that the different branches of this function are continuous throughout the zone. Consequently, in the reduced zone scheme restrictions on labeling the bands can be added so that the energies of a given band are a continuous function of  $\vec{k}$  throughout the reduced zone and are equal at conjugate boundary points of the reduced zone.

In practice the most convenient fundamental region is the symmetrical region constructed in the following way. The planes which perpendicularly bisect all the reciprocal lattice vectors drawn from the origin are constructed. The region which can be reached from the origin without crossing

any plane satisfies the requirements for a fundamental region and is also a possible unit cell of the reciprocal lattice. This region is also called the first Brillouin zone. Pictures of the first Brillouin zone of the simple cubic, face-centered cubic, and body-centered cubic lattices are given in Appendix A.

The second procedure for choosing the fundamental regions is called the extended zone scheme. In this scheme all reciprocal space is divided into separate fundamental regions. Each different wave function  $\psi_{\vec{n}\vec{k}}$  of the reduced zone scheme is now assigned to a separate vector  $\vec{k}' = \vec{k} + \vec{E}_m$  in the extended zone scheme. The set of wave functions and energies belonging to the  $\vec{k}$  vectors of the same fundamental region are said to belong to the same band. Thus, a wave function and its corresponding energy are usually denoted by

$$\psi_{\vec{k}}(\vec{r}) = \exp(2\pi i \vec{k} \cdot \vec{r}) u_{\vec{k}}(\vec{r}) \quad \text{and} \quad E(\vec{k}), \quad (2.12)$$

respectively; and the different bands are denoted only implicitly by the number of the region in which the end of the  $\vec{k}$  vector lies. The energy is now a single-valued function of  $\vec{k}$  throughout all reciprocal space.

A fundamental region may be composed of one or more sections. A section is the region which can be reached from any one point of the fundamental region without crossing any boundary of the fundamental region. A restriction can be added that the wave functions are to be assigned to the sections in such a way that the energy is a continuous function of  $\vec{k}$  within each section. In any special case it may be desirable to require additional continuity properties. However, for purposes of general analysis only the above property will be required. It follows from the fact that all fundamental regions are equivalent that each fundamental region in the extended zone scheme can be divided into parts so that each part, which is

not necessarily a section, can be brought by one and only one reciprocal lattice translation to the inside of the reduced zone; and these parts then just fill the reduced zone without any overlapping of the parts. In the extended zone scheme it is not required that the different parts of an energy band join continuously when brought within the reduced zone.

The fundamental regions in the extended zone scheme can be chosen in an infinite variety of ways. One of the most useful schemes is that defined by Brillouin. This is described in Section 2.2. A few of the other possible zone schemes are discussed in Section 2.3. The words "zone" and "Brillouin zone" are also used in the literature to denote regions in reciprocal space which are not fundamental regions. This use is discussed in Section 2.4.

## 2.2. BRILLOUIN ZONES

The only extended zone scheme that has been useful in practice is the one worked out by Brillouin. The zones are constructed by an extension of the method used to form the reduced zone. The perpendicularly bisecting planes are constructed for all the reciprocal lattice vectors drawn from the origin. These planes divide reciprocal space into small sections. Each section is assigned a number equal to one plus the number of planes passing between the section and the origin. All sections with number  $N$  form the  $N^{\text{th}}$  Brillouin zone. Although it is not simple to do, it can be shown<sup>8</sup> that each Brillouin zone is a fundamental region and that all of each section can be moved to within the first Brillouin zone by one and only one reciprocal lattice translation.

Appendix A contains photographs of models showing the outside surfaces of the first four Brillouin zones of the simple cubic, body-centered cubic, and face-centered cubic lattices. In addition drawings are given of

the outside surfaces of the first eight Brillouin zones for the body-centered and face-centered cubic lattices. It is believed that the drawings of zones five through eight have not been given before in the literature.

The term "Brillouin zone" is often used in the literature to refer to any region of reciprocal space of interest for a particular problem. It has also been used to denote an energy band in the reduced zone scheme. In this paper the term "Brillouin zone" will always refer to a zone as defined by Brillouin.

### 2.3. OTHER EXTENDED ZONE SCHEMES

The geometrically simplest extended zone scheme is obtained by the periodic repetition of the central reduced zone to fill all reciprocal space. Each energy band of the reduced zone scheme can be assigned to a different zone in the extended zone scheme. This zone scheme will be useful in certain theoretical derivations given later in this study.

Seitz<sup>1</sup> has shown that another extended zone scheme arises in the following way. Suppose the crystal potential can be written as the sum  $V(\vec{r}) = V_0(\vec{r}) + V_p(\vec{r})$ , where the symmetry of  $V(\vec{r})$ , including translational, is a subgroup of the symmetry of  $V_0(\vec{r})$  and  $V_p(\vec{r})$  is a small perturbation on  $V_0(\vec{r})$ . When  $V(\vec{r}) = 0$ , considered as the limit of  $V(\vec{r})$  decreased to zero, the electrons are free; and there are degeneracies in the energy on and only on the Brillouin zone boundaries of the lattice of  $V(\vec{r})$ . Consider what happens to the electron energies as  $V_0(\vec{r})$  is adiabatically increased from zero to its final value while  $V_p(\vec{r})$  is still zero. As  $V_0(\vec{r})$  is increased, three things may happen to the degeneracies: (1) degeneracies which existed on certain zone boundaries are removed, (2) degeneracies which existed on certain zone boundaries remain on those boundaries, and (3) degeneracies which existed on certain zone boundaries now exist on certain



curved surfaces (curved lines in two dimensions). The old zone boundaries of cases (1) and (2) and the new curved surfaces of case (3) divide reciprocal space into sections. The sections can be grouped into zones, each of which is a fundamental region. This last result follows from the symmetrical form of Brillouin zones and the periodicity of the energy. If part of the surface at the point  $\vec{k}$  between the  $N^{\text{th}}$  and  $N + 1^{\text{st}}$  Brillouin zone bulges into the  $N + 1^{\text{st}}$  zone, then the surface at the conjugate point  $\vec{k}'$  must bulge an equal amount into the  $N^{\text{th}}$  zone. Thus, the new zones are also fundamental regions. In this way an extended zone scheme is constructed which forms a logical starting point for considering the perturbed problem. These zones may appropriately be named "Seitz zones." A two-dimensional example of a Seitz zone scheme is given in Section 5.1.

#### 2.4. JONES ZONES

In Chapter I a procedure was briefly described for constructing a zone for which an energy gap exists or almost exists. Following Reitz, this zone will be called a "Jones zone." Unlike Brillouin zones, the Jones zone for a given lattice is not uniquely defined, because its form depends on the crystal potential. The usual method of constructing Jones zones will now be given in more detail than in the preceding chapter. According to the nearly-free-electron approximation the energy difference on crossing a plane forming a Brillouin zone boundary is  $2V(\vec{B}_n)$ , where  $V(\vec{B}_n)$  is the Fourier coefficient of the crystal potential corresponding to the plane  $\vec{B}_n$ . On making the approximation that the crystal potential is the sum of identical atomic-like potentials located at the positions of each atom, then it follows that  $V(\vec{B}_n) = V'(\vec{B}_n) S(\vec{B}_n)$ , where  $V'(\vec{B}_n)$  is the Fourier coefficient of a potential formed by atoms located only at the origins of the unit cells and  $S(\vec{B}_n)$  is the geometrical structure factor of the unit cell. It turns

out that  $V'(\vec{B}_n)$  is usually a slowly varying function of  $\vec{B}_n$ , so that large fluctuations in  $V(\vec{B}_n)$  and in particular the vanishing of  $V(\vec{B}_n)$  are due to corresponding changes in the geometrical structure factor  $S(\vec{B}_n)$ . If the nearly-free-electron approximation has sufficient validity to maintain a correlation between large Fourier coefficients of the potential and large energy differences across the corresponding planes in an extended zone scheme, then it follows that the boundaries of the Jones zone should be planes with large geometrical structure factors. In practice the volume of the Jones zone formed by the planes with the largest geometrical structure factors has usually been approximately just sufficient to contain the conduction electrons. The Jones zones considered in this study will be constructed by the above procedure.

It follows from the above method of construction that the Jones zone contains all of one or more Brillouin zones and sometimes contains only parts of one or more additional Brillouin zones. A Jones zone which contains parts of Brillouin zones may or may not contain an integral number of fundamental regions.

The term "Jones zone" ordinarily means the central zone containing the origin of reciprocal space. However, a Jones zone scheme can be defined. The outer zones are constructed and numbered in the same way as the Brillouin zones, except that only those planes are used which have large geometrical structure factors. The Jones zones are not uniquely defined in that there is an arbitrariness in the choice of which planes are to be used in their construction.

The assignment of the energy bands to the Jones zones is not always unique but is guided by the general rule that the energies within a zone are to be less than the energies in the next higher zone insofar as

possible. The general properties of the electron energies in Jones zones are discussed in the following chapter. It is shown there that for various reasons a discontinuity in the energy may not exist at every point of a Jones zone boundary constructed according to the above procedure. Thus, the traditional method of constructing Jones zones does not always lead to zones having an energy gap. In such cases it might be desirable to choose the boundaries of the Jones zone by a new procedure.

## CHAPTER III

### GENERAL PROPERTIES OF ELECTRON ENERGIES IN JONES ZONES

The importance of the Jones zone is due to the energy gap which is supposed to exist for it. Although a superficial application of the nearly-free-electron approximation predicts that an energy gap should exist for every Jones zone if the potential is "strong" enough, Jones<sup>9</sup> has shown by a careful application of the nearly-free-electron approximation that an energy gap cannot exist for a possible Jones zone of the hexagonal close-packed structure. That is, there must always be a degeneracy between the first and second Jones zones. This result was later confirmed by Herring<sup>10</sup> by using group-theoretical methods. This work suggests the need for a general investigation as to when degeneracies between the true electron energies in different Jones zones must occur. The first part of this chapter presents some results of such an investigation.

The chapter concludes with a discussion as to when it is correct in principle to simplify the nearly-free-electron approximation for calculating the electron energies in Jones zones by neglecting the plane waves and zone boundary planes corresponding to the zero Fourier coefficients of the crystal potential.

#### 3.1. DIRECTIONAL, SYMMETRY, AND ACCIDENTAL DEGENERACIES

In the reduced zone scheme it is known that the energy bands often touch or overlap. In such cases the energy degeneracies are of three types. For completeness these will be described briefly. A directional degeneracy is said to occur whenever the energy in one band at one wave vector is equal

to the energy in another band at another wave vector (except for certain special cases which obviously belong to the following types). The end points of the wave vectors of either band for which directional degeneracies occur usually fill a three-dimensional region of the reduced zone. A symmetry degeneracy is said to occur whenever the energies in two bands must be equal at the same wave vector because of the symmetry or reality of the crystal potential. An accidental degeneracy is said to occur whenever the energies in two bands are equal at the same wave vector but are not required to be equal by the symmetry or reality of the potential. Symmetry and accidental degeneracies have been shown by Bouckaert, Smoluchowski, and Wigner<sup>7</sup> and by Herring<sup>11</sup> to occur only at certain points, lines, and planes of the reduced zone. Reference should be made to the original articles cited for more detailed information about these degeneracies.

In an extended zone scheme these same degeneracies must still exist at points which differ from the corresponding points of the reduced zone scheme by reciprocal lattice vectors. Whether or not such degeneracies will occur between the energies in different Jones zones usually can only be determined by an actual calculation of the electron energies. Occasionally, as in the hexagonal close-packed structure mentioned above, it is possible to predict that symmetry degeneracies must occur. The important point is that, since directional, symmetry, and accidental degeneracies are known to occur frequently among the higher bands in the reduced zone, these degeneracies cannot be assumed to be absent in Jones zones.

### 3.2. SHAPE DEGENERACIES

The three types of degeneracies discussed in the preceding section could exist for all Jones zones. For certain Jones zones there is in addition

an effect which is so similar to a degeneracy that it will be convenient to classify it as a fourth type of degeneracy. As this effect does not seem to have been generally treated before, it will be discussed in detail. This effect is due only to the shape of the Jones zone and not to any particular form of the energy bands, and it exists only in those Jones zones in which an integral number of fundamental regions cannot be constructed.

For such Jones zones only a certain number of fundamental regions can be constructed within the zone, and then in order to fill the zone one or more additional fundamental regions must be constructed which are composed of sections lying wholly inside or wholly outside the Jones zone. (A section now means the region which can be reached from a given point of the fundamental region without crossing either a boundary of the fundamental region or a Jones zone boundary.) Let the continuous energy bands of the reduced zone scheme be cut, if necessary, and replotted with one to each fundamental region. It follows that the energies in each region must be equal in a limiting sense at all conjugate boundary points. The equality of the energies of the same region which exists at conjugate boundary points lying on opposite sides of the Jones zone boundary will be called a shape degeneracy, although it is not a true degeneracy in the strict sense of the word. Of course, in special cases symmetry and accidental degeneracies between different bands might also exist at such conjugate points.

It should be noted that shape degeneracies must always exist if the volume of the Jones zone is not an integral multiple of the volume of the reduced zone. Also, shape degeneracies must always exist if there is a part of the Jones zone boundary which is not connected to any other part of the zone boundary by any reciprocal lattice vector. This is because in such cases there must be sections of the same fundamental region both in-

side and outside the Jones zone. In the following examples it will be seen that the parts of the zone boundary faces which are not connected to other parts by reciprocal lattice vectors cause the faces to be asymmetric with respect to the center of the plane forming the face. This criterion of asymmetry has been in practice a simple and reliable guide for predicting shape degeneracies in all Jones zones investigated in this study. However, the criterion of asymmetry may not be rigorously valid because it would seem to be possible to have a Jones zone, constructed by the procedure of Section 2.4, which has asymmetric faces all parts of which are connected to other parts of the zone boundary by reciprocal lattice vectors.

Shape degeneracies exist on surfaces (lines in two dimensions), but the positions of the surfaces are not unique because of the arbitrariness in the choice of the fundamental regions. However, as will be seen from the examples below, the fundamental regions can always be chosen so that the energy will be continuous across those parts of the Jones zone boundary which are not connected to any other part of the boundary by any reciprocal lattice vector. Additional shape degeneracies may exist either on or off the Jones zone boundary. A property of particular importance is that shape degeneracies will almost always be accompanied by directional degeneracies between points inside and outside the Jones zone.

The following simple examples illustrate the nature of the shape degeneracies to be expected in the Jones zones of actual metals. All examples are for the two-dimensional square reciprocal lattice.

The (20) Jones Zone.—The Jones zone formed by the (20) family of planes will be used extensively in Chapter V. No shape degeneracies exist for this zone because it is filled by exactly four fundamental regions, for example as shown in Fig. 3.1. In addition to all of the first three

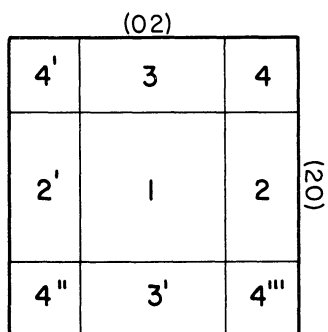


Fig. 3.1. The (20) Jones zone.

Brillouin zones, the (20) Jones zone contains parts of the fourth, fifth, and sixth Brillouin zones (see Fig. 5.1), showing that the existence of only parts of Brillouin zones inside the Jones zone does not necessarily imply a shape degeneracy.

The (30)(31) Jones Zone.—A considerable

amount of shape degeneracy exists in the (30)(31) Jones zone. To see this, construct an extended zone scheme by the periodic repetition of the re-

duced zone, as in Fig. 3.2. In this scheme the energy is continuous across those parts of the zone boundaries formed by the (31) planes, so that there

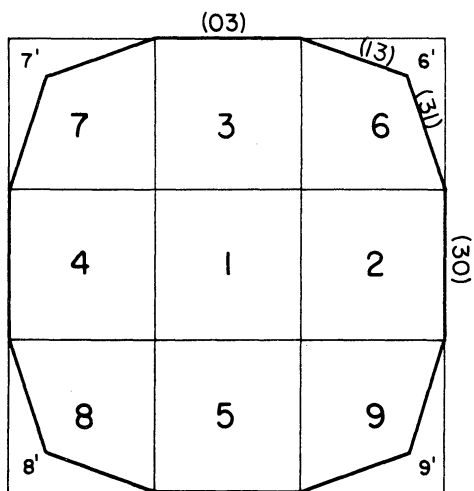


Fig. 3.2. The (30)(31) Jones zone.

are shape degeneracies in fundamental regions 6, 7, 8, and 9. Since on the zone boundaries no finite part of the (31) planes is connected to any other by reciprocal lattice vectors, the shape degeneracies cannot be essentially removed as they were by the proper choice of the regions for the (20) Jones zone. The shape degeneracies in, say, regions 6 and 7 can be removed, but this can be done only by introducing additional shape degeneracies

in other regions. The volume of the (30)(31) Jones zone is eight times that of the reduced zone, showing that a shape degeneracy can exist even if the volume of the Jones zone is an integral multiple of the volume of the reduced zone. That is, it is sometimes impossible to construct an integral number of fundamental regions within a Jones zone whose volume is an



integral multiple of the volume of the reduced zone.

The (50)(43) Jones Zone.—As a last example consider the (50)(43) Jones zone. The volume of this zone is twenty and five twenty-first times the volume of the reduced zone, so there are necessarily shape degeneracies. A possible extended zone scheme using all or parts of only twenty-one fundamental regions inside the Jones zone is shown in Fig. 3.3. In this scheme

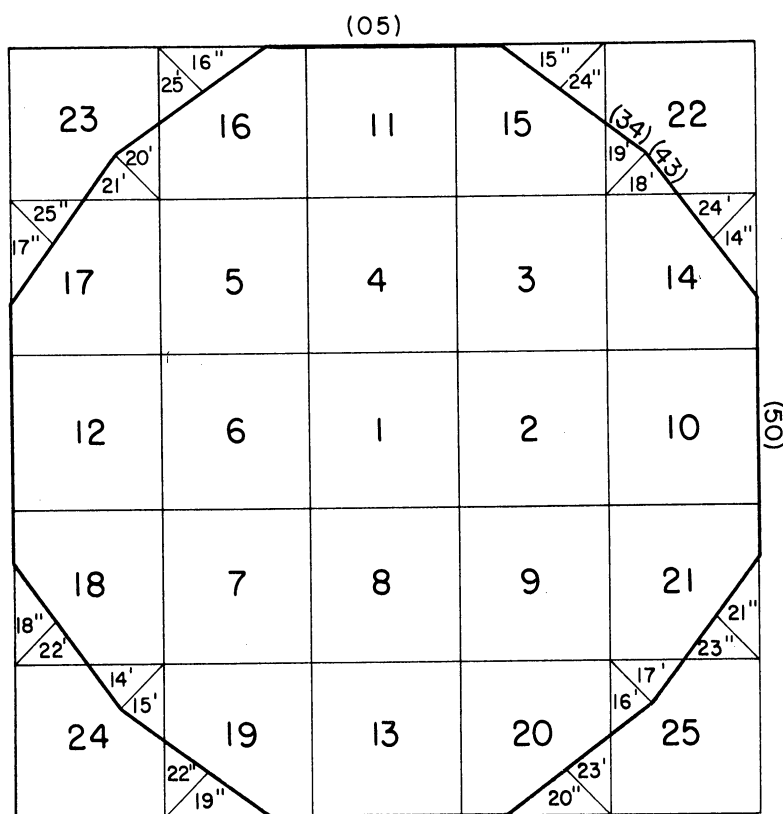


Fig. 3.3. The (50)(43) Jones zone.

parts of some of the squares have been interchanged, so that, for example, section 14' lies inside the Jones zone in the original twenty-fourth square. The part of the Jones zone boundary between sections 14 and 14" is not connected by any reciprocal lattice vector to any other part of the zone boundary, and thus the continuity of the energy across this part of the boundary cannot be essentially removed. There are additional shape de-

degeneracies between conjugate points on the boundaries of sections 14' and 14'', but the shape of these boundaries can be changed within wide limits. A similar situation exists in regions 15 through 21. The general nature of the shape degeneracies in the (50)(43) zone should be typical of that to be found in large three-dimensional zones, such as the  $\gamma$ -brass zone.

Appendix C contains an investigation of some important three-dimensional Jones zones to determine whether or not shape degeneracies must exist for them. It is shown that shape degeneracies do exist in some cases, for example in the  $\gamma$ -brass zone.

### 3.3. POSSIBLE OMISSION OF CERTAIN PLANES FORMING ZONE BOUNDARIES

When the central Jones zone is larger than the first Brillouin zone, certain Fourier coefficients of the crystal potential are much larger than the others. Let us see to what extent this property can be used, first, to simplify an approximate calculation of the electron energies in which certain small coefficients are set equal to zero and, second, to simplify the extended zone scheme by omitting certain of the planes used in forming the zone boundaries.

Consider those reciprocal lattice vectors whose corresponding coefficients are large. The sums and differences of all integral multiples of these vectors constitute a set  $\vec{B}'$  of vectors which themselves form a reciprocal lattice. Note that the Fourier coefficients of some of the vectors of the set  $\vec{B}'$  may be small or zero. If the set  $\vec{B}'$  is smaller than the original set  $\vec{B}$  of all reciprocal lattice vectors, then another set  $\vec{B}''$ , containing no vectors of set  $\vec{B}'$ , can be found such that

$$\text{set } \vec{B} = \text{set } \vec{B}' + \text{set } \vec{B}'' . \quad (3.1)$$

The Fourier coefficients can be divided into corresponding sets such that

$$\text{set } V(\vec{B}) = \text{set } V(\vec{B}') + \text{set } V(\vec{B}'') . \quad (3.2)$$

All the coefficients in the set  $V(\vec{B}'')$  are small; and therefore the crystal potential can be divided into two terms such that

$$V(\vec{r}) = V_0(\vec{r}) + V_p(\vec{r}) , \quad (3.3)$$

where  $V_p(\vec{r})$  is a small perturbation on  $V_0(\vec{r})$ . A straightforward calculation shows that the volume of the reduced zone of the lattice of set  $\vec{B}'$  must be an integral multiple of the volume of the reduced zone of the original reciprocal lattice. Physically, this means that the true crystal can be considered as a small perturbation of another crystal which has a smaller direct lattice unit cell and hence a larger reciprocal lattice unit cell.

The importance of the above division is the following. Consider the approximate, unperturbed problem in which the coefficients of the set  $V(\vec{B}'')$  are set equal to zero. In the matrix formulation of quantum mechanics in which the true eigenfunctions are expanded in terms of the complete orthogonal set of plane waves  $\exp[2\pi i(\vec{k} - \vec{B}_n) \cdot \vec{r}]$ , the matrix elements are

$$\langle \vec{k} - \vec{B}_m | V(\vec{r}) | \vec{k} - \vec{B}_n \rangle = V(\vec{B}_n - \vec{B}_m) . \quad (3.4)$$

There can be no nonzero matrix elements between plane waves specified by vectors belonging to different sets  $\vec{B}'$  and  $\vec{B}''$ , because a vector  $\vec{B}_m'' - \vec{B}_n'$  must necessarily belong to the set  $\vec{B}''$ . This means that the infinite secular determinant can be split into two parts as shown schematically in Fig. 3.4. The  $\det \vec{B}'$  is the secular determinant for the problem obtained by considering only the plane waves and zone boundary planes corresponding to the vectors of set  $\vec{B}'$ . A solution of this determinant is also a true solution of the original secular determinant. Thus, for the approximate, unperturbed problem it is correct to neglect all plane waves and zone boundary planes corresponding to the vectors of set  $\vec{B}''$ . The solutions of the  $\det \vec{B}''$  give the extra solu-

	SET $\vec{B}'$	SET $\vec{B}''$
SET $\vec{B}'$	Det $\vec{B}'$	0
SET $\vec{B}''$	0	Det $\vec{B}''$

Fig. 3.4. Form of secular determinant.

tions of the original secular determinant which are required by the fact that the periodicity of the original reciprocal lattice is smaller than the periodicity of the lattice formed by the vectors of set  $\vec{B}'$ .

In practice the set  $\vec{B}'$  is often identical with the original set  $\vec{B}$ . In such cases no plane waves and zone boundary planes can be neglected.

To see this, choose a new set  $\vec{B}'''$ , which is smaller than the set  $\vec{B}$  but contains all vectors whose corresponding coefficients are large. Let set  $\vec{B} = \text{set } \vec{B}''' + \text{set } \vec{B}^{iv}$ . Then there must exist many vectors  $\vec{B}_m^{iv}$  and  $\vec{B}_n'''$  such that the coefficients corresponding to the vectors  $\vec{B}_m^{iv} - \vec{B}_n'''$  are large. This means that there are large matrix elements connecting states of set  $\vec{B}'''$  with states of set  $\vec{B}^{iv}$ , and hence the solutions of the det  $\vec{B}'''$  are not in general true solutions of the original secular determinant.

The following examples illustrate typical cases when plane waves and zone boundary planes can and cannot be neglected. Both examples are for the two-dimensional square reciprocal lattice.

The (20) Jones Zone.—Suppose that the only large Fourier coefficients of the potential are those corresponding to the (20) family of planes. The set  $\vec{B}'$  consists of all lattice vectors whose components are even integers times the basic translation vectors, and the new reciprocal lattice is again a square lattice but with twice the lattice spacing. In the vicinity of the (20) Jones zone only the plane waves and zone boundary planes for the (20) and (22) families of vectors have to be considered for the unperturbed problem and those for the (10), (11), and (21) families can

be neglected. The complications which arise in computing and plotting the energy in the (20) Jones zone when the (10), (11), and (21) families are not neglected are discussed in Chapter V for a particular numerical example.

The (30)(22) Jones Zone.—When the only large Fourier coefficients of the potential are those corresponding to the (30) and (22) families of planes, the set  $\vec{B}'$  will include the vector  $(\vec{30}) + (22) + (2\bar{2}) = (10)$ . Similarly, all vectors of the (10) family are included in the set  $\vec{B}'$ , so that the set  $\vec{B}'$  is identical with the original set  $\vec{B}$ . Hence there are no plane waves and zone boundary planes which can in general be omitted in calculating the energy. The boundary of the (30)(22) Jones zone coincides with the outer boundary of the seventh Brillouin zone (see Fig. 5.1), showing that it may be impossible to neglect plane waves and zone boundary planes even if the Jones zone contains an integral number of fundamental regions.

Appendix C contains an analysis of some important large Jones zones to see if their interior zone boundary planes and the corresponding plane waves can be neglected in computing the approximate electron energies. It turns out that in most cases, for example that of  $\gamma$  brass, it is not correct even in an approximate calculation to consider only the large Fourier coefficients and their corresponding plane waves and zone boundary planes.

## CHAPTER IV

### ONE-DIMENSIONAL PROBLEMS WITH COSINE POTENTIALS

Much of the remainder of this work is devoted to the study of certain two- and three-dimensional numerical problems. These examples illustrate important concepts in zone theory such as those discussed in the preceding chapter as well as others to be introduced later. As these concepts have to do only with the electron energies and not with the electron wave functions, it is sufficient to consider highly simplified problems which do not have accurate crystal potentials and electron wave functions but which do have the essential features of the energies of the conduction electrons in actual metals. One of the simplest such problems and one which is closely related to the study of Jones zones is obtained when the Fourier series of the crystal potential contains only a few nonzero exponential terms which can be combined into cosines. In order to get a numerically simple problem the potential must be such that a separation of variables can be made in the Schrödinger equation. This chapter is concerned with finding both analytical and numerical solutions of the resulting one-dimensional Schrodinger equation.

#### 4.1. ONE-DIMENSIONAL EQUATION AND DIMENSIONLESS VARIABLES

On separation of variables the considerations above lead to the study of the following one-dimensional Schrödinger equation

$$(-\hbar^2/2m)(d^2/dx'^2)\psi + 2V'(100)\cos(2\pi x'/a)\psi + 2V'(200)\cos(4\pi x'/a)\psi = E'\psi, \quad (4.1)$$

in which  $a$  is the lattice constant and the primes distinguish certain

symbols with dimensions from the dimensionless symbols introduced below.

It is convenient to measure energies relative to the energy

$$E_0' = h^2/2ma^2 \quad (4.2)$$

of a free electron with wave vector at the center of a zone face of the (20) or (200) Jones zones. Thus, introduce dimensionless quantities

$$E = E'/E_0', \quad V_1 = V'(100)/E_0', \text{ and } V_2 = V'(200)/E_0' . \quad (4.3)$$

The energy  $E_0'$  is about ten electron volts for typical metals so that the dimensionless energies given hereafter should be multiplied by ten to get representative energies in electron volts. The dimensionless length

$$x = \pi x'/a \quad (4.4)$$

varies from zero to  $\pi$  within the unit cell. In terms of these dimensionless variables the Schrödinger equation (4.1) becomes

$$(d^2/dx^2)\psi + 4(E - 2V_1 \cos 2x - 2V_2 \cos 4x)\psi = 0 . \quad (4.5)$$

The Bloch solution of this equation has the form

$$\psi(x) = \exp(2ikx) u(x), \text{ where } u(x + \pi) = u(x) . \quad (4.6)$$

The boundaries of the Brillouin zones occur at  $k = \pm 1/2, \pm 1, \pm 3/2, \dots$ ; and the (dimensionless) energies of a free electron ( $V_1 = V_2 = 0$ ) with wave vector at these boundaries are  $E = 1/4, 1, 9/4, \dots$ .

#### 4.2. ANALYTICAL SOLUTIONS

The Schrödinger equation (4.5) is a special case of Hill's equation, since there are only two cosine terms. Ince<sup>12</sup> has obtained solutions

of the general Hill equation by extending a method due to Whittaker<sup>13</sup> for Mathieu's equation. The solutions are in the form of power series expansions in  $V_1$  and  $V_2$ . Each expansion converges rapidly enough to be useful only in a restricted region of reciprocal space in an extended zone scheme, so that three expansions have to be used to cover the first, second, and inner parts of the third Brillouin zones. In the first of these expansions, called the  $\kappa$ -expansion,  $E$  and  $u(x)$  are expanded in powers of  $V_1$  and  $V_2$  with coefficients which are functions of  $\kappa = 2k$ . This expansion diverges for values of  $k$  on the zone boundaries and converges well only for values of  $k$  far from the zone boundaries. In the other two expansions,  $E$ ,  $k$ , and  $u(x)$  are expanded in powers of  $V_1$  and  $V_2$  with coefficients which are functions of a parameter  $\sigma$ . Each of these expansions converges well only in the vicinity of one zone boundary. In one of these, called the  $\sigma$   $1/4$ -expansion, the leading term in the series for  $E$  is the energy  $1/4$  of a free electron at the boundary of the first Brillouin zone; and this expansion converges well only for values of  $k$  near the first zone boundary. Similarly, in the other, called the  $\sigma$   $1$ -expansion, the series for  $E$  begins with  $1$ ; and this expansion converges well only near the second zone boundary.

Ince obtained the most important terms in the three expansions when  $V_1$  is greater than  $V_2$ . However, for problems in connection with Jones zones  $V_1$  is less than  $V_2$ ; and hence it was necessary to extend Ince's results to include high-degree terms in  $V_2$ . The details of the method for doing this and the results obtained are reported in Appendix B. Since general formulas for the coefficients in the various expansions are not known, a recurrence relation method was used in which the coefficients of a term of a given degree could be calculated as soon as all the coefficients of



terms of lower degree had been derived. In this way all terms through the fifth degree in  $V_1^i V_2^j$  ( $i + j \leq 5$ ) were calculated in the series for  $E$  and  $k$ . To do this, certain terms through the fourth degree in the series for  $u(x)$  had to be calculated, although the wave functions are not otherwise needed. As a check on the accuracy of the work, all calculations were done twice. In addition to obtaining new results, a few errors were discovered in Ince's work.

When either  $V_1 = 0$  or  $V_2 = 0$ , the Schrödinger equation (4.5) reduces to Mathieu's equation and the solutions discussed above reduce to known solutions of Mathieu's equation.

#### 4.3. NUMERICAL PROBLEMS

The illustrative examples of the following chapters are based on two numerical problems. In one of these, the unperturbed problem,

$$V_1 = 0.00 \quad \text{and} \quad V_2 = 0.30 \quad ; \quad (4.7)$$

and in the other, the perturbed problem,

$$V_1 = (1/10) V_2 = 0.03 \quad \text{and} \quad V_2 = 0.30 \quad . \quad (4.8)$$

The value of  $V_2$  was chosen to give a small amount of directional degeneracy in the (20) Jones zone, and the ratio of  $V_1$  to  $V_2$  in the perturbed problem was chosen as typical of the ratio of weak to strong Fourier coefficients in actual metals.

The expansions discussed in the preceding section and derived in Appendix B were used to calculate  $E$  as a function of  $k$  for the perturbed and unperturbed problems. Unfortunately, it was not possible to make an estimate of the error made in using only a finite number of terms of the infinite series. However, the way the  $E$ -versus- $k$  curves for expansions

valid in different regions closely approached each other or crossed with almost equal tangents strongly indicates that the error in the energy in these joining regions is less than about  $\pm 0.002$ , which is sufficiently accurate for the following examples. The calculated energies of the unperturbed problem at the origin and on the zone boundaries were compared with the true solutions of Mathieu's equation which are tabulated<sup>14</sup> at only these positions. This indicates that the error in the energy at these points is less than  $\pm 0.00002$ .

Figure 4.1 shows part of the second energy band plotted in the reduced zone scheme for the perturbed problem. Curves computed by all three expansions are shown, although that by the  $\sigma 1$ -expansion is not used in this region. A composite E-versus-k curve was constructed in this region by using the  $\sigma 1/4$ -expansion to the right of, say,  $k = 0.44$  and the  $\kappa$ -expansion to the left of this point with a slight adjustment of these curves near  $k = 0.44$  to make them join smoothly. A similar procedure was used at other points where different expansions had to be joined.

The final composite energy curve for the perturbed problem is shown as the solid curve in Fig. 4.2. The dashed curve in this figure is the energy of a free electron. The energy gap between the second and third energy bands is 0.6002 with center at 0.9890. The predictions of the nearly-free-electron approximation of a gap of  $2V_2 = 0.60$  with center at 1.00 are close to the correct values. The gap between the first and second energy bands is 0.0423 with center at 0.1908, whereas the nearly-free-electron approximation predicts a gap of  $2V_1 = 0.06$  with center at 0.25. The reason for the failure of the nearly-free-electron approximation in this case is, of course, the strong perturbation by the coefficient  $V_2$ .

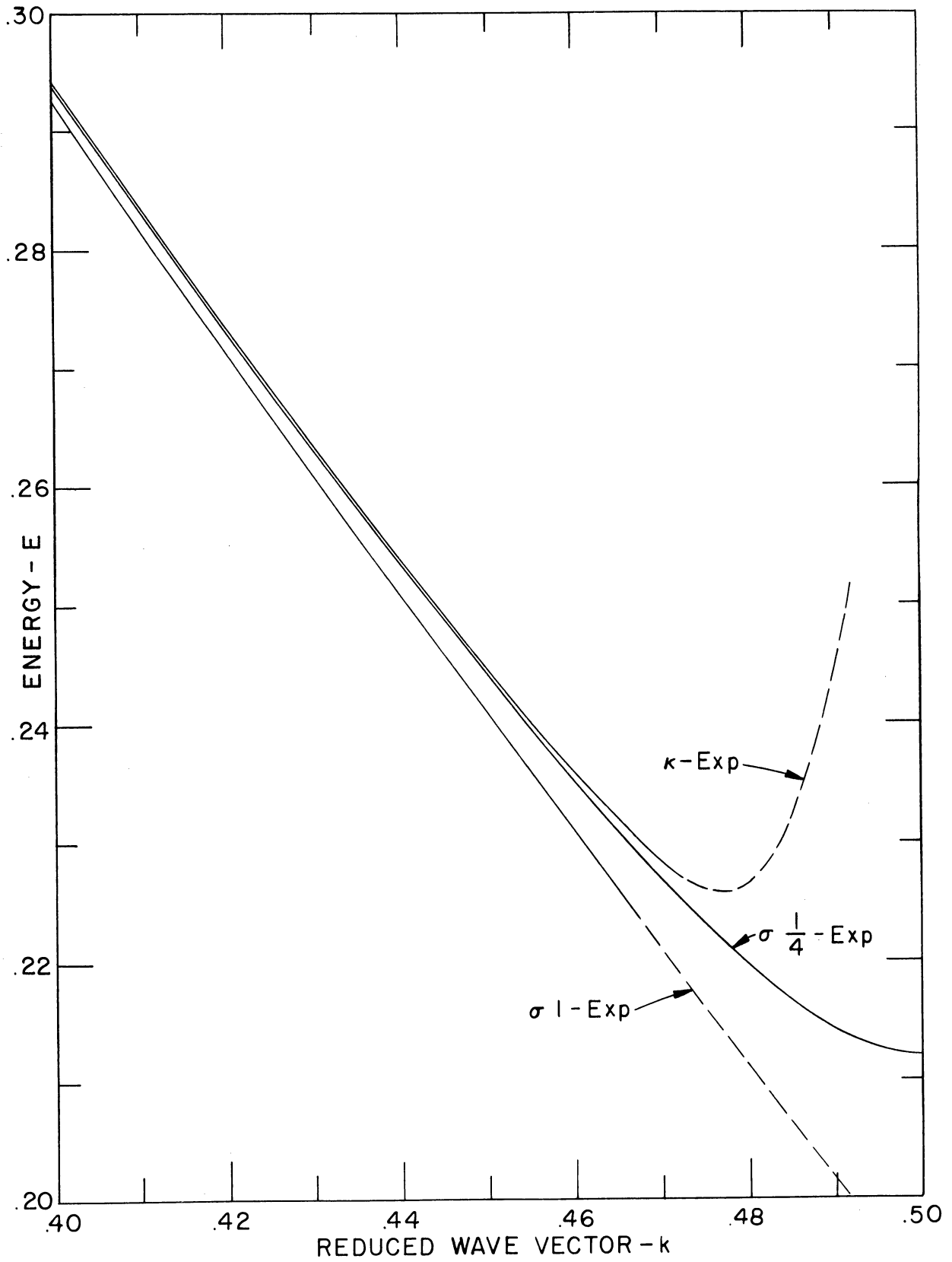


Fig. 4.1. Electron energies by different expansions.

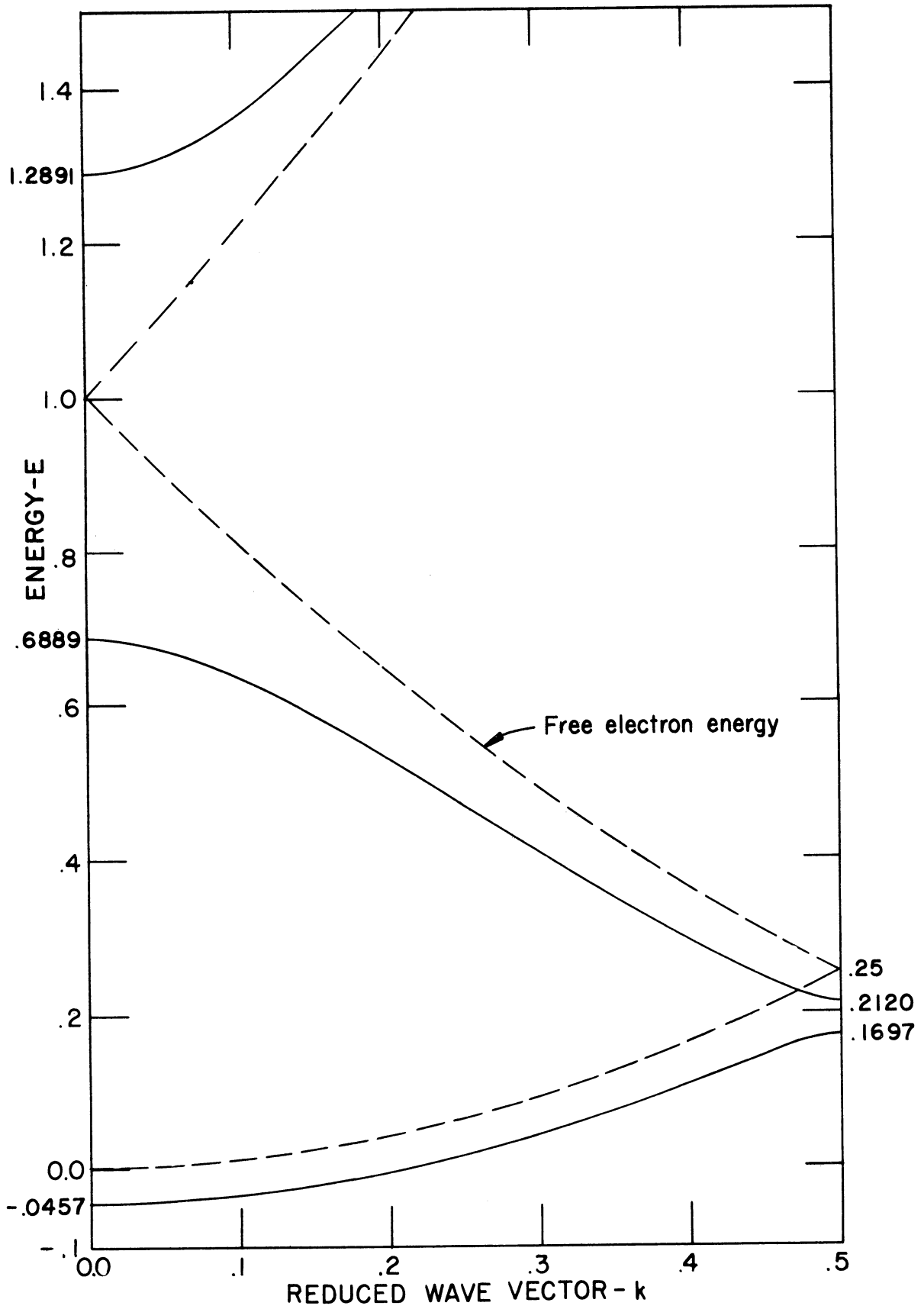


Fig. 4.2. Composite energy curve for perturbed problem and energy of free electron.

For purposes of comparison it is convenient to consider the unperturbed problem as a limiting case of the perturbed problem obtained by letting  $V_1$  approach zero. This is somewhat artificial since the true first Brillouin zone for the unperturbed problem is the sum of the first and second Brillouin zones of the perturbed problem. The composite energy curve for the unperturbed problem is shown in Fig. 4.3. The energy gap is 0.5991 with center at 0.9887. This curve differs appreciably from that for the perturbed problem only in the vicinity of the first zone boundary.

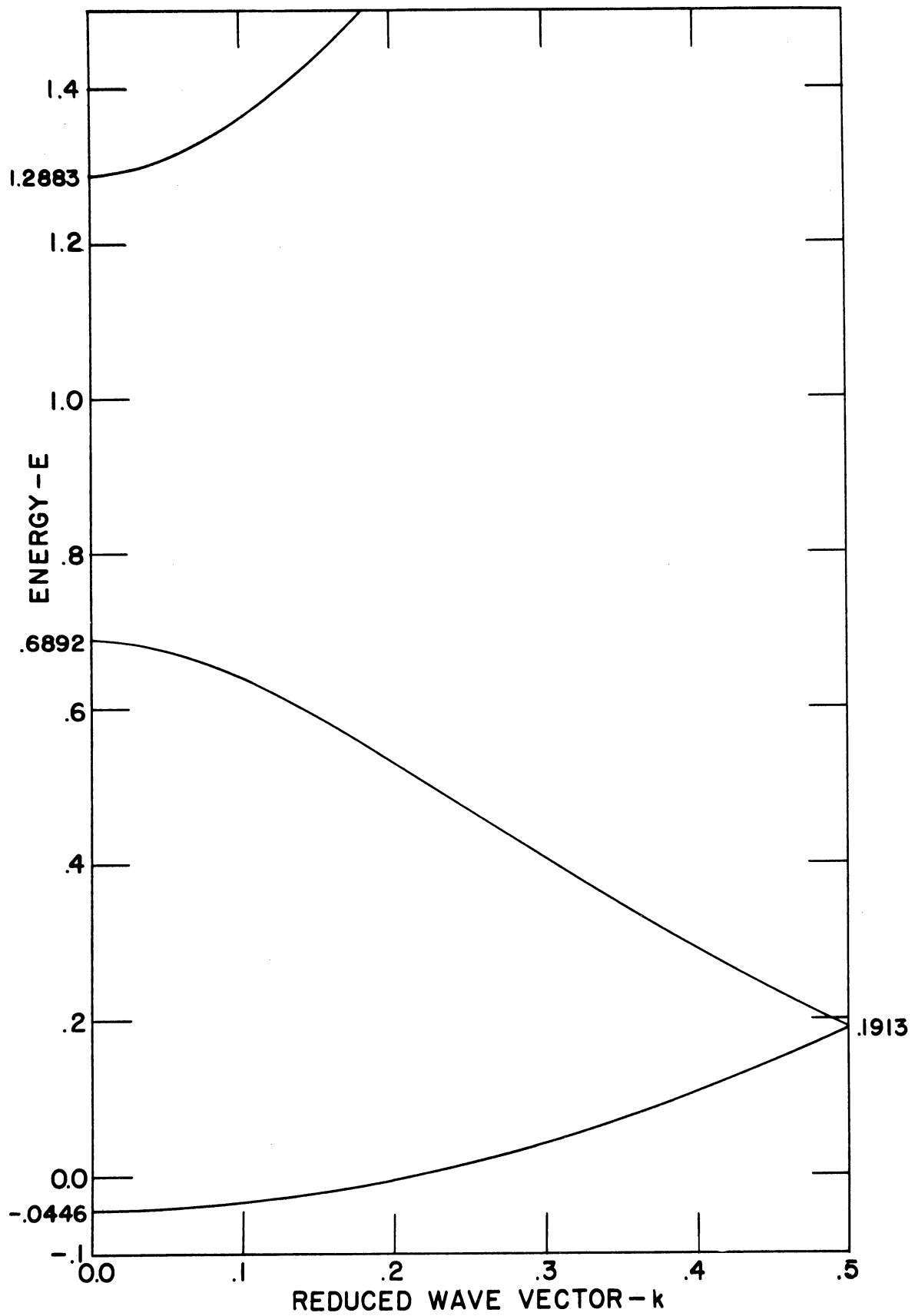


Fig. 4.3. Composite energy curve for unperturbed problem.

## CHAPTER V

### THE (20) JONES ZONE WITH COSINE POTENTIALS

Interesting two-dimensional problems can be obtained from the results of the preceding chapter by combining two one-dimensional problems in the  $x$  and  $y$  directions. The electron energies can be represented either as an energy surface plotted over the  $k_x k_y$  plane or as contour lines of constant energy plotted in the  $k_x k_y$  plane. The Brillouin zone scheme of the square reciprocal lattice is shown in Fig. 5.1.

The electron energies of the unperturbed problem

$$[V(10) = V(01) = V_1 = 0 \text{ and } V(20) = V(02) = V_2 = 0.30] ,$$

plotted in different ways in the extended zone scheme, illustrate the results of Section 3.3 on omitting certain planes forming zone boundaries and also form the basis for deriving the Seitz zone scheme, as discussed in Section 2.3. The unperturbed problem can also be used to infer information about the (20)(21) Jones zone. An analysis of the same zone by the nearly-free-electron approximation shows how shape degeneracies are predicted by this approximation method.

The perturbed problem ( $V_1 = 0.03$  and  $V_2 = 0.30$ ) is of some interest in showing the effect on the energy contours of weak Fourier coefficients of the potential corresponding to zone boundary planes which cut inside a Jones zone. Further insight into this effect is obtained by comparing the density of states for the unperturbed and perturbed problems. This work also forms the starting point for the corresponding three-dimensional problems treated in Chapter VI.

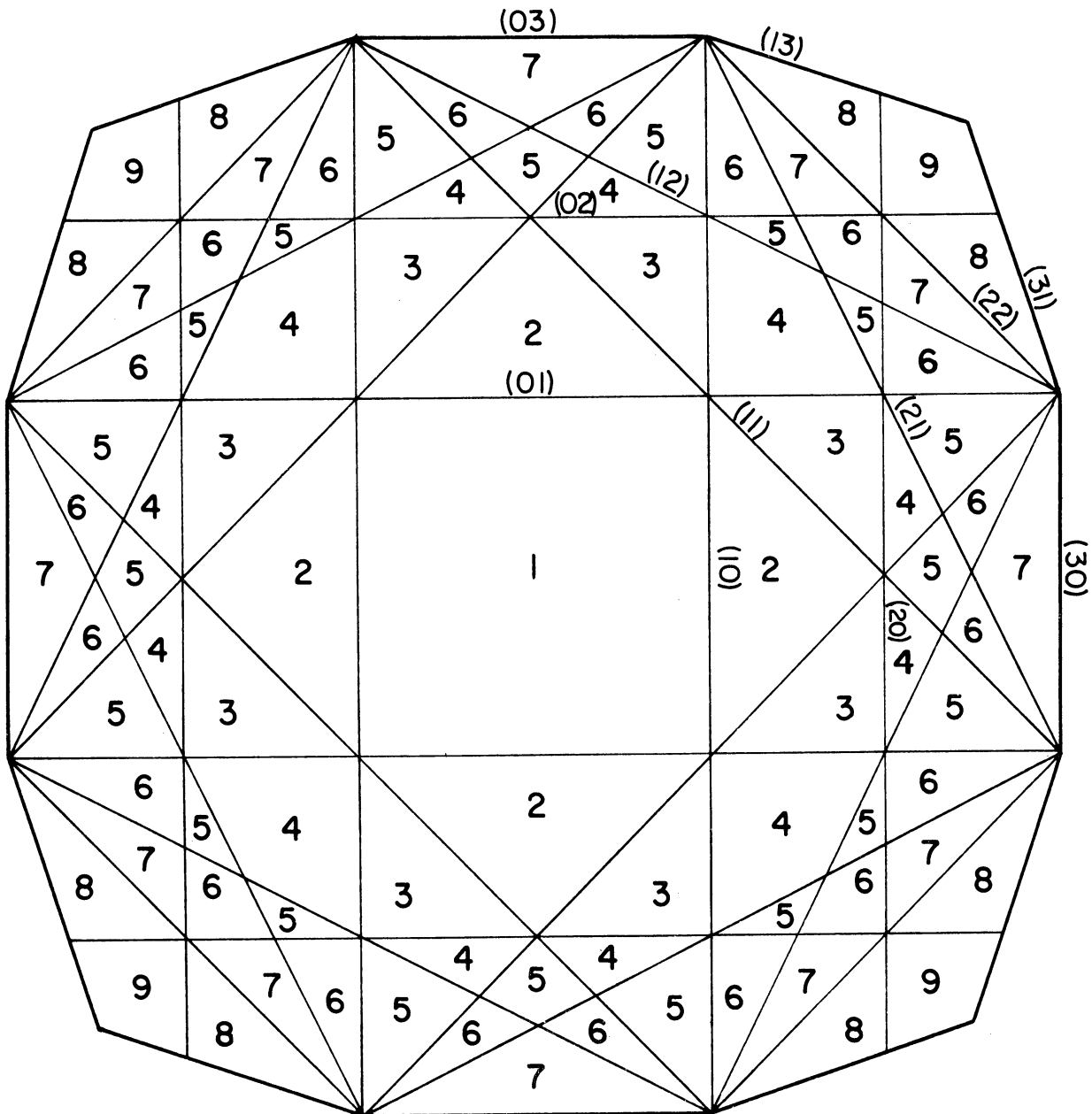


Fig. 5.1. Brillouin zones, square reciprocal lattice.

### 5.1. ENERGY CONTOURS

As shown in Section 3.3, the energy contours for the unperturbed problem can be correctly plotted in the (20) Jones zone without considering the (10), (11), and (21) families of planes. The resulting set of energy contours, which is also the most natural one for this simple problem, is shown in Fig. 5.2. The coefficient  $V_2$  was chosen to give a small amount



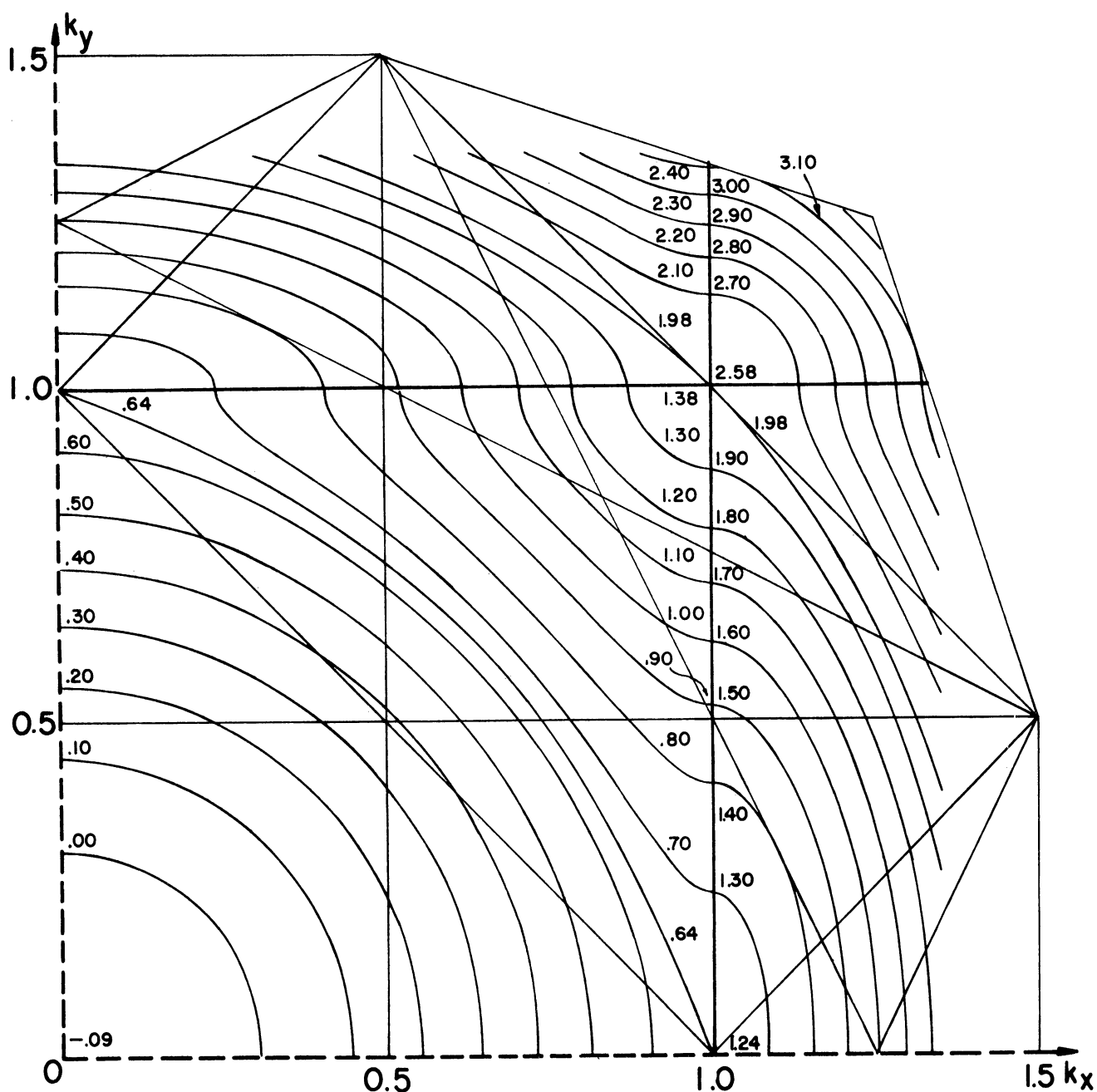


Fig. 5.2. Energy contours for the unperturbed problem.

of directional degeneracy. There is no symmetry or shape degeneracy for the (20) zone, but there is accidental degeneracy along certain lines. This cannot be seen directly from the single quadrant shown in the figure. However, by using symmetry it can be verified that accidental degeneracy exists, for example, between points on part of a vertical oval in zone 6

near the point (11) (see Fig. 5.3) and points on part of a vertical oval in zones 4 and 5 near point  $(\bar{1}0)$ . Corresponding points on these two ovals differ by a reciprocal lattice vector.

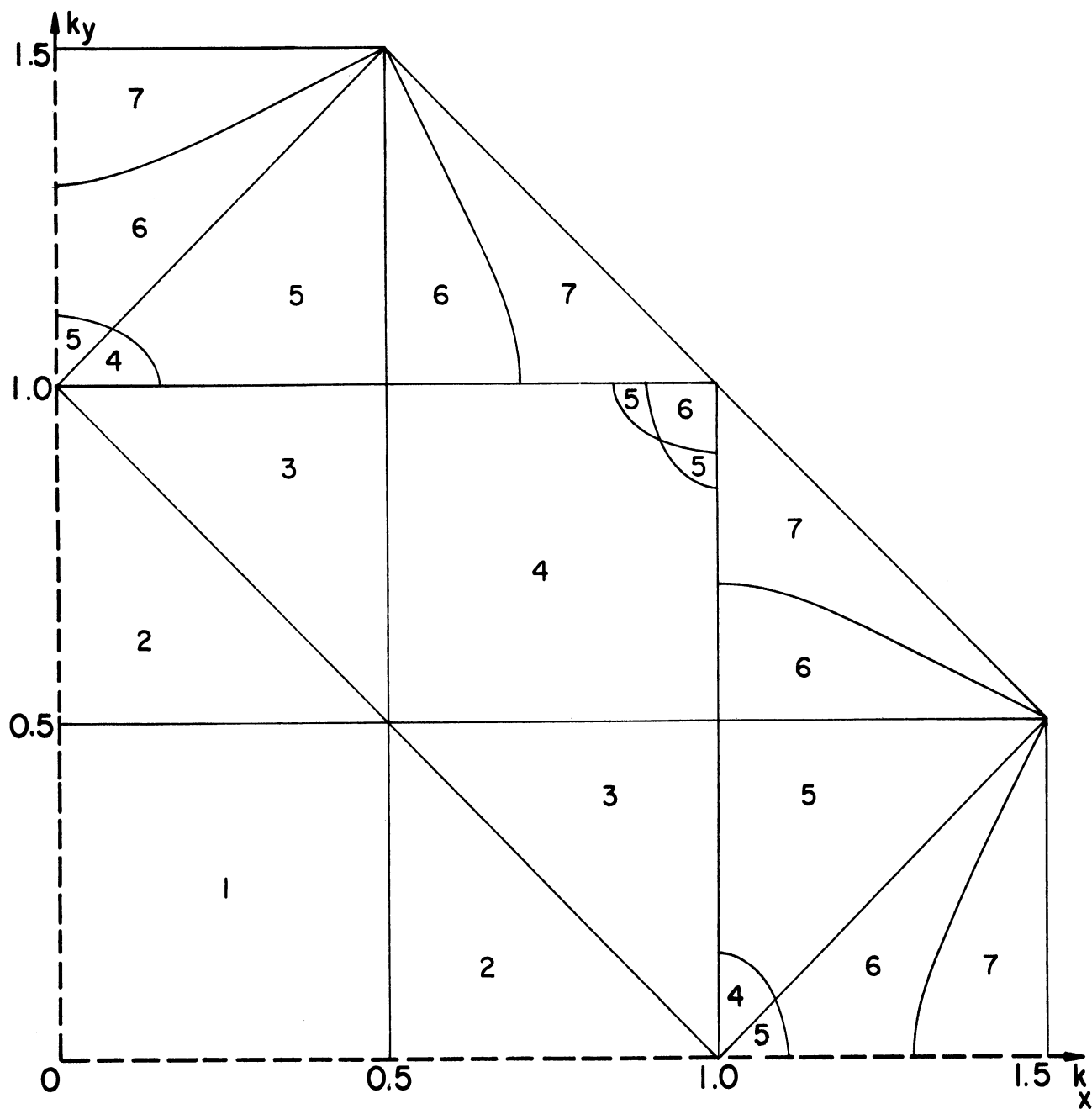


Fig. 5.3. Seitz zones for the unperturbed problem.

As  $V_2$  decreases to zero, the part of the vertical oval near the point (11) becomes larger and straightens out until it coincides with the segment of the (21) zone boundary lying inside the (20) Jones zone. In a similar way it can be verified that the accidental degeneracies existing on the other curved lines in Fig. 5.3 correspond to accidental degeneracies which existed on segments of the (21) family of zone boundaries for the free-electron case. Accidental degeneracies still exist on the (10) and (11) families of zone boundaries, but the degeneracy has been removed on the (20) family of zone boundaries. Thus, in accordance with the discussion of Section 2.3, the Seitz zone scheme of Fig. 5.3 is the appropriate one to use in treating the perturbed problem, because the first-order effect of a small but general perturbation will be to remove the remaining degeneracies which exist on these zone boundaries (except where symmetry degeneracies must exist).

Slater<sup>15</sup> has remarked that the effect of a superlattice is to introduce new Brillouin zone boundary planes with weak Fourier coefficients of the potential. These planes cut inside the previous zones and may cause a splitting of the original energy bands. Katz<sup>16</sup> has pointed out that directional degeneracies will prevent these gaps from occurring unless the new zone boundaries almost coincide with a constant energy surface. It should be noted that the new zone boundaries under consideration are those of the Seitz zone scheme and not in all cases the new Brillouin zone boundary planes.

The energy as plotted in Fig. 5.2 is discontinuous in the reduced zone scheme in the sense that when the different sections of the same Brillouin zone are translated back within the reduced zone, the energy contours in the different sections will not join continuously. In order to get a

set of contours which will join continuously in the reduced zone, the energy contours of Fig. 5.2 must be replotted in a much more complicated way in the extended Brillouin zone scheme. One way this can be done is indicated in the upper-left part of Fig. 5.4. For example, in the upper of

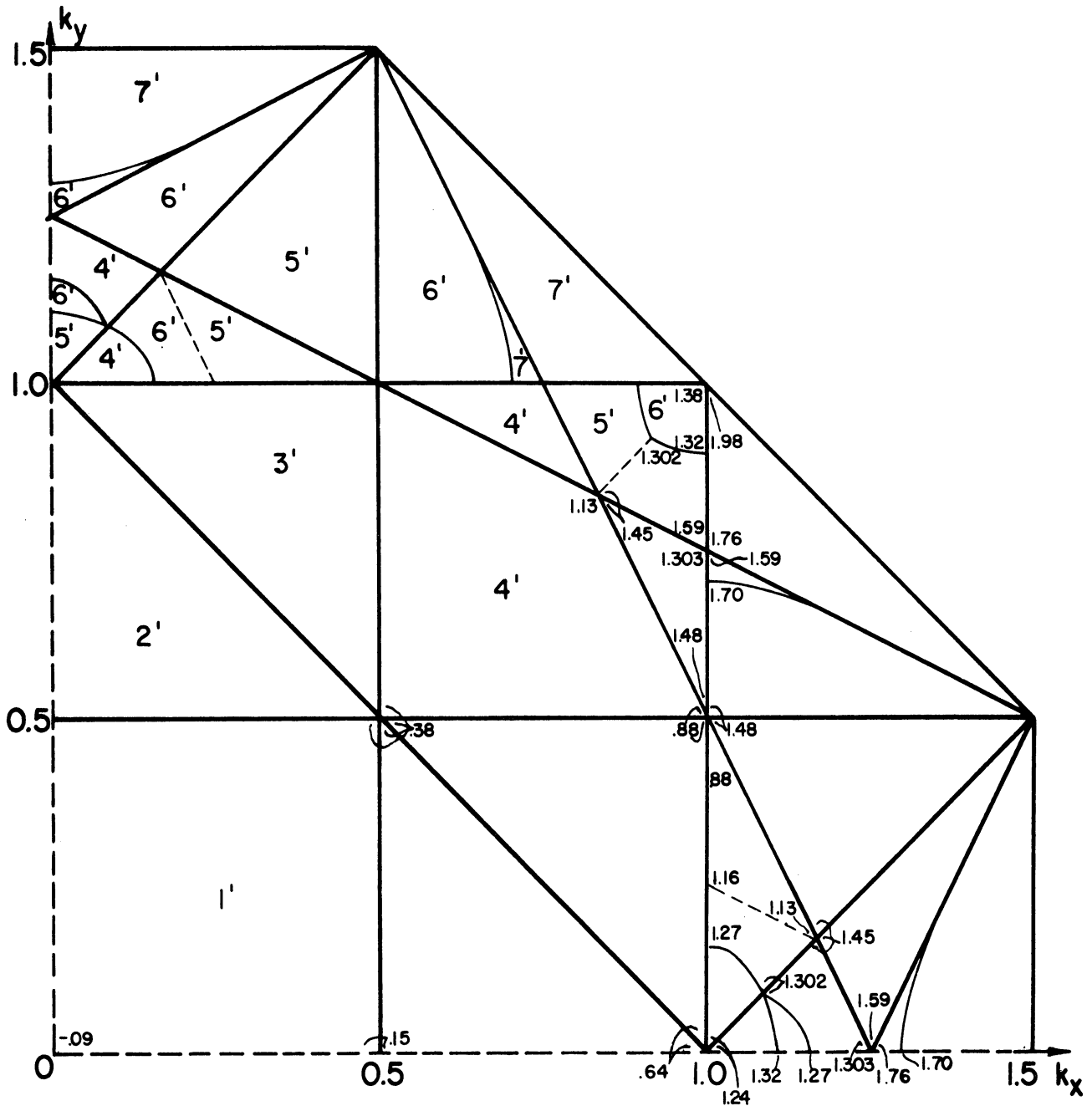


Fig. 5.4. Alternative method of plotting the energy for the unperturbed problem.

the two sections of the fifth zone lying inside the (20) Jones zone, energy contours must be plotted which are plotted in Fig. 5.2 in that part of a section of the fourth zone which is a reciprocal lattice vector distance away. Similarly, in the other sections or parts of sections energy contours must be plotted which in Fig. 5.2 are plotted in the zones indicated by the primed numbers. The resulting energy at important points of the zones is indicated in the lower-right part of Fig. 5.4. The energy contours are now continuous within each section and continuous between neighboring sections of the same Brillouin zone when brought back within the reduced zone, but the pattern of energy contours in the extended zone scheme is much more complicated than that of Fig. 5.2.

If the coefficient  $V_2$  had been chosen somewhat larger, then the energy everywhere inside the (20) Jones zone, plotted as in Fig. 5.2, would have been less than the energy at every point outside the zone. Alternatively, when plotted as in Fig. 5.4, the energy at every point of the first four Brillouin zones would have been less than the energy at every point of the fifth and higher Brillouin zones. The contour pattern of Fig. 5.4 is the one given by the nearly-free-electron approximation when all Brillouin zone boundaries and their corresponding plane waves are used. This can be seen by studying the contours as  $V_2$  is increased from zero. Thus, even for the nearly-free-electron approximation the Jones zone is not necessarily the same as the zone containing the contours of energy less than that of the energy gap.

Another possible difference between the Jones zone and the zone associated with the energy gap is illustrated by introducing a strong perturbation due to the (21) family of Fourier coefficients. If  $V(20)$  is sufficiently greater than  $V(21)$ , the energy everywhere inside the (20)

zone, plotted as in Fig. 5.2, will still be less than the energy everywhere outside the zone. The importance of this is the following. According to the usual procedure for choosing Jones zones, the Jones zone for this perturbed problem is the (20)(21) zone. The volume of this zone is three and two-thirds times that of the reduced zone, so a shape degeneracy must exist for this zone. This problem is a simple example of a case in which an energy gap cannot exist for a Jones zone, but the Fourier coefficients corresponding to the Jones zone boundary planes cause an energy gap to occur at a volume different from the volume of the Jones zone—for this problem the gap occurs at four times the volume of the reduced zone. These examples strongly suggest that in many actual metals, such as  $\gamma$  brass, an energy gap may occur or almost occur such that the electron states with energies below the gap fill a volume close to but not exactly equal to the volume of the Jones zone. This point is discussed further in Appendix C for the Jones zones of several important alloy structures. Up to now no simple Jones zone with a shape degeneracy has been found for which the volume occupied by the states below the energy gap is less than the volume of the Jones zone, but this may be possible in larger and more complicated zones or it may be necessary to use second- or higher-order perturbation theory to analyze the zones.

To return to the numerical problems of Chapter IV, the energy contours within the (20) Jones zone for the two-dimensional perturbed problem ( $V_1 = 0.03$  and  $V_2 = 0.30$ ) are shown in Fig. 5.5. There are no unusual features about the pattern, but it is included here because it will be used in Section 5.3 in connection with a study of the density of states.

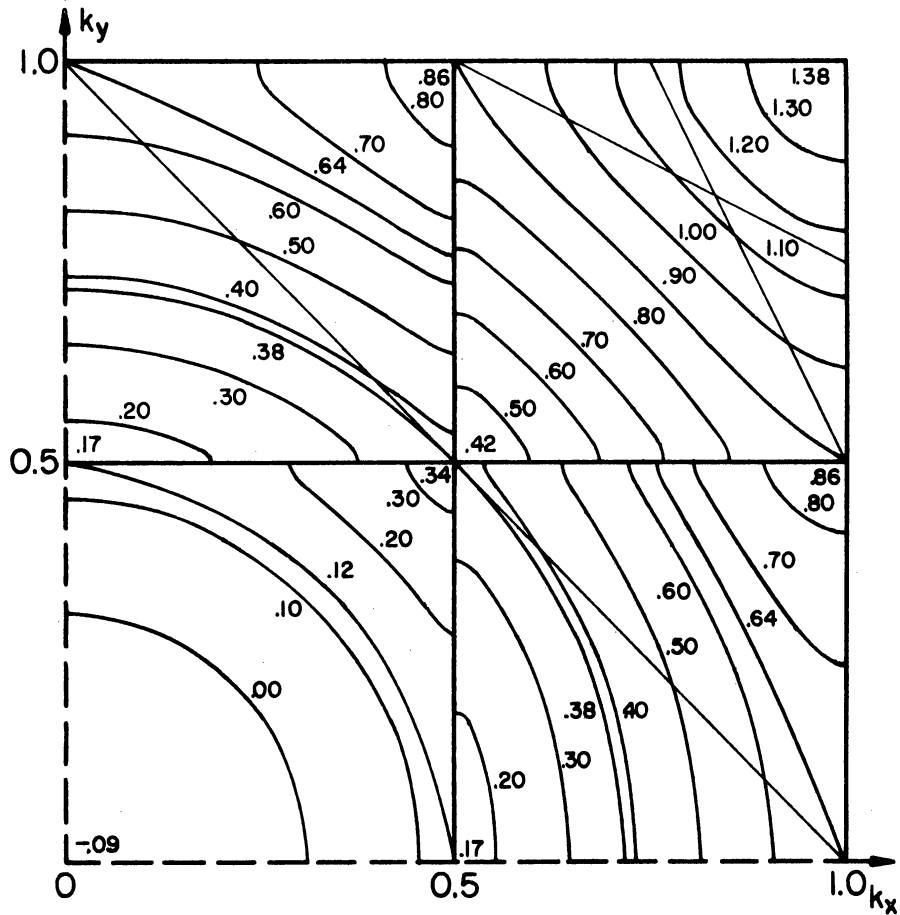


Fig. 5.5. Energy contours for the perturbed problem.

## 5.2. NEARLY-FREE-ELECTRON APPROXIMATION

The central result of the nearly-free-electron approximation is that, except for edge effects, the energy changes across every zone face by an amount equal to twice the corresponding Fourier coefficient of the crystal potential. From this result the erroneous conclusion has been drawn in the past that an energy gap could exist for every Jones zone provided the potential was strong enough. That the nearly-free-electron approximation does not actually predict this conclusion for Jones zones with shape degeneracies can be seen by studying the (20)(21) Jones zone discussed in the preceding section.

The electron energies, correct to first order, at points of inter-

section of two or more zone planes are the following:

Points:  $(\pm 1, 0)$   $(0, \pm 1)$

$$E = 1 + V(20) \pm 2V(11)$$

$$E = 1 - V(20) \quad (\text{double})$$

Points:  $(\pm 1, \pm 1/2)$   $(\pm 1/2, \pm 1)$

$$E = (5/4) + V(20) \pm [V(21) + V(10)]$$

$$E = (5/4) - V(20) \pm [V(21) - V(10)]$$

Points:  $(\pm 5/6, \pm 5/6)$   $(\pm 7/6, \pm 1/6)$   $(\pm 1/6, \pm 7/6)$

$$E = (25/18) + (1/2)[V(11) \pm \sqrt{V(11)^2 + 8V(21)^2}]$$

$$E = (25/18) - V(11)$$

Points:  $(\pm 1, \pm 3/4)$   $(\pm 3/4, \pm 1)$   $(\pm 5/4, 0)$   $(0, \pm 5/4)$

$$E = (25/16) + (1/2) [V(20) \pm \sqrt{V(20)^2 + 8V(21)^2}]$$

$$E = (25/16) - V(20).$$

The energies are equal at points on the (21) plane equidistant from the center  $(1, 1/2)$  of the plane, for example, at points  $(5/6, 5/6)$  and  $(7/6, 1/6)$  and at points  $(3/4, 1)$  and  $(5/4, 0)$ . This is a special case of a general property of the nearly-free-electron approximation. The points on the (21) plane between  $(1, 1/2)$  and  $(5/6, 5/6)$  form part of the boundary of the (20) (21) Jones zone, so that the nearly-free-electron approximation does predict an equality of the energy at points inside and outside the (20) (21) Jones zone. This is the shape degeneracy discussed earlier.

In the (20) (21) Jones zone the plane waves corresponding to the (10) and (11) families of planes cannot be neglected, according to general theory, in applying the nearly-free-electron approximation. As an example of the error caused by such an omission, consider the energies at the point  $(1, 1/2)$ . If the plane wave corresponding to the (01) plane is neglected,



the resulting energies to first order are  $E = 5/4$  and  $E = (5/4) \pm \sqrt{V(20)^2 + V(21)^2}$ , which are incorrect both in the number of energy levels and in the dependence on the large coefficients.

### 5.3. DENSITY OF STATES

There are no essential differences in the complexities of the two-dimensional energy contours and the three-dimensional energy surfaces. On the other hand, as pointed out by van Hove,<sup>17</sup> there are rather striking differences between the density-of-states functions for the two- and three-dimensional problems. For this reason it is not very instructive to analyze the density of states for the energy contours given above. However, these functions will be needed in Chapter VI in order to compute the density of states for certain three-dimensional problems.

The contribution to the total density of states was determined only for those contours of Figs. 5.2 and 5.5 lying inside the (20) Jones zone. The procedure was to plot these and certain additional contours on a scale approximately five times larger, and then to measure the area between successive contours with a planimeter. If

$$A(E) = \text{area inside both the (20) Jones zone and the contour of energy } E, \quad (5.1)$$

then the average density of states for the energy interval from  $E$  to  $E'$  is

$$N_{\text{avg}} = \frac{A(E') - A(E)}{E' - E} \quad (5.2)$$

A smooth curve was then drawn through these average values to get the final dimensionless density of states  $N(E)$ . If primes are again used to denote certain quantities with dimensions, then

$$k = ak' \quad (5.3)$$

and

$$N(E) = \frac{\int d\vec{k}}{dE} = \frac{E_0' V_a' \int d\vec{k}'}{dE'} = E_0' V_a' N'(E'), \quad (5.4)$$

where  $V_a'$  is the volume of the unit cell of the direct lattice and  $\int d\vec{k}$  extends between the energy surface  $E$  and the surface  $E + dE$ . The dimensionless density of states  $N(E)$  is the number of energy levels (two electrons per level) per unit cell per unit (dimensionless) energy range.

This graphical method is not sufficiently accurate to determine the density of states in the immediate vicinity of its singular points, but the nature of the function at these points is determined by the results of van Hove which, for a two-dimensional problem, state that (1) at a minimum (m) in the energy the density of states increases discontinuously, (2) at a saddle point (S) in the energy there is a logarithmic infinity in the density of states, and (3) at a maximum (M) in the energy the density of states decreases discontinuously.

Table 5.1 gives a typical location, the type of each critical point, and the energy for all the critical points inside the (20) Jones zone of the energy as plotted in Figs. 5.2 and 5.5. The density-of-states functions for both the unperturbed and the perturbed problems are shown in Fig. 5.6.

TABLE 5.1

## CRITICAL POINTS OF THE ENERGY

UNPERTURBED PROBLEM			PERTURBED PROBLEM		
Location	Type	Energy	Location	Type	Energy
0 0	m	- .0892	$1/2^+ 1/2^+$	m	.4240
$1^- 0$	S	+ .6446	$1^- 0$	S	.6432
$1^- 1^-$	M	1.3784	$1^- 1/2^-$	M	.8586
			$1^- 1/2^+$	S	.9009
			$1^- 1^-$	M	1.3778

m = Minimum Point

S = Saddle Point

M = Maximum Point

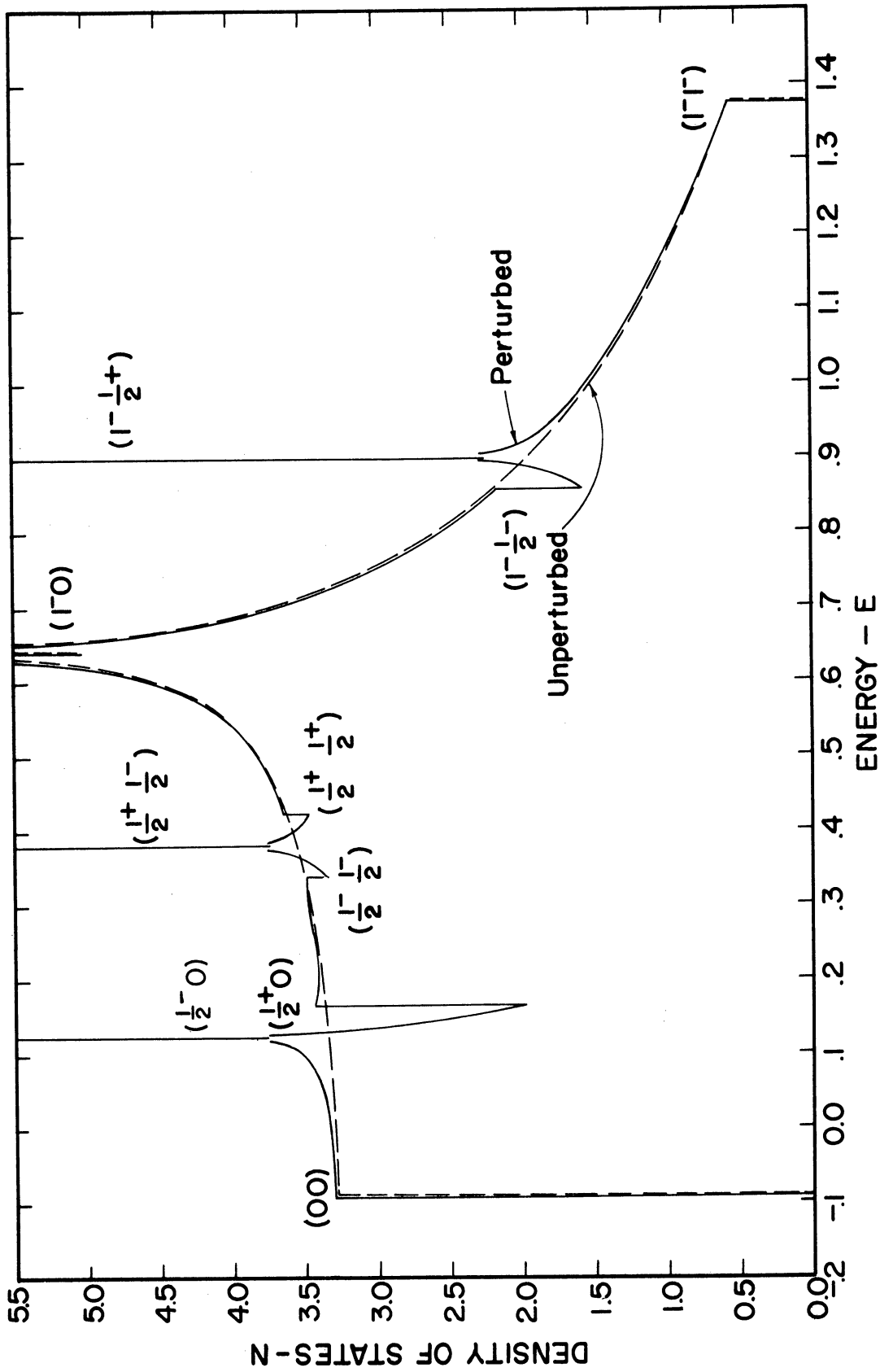


Fig. 5.6. Density of states, two-dimensional problems. The numbers in parentheses are the critical points of Table 5.1.

## CHAPTER VI

### THE (200) JONES ZONE WITH COSINE POTENTIALS

Three-dimensional problems are easily constructed by combining one-dimensional problems in the  $z$  direction with the two-dimensional problems of the preceding chapter. The main interest in these three-dimensional problems lies in the density-of-states functions and the effect on these functions of weak Fourier coefficients of the potential corresponding to zone planes which cut inside the Jones zone.

The separability of the problems made it practical to compute more accurate density-of-states functions than those usually given in the literature. The structure of the functions given here is of pedagogic value in illustrating the types of peaks and valleys which are likely to occur in density-of-states curves. The density of states for the unperturbed problem gives, by comparison, an indication of the accuracy of an approximate method of calculating the density of states due to Jones and is also the basis for deriving other functions of more direct interest, such as the total energy of all the electrons. These derived functions are discussed in the following chapter.

#### 6.1. ENERGY SURFACES

The energy surfaces for the three-dimensional problems are described by the equation

$$E_2(k_x, k_y) + E_1(k_z) = E, \quad (6.1)$$

in which  $E_1(k_z)$  is a one-dimensional energy function of Chapter IV and  $E_2(k_x, k_y) = \text{constant}$  describes the two-dimensional energy contours of

Chapter V. The intersection of every plane parallel to the  $k_x k_y$  plane with the energy surfaces gives a set of energy contours of the same shape as those of Chapter V.

Figure 6.1 gives the critical energies of the unperturbed problem within the (200) Jones zone and also shows the shape of that energy

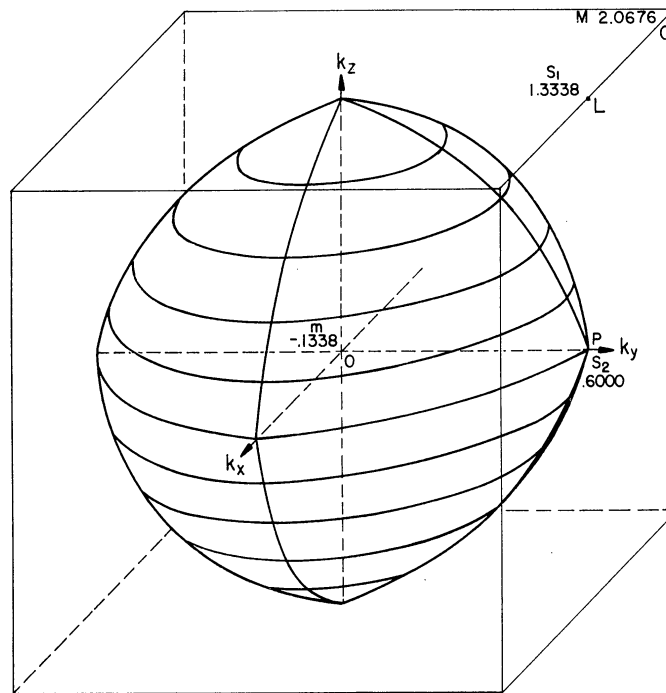


Fig. 6.1. Critical energies and a critical energy surface for the unperturbed problem. See Section 6.2 for definitions of minimum (m), saddle ( $S_1 S_2$ ), and maximum (M) critical points.

surface which just touches the zone faces. Although this surface is approximately spherical over much of its area, the conical points cause its volume to be significantly less than the volume of the sphere enclosed by the (200) zone. Numerical values are given in the next chapter. The lowest energy outside the (200) zone is 1.1991 at point P. The considerable amount of directional degeneracy which exists for this problem is due to the large deviation of the shape of the cube from the shape of the enclosed energy surfaces.

The critical energies of the perturbed problem are shown in Fig. 6.2 at typical locations of the critical points of the energy surfaces. The nature of these critical points and their effect on the density of states is discussed in the next section.

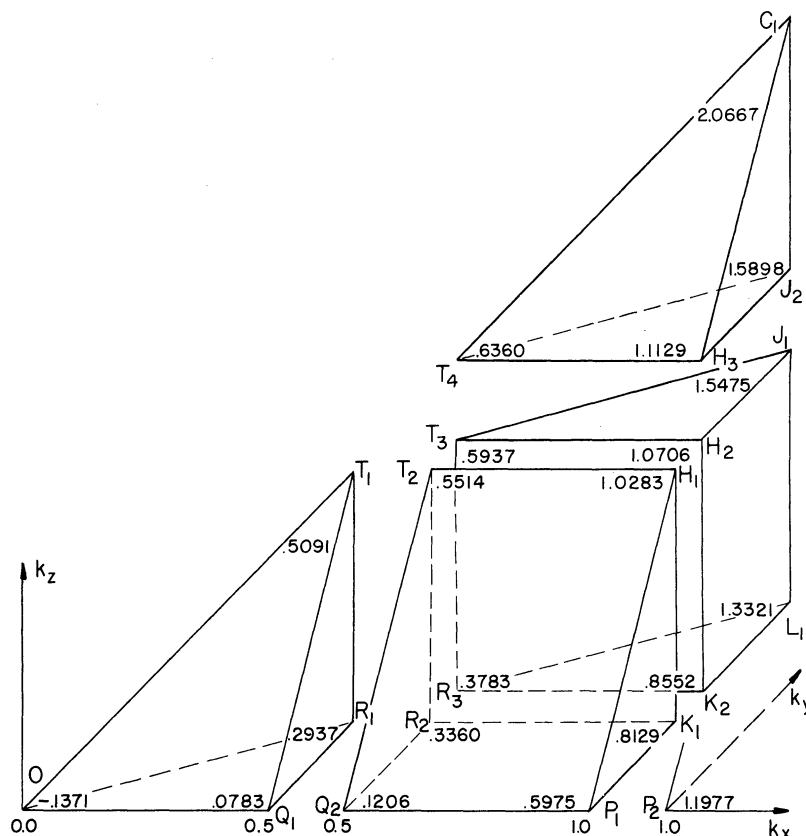


Fig. 6.2. Critical energies for the perturbed problem.

## 6.2. DENSITY OF STATES

The density of states was determined in the following way for the energy surfaces indicated in Figs. 6.1 and 6.2. The average density of states for the energy interval from  $E$  to  $E'$  is

$$N_{\text{avg}} = \frac{V(E') - V(E)}{E' - E} \quad (6.2)$$

In this formula

$$V(E) = \text{volume inside both the (200) Jones zone and the surface of energy } E \quad (6.3)$$

$$= \int_{k_z, \min}^{k_z, \max} A(k_z; E) dk_z, \quad (6.4)$$

where

$$A(k_z; E) = A(E_2) \quad \text{and} \quad E_2 = E - E_1(k_z) \quad . \quad (6.5)$$

The integral (6.4) was evaluated graphically by plotting  $A(k_z; E)$  as a function of  $k_z$  for different values of  $E$  and measuring the area between successive curves with a planimeter.

The nature of the density of states near the critical energies is given by the results of van Hove.<sup>17</sup> For the problems considered here the energy surface in the immediate vicinity of one of its critical points, taken as origin, is of the form

$$E = E_c \pm C_x k_x^2 \pm C_y k_y^2 \pm C_z k_z^2, \quad (6.6)$$

in which  $C_x$ ,  $C_y$ , and  $C_z$  are positive constants. Near each critical energy the density of states has the form indicated in Table 6.1, in which the  $B$ 's are positive constants and the functions  $O(E - E_c)$  are of order  $E - E_c$  for  $E \rightarrow E_c$ .

TABLE 6.1

FORM OF THE DENSITY OF STATES NEAR THE CRITICAL ENERGIES

Type of Critical Energy	Number of Plus Signs, Eq. 6.6	Energy Range	Form of Density of States
Minimum ( $m$ )	Three	$E \leq E_c$	$N_c + O(E - E_c)$
		$E \geq E_c$	$N_c + B\sqrt{E - E_c} + O(E - E_c)$
Saddle ( $S_2$ )	Two	$E \leq E_c$	$N_c - B\sqrt{E_c - E} + O(E - E_c)$
		$E \geq E_c$	$N_c + O(E - E_c)$
Saddle ( $S_1$ )	One	$E \leq E_c$	$N_c + O(E - E_c)$
		$E \geq E_c$	$N_c - B\sqrt{E - E_c} + O(E - E_c)$
Maximum ( $M$ )	None	$E \leq E_c$	$N_c + B\sqrt{E_c - E} + O(E - E_c)$
		$E \geq E_c$	$N_c + O(E - E_c)$



The density of states for the unperturbed problem is shown in Fig. 6.3. The density of states due to the parts of the energy surfaces of free electrons lying inside the (200) zone, computed from formulas of Stoner,<sup>18</sup> is

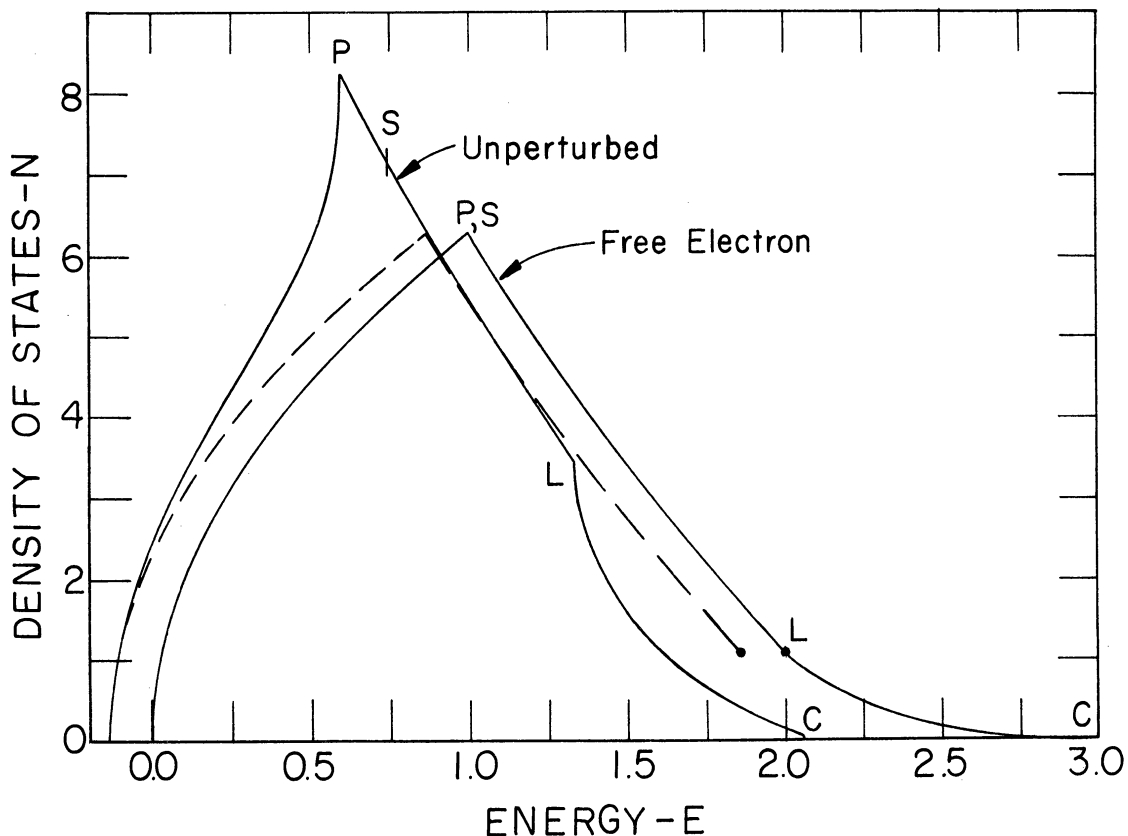


Fig. 6.3. Density of states for the unperturbed problem and for free electrons in the (200) zone.

also shown. The dashed curve is this density of states for free electrons translated so as to coincide with that for the unperturbed problem at the bottom of the band. That the part of the curve from P to L for the unperturbed problem is to a close approximation an extension of the corresponding part of the translated curve for free electrons follows from a result due to Jones given in the next section. Because of this property a good sketch of the density of states can be made if one knows the type and value of the critical energies occurring in the zone and the density of states for the zone for free electrons. This procedure becomes less accurate the farther

the energy surfaces deviate from spheres.

Figure 6.4 shows the structure of the density of states for the perturbed problem. There are several points of interest concerning the fine structure of this curve. The first is the obvious fact that the difference between the density of states for the perturbed and unperturbed problems is too small to cause an observable effect. This should be a typical result for weak coefficients corresponding to interior zone planes, unless either the Seitz zone boundary corresponding to the perturbing plane almost coincides with a constant energy surface or else the ratio of weak to strong coefficients is appreciably greater than the one-tenth used here. The second point is that the coefficients B in Table 6.1 are proportional to  $1/\sqrt{C_x C_y C_z}$  and hence to the square root of the product of the three principal effective masses of the electron with wave vector at the critical point of the energy surface. Thus, a large change in the density of states will occur only at those critical energies for which the product of the principal effective masses at the critical points is large. The coefficient B is also proportional to the number of times ( $w$ ) the corresponding critical point occurs in the zone, proper allowance being made for the amount of solid angle in the zone at each critical point. These results are easily verified for the perturbed problem, because the principal effective masses are the (dimensionless) effective masses of the one-dimensional problem—roughly 1 at  $k = 0$ , 0.05 at  $k = 1/2$ , and 0.15 at  $k = 1$ . Table 6.2 gives a typical location and the type of each critical energy of the perturbed problem and also the factor  $w/\sqrt{C_x C_y C_z}$ . There is an obvious correlation between this factor and the size of the corresponding singularity in the density of states in Fig. 6.4. More precisely, the radius of curvature at the singularity on the side of the vertical tangent is proportional to  $w^2/C_x C_y C_z$ .

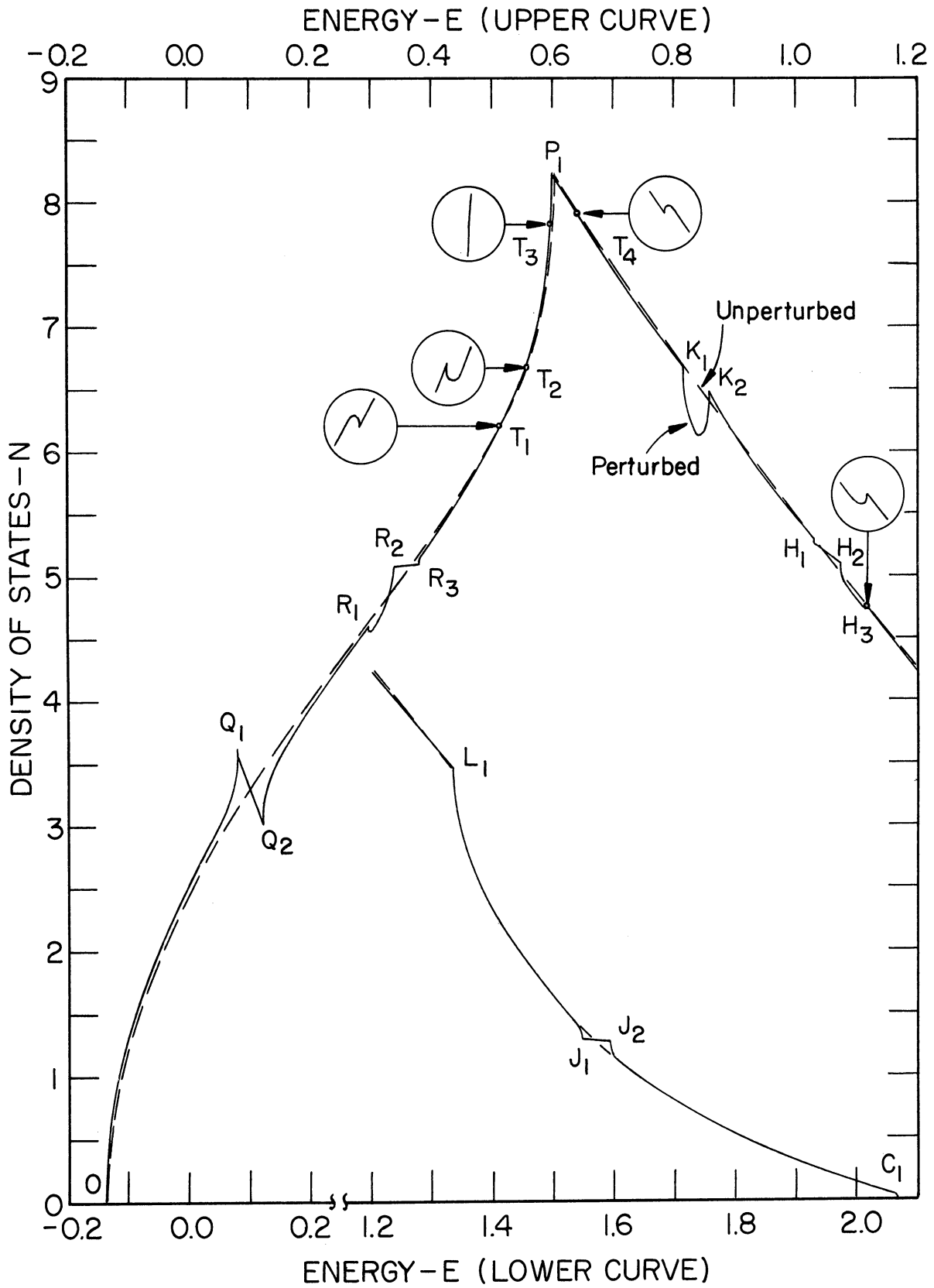


Fig. 6.4. Density of states for the perturbed problem.

The third point of interest is the occurrence of a critical energy of type  $S_1$  followed by a critical energy of type  $S_2$ . This produces a U-shaped dip in the density of states, as at  $K_1K_2$ , which could be quite deep under certain conditions. Such a dip would strongly influence properties which depend on the electrons with energies at the dip but, if narrow, would have little effect on properties which depend on the total energy of all the electrons.

TABLE 6.2

EFFECTIVE MASSES AT CRITICAL POINTS OF  
THE ENERGY, PERTURBED PROBLEM

$w$  = Number of Times Critical Point Occurs  
 $1/C_x C_y C_z$  = Product of the Three Effective Masses

Critical Point	Typical Location	Type	$\frac{w}{\sqrt{C_x C_y C_z}}$	Critical Point	Typical Location	Type	$\frac{w}{\sqrt{C_x C_y C_z}}$
0	0 0 0	m	1.075	$K_1$	$1^- 1/2^- 0$	$S_1$	0.584
				$K_2$	$1^- 1/2^+ 0$	$S_2$	.560
$Q_1$	$1/2^- 0 0$	$S_2$	.714	$H_1$	$1^- 1/2^- 1/2^-$	M	.065
$Q_2$	$1/2^+ 0 0$	m	.684	$H_2$	$1^- 1/2^+ 1/2^-$	$S_1$	.124
$R_1$	$1/2^- 1/2^- 0$	$S_1$	.158	$H_3$	$1^- 1/2^+ 1/2^+$	$S_2$	.059
$R_2$	$1/2^+ 1/2^- 0$	$S_2$	.303	$L_1$	$1^- 1^- 0$	$S_1$	.540
$R_3$	$1/2^+ 1/2^+ 0$	m	.145	$J_1$	$1^- 1^- 1/2^-$	M	.119
$T_1$	$1/2^- 1/2^- 1/2^-$	M	.012	$J_2$	$1^- 1^- 1/2^+$	$S_1$	.114
$T_2$	$1/2^+ 1/2^- 1/2^-$	$S_1$	.034	$C_1$	$1^- 1^- 1^-$	M	.074
$T_3$	$1/2^+ 1/2^+ 1/2^-$	$S_2$	.032				
$T_4$	$1/2^+ 1/2^+ 1/2^+$	m	.010				
$P_1$	$1^- 0 0$	$S_2$	1.319				
$P_2$	$1^+ 0 0$	m	1.135				

## 6.3. JONES'S APPROXIMATION TO THE DENSITY OF STATES

In a calculation of the  $\alpha\beta$  phase boundaries of brass, Jones<sup>4</sup> made an approximate analytical calculation of the density of states. Some indication of the accuracy of this approximate method is provided by applying this method to the unperturbed problem and comparing the results with the

correct results given in the preceding section.

The first step in Jones's method is to use the nearly-free-electron approximation to represent the energy surfaces near the center of a zone boundary plane. These approximate surfaces have cylindrical symmetry about the normal to the plane. The density of states is given by the surface integral over a constant energy surface of  $1/\sqrt{\text{grad } E}$ . To evaluate this integral the zone is divided into pyramids with vertices at the center and the zone boundaries as bases. The pyramids are approximated by right circular cones of the same solid angle. If the zone boundary consists of  $f$  similar faces, the original surface integral is approximated by  $f$  times the surface integral over that part of the surface within a cone. Because of the cylindrical symmetry, this integral can be evaluated explicitly. Jones's results in dimensionless variables for a zone bounded by  $f$  planes of the family  $\vec{B}_n$  are

$$N(E) = f\pi(k_M - k_m), \quad (6.7a)$$

in which

$$E = k_c^2 + \frac{4(f-1)}{(f-2)^2} k_m^2 + (k_c - k_m)^2 - \sqrt{4k_c^2(k_c - k_m)^2 + |V(\vec{B}_n)|^2}, \quad (6.7b)$$

$$k_c = |\vec{B}_n|/2, \quad E_c = k_c^2 - |V(\vec{B}_n)|, \quad (6.7c)$$

$$E = k_c^2 + (k_c - k_M)^2 - \sqrt{4k_c^2(k_c - k_M)^2 + |V(\vec{B}_n)|^2} \text{ for } E \leq E_c, \quad (6.7d)$$

and

$$k_M = k_c \text{ for } E \geq E_c. \quad (6.7e)$$

For the unperturbed problem these equations yield the curve denoted "Jones Approximation" in Fig. 6.5. This is to be smoothly connected with the curve for free electrons near the bottom of the band. More accu-

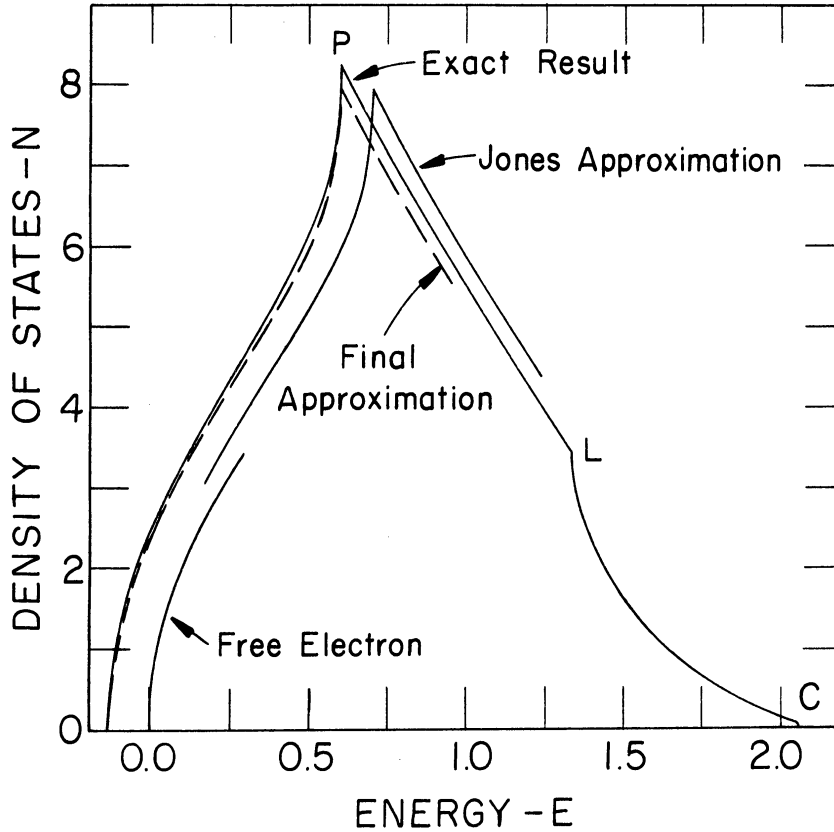


Fig. 6.5. Density of states by Jones's approximation for the unperturbed problem.

rate results are obtained by translating these curves so that they pass through the critical energies at the origin and at the center of the zone face, as calculated, say, by second-order perturbation theory. This procedure gives the dashed curve in Fig. 6.5, which lies about three percent below the exact solution. For spherical energy surfaces the procedure of integrating over cones instead of pyramids introduces no error. Since the energy surfaces of the unperturbed problem are very nearly spherical in the boundary region between the cone and the pyramid, the approximation of pyramids by cones should cause very little error for this problem. Thus, even though the energy discontinuity is large for this problem, the use of the nearly-free-electron approximation causes only a three-percent error in the density of states.

The equations (6.7) have the approximate explicit solution

$$N(E) = 2\pi\sqrt{E} - f\pi(\sqrt{E} - k_c) - \frac{f(f-2)\pi}{8} \frac{|V(\vec{B}_n)|^2}{fk_c^2\sqrt{E} - (f-2)k_cE} \quad \text{for } E \geq E_c. \quad (6.8)$$

The first term is the total density of states for free electrons. The first and second terms give the density of states of free electrons due to the parts of the energy surfaces within the  $(\vec{B}_n)$  zone. The third term shows that for this approximate solution the density-of-states curve between the peak P and the point L differs from the extension of the corresponding part of the curve for free electrons only by terms of second and higher order in  $V(\vec{B}_n)$ . This is the theoretical justification for the approximate method of sketching the density of states given in the preceding section.

## CHAPTER VII

### TOTAL ELECTRON ENERGY AND THE HUME-ROTHERY RULES

The Hume-Rothery rules state that each type of intermediate phase of certain alloys occurs near a definite ratio of the number of electrons to the number of atoms or, better, at a definite number of electrons per unit cell. The usual interpretation of these rules is based on the approximation that at zero degrees absolute the change in the free energy of the phases with composition is due only to the change in the total energy of the electrons with composition. Zone theory is used to predict for a given phase the number of electrons with energies less than that at which the main peak in the density of states occurs. The assumption has been made in the past that if the number of electrons is increased beyond this value, then the total energy of the electrons will increase rapidly and a transition to another phase with lower energy will be probable.

In this chapter the total energy of the electrons is investigated. First, certain simple but general continuity properties are established which show what changes in the density of states are necessary to cause a sharp increase in the total energy of the electrons. Next, accurate total energy functions are derived for the three-dimensional problems of the preceding chapter. A study of these results leads to a better qualitative understanding of the nature and difficulties of the phase boundary problem.

For simplicity the study will be made for a substance at zero degrees absolute. In theoretical work quantities such as the density of states and total energy will be taken per unit volume of crystal but in



the numerical examples such quantities will be referred to a volume  $V_a$ , the volume of the unit cell of the perturbed problem.

### 7.1. CONTINUITY PROPERTIES OF THE TOTAL ENERGY OF THE ELECTRONS

Insight into the possible occurrence of an abrupt change in slope of the total electron energy function is obtained from a study of the continuity properties of this and related functions. Let  $C^{(i)}$  denote the class of functions with a piece-wise continuous  $i + 1^{\text{st}}$  derivative (the discontinuity in the  $i + 1^{\text{st}}$  derivative may be infinite).

Consider first the energy range from the lowest energy  $E_m$  of a band up to the first energy gap, if there is one, otherwise to infinity. In this interval the density of states  $N(E)$  in three dimensions is greater than zero and of class  $C^{(0)}$ . It is assumed that only the types of critical points of Table 6.1 occur in the energy surfaces. It is further assumed that at least one singularity in the density of states occurs in the energy interval, otherwise all functions and their derivatives are continuous. If  $N(E)$  is the number of levels per unit energy range per unit volume, then the number of electrons  $n(E)$  per unit volume with energies less than  $E$  is

$$n(E) = 2 \int_{E_m}^E N(E') dE' , \quad \text{of class } C^{(1)} ; \quad (7.1)$$

thus

$$N(E) = \frac{1}{2} \frac{dn}{dE} . \quad (7.2)$$

In this energy interval the inverse function

$$E = E(n) \quad \text{is of class } C^{(1)} . \quad (7.3)$$

The total energy  $U(E)$  per unit volume of the electrons with energies less than  $E$ , considered as a function of  $E$ , is

$$U(E) = 2 \int_{E_m}^E (E' - E_m) N(E') dE' , \quad \text{of class } C^{(1)} . \quad (7.4)$$

The derivative of  $U$  with respect to  $n$  is

$$\frac{dU}{dn} = \frac{dU}{dE} \frac{dE}{dn} = E(n) - E_m , \quad \text{of class } C^{(1)} . \quad (7.5)$$

The total energy of the electrons, considered as a function of the number of electrons, is

$$U(n) = \int_0^n [E(n') - E_m] dn' , \quad \text{of class } C^{(2)} . \quad (7.6)$$

At an energy gap the continuity properties are different. The number of electrons  $n(E)$  is constant across the gap. Hence, the inverse function  $E(n)$  has a finite discontinuity, and the total energy of the electrons  $U(n)$  is continuous but has a finite discontinuity in its first derivative at the energy gap. According to relation (7.5), the change in the slope of the total energy function  $U(n)$  is the width of the energy gap.

These continuity properties indicate that a sharp change in the slope of the total energy function  $U(n)$  will occur only where there is an appreciable energy gap or where the density of states is very small over an appreciable range of energies. The  $U(n)$  curve is "straightest" for values of  $n$  near that corresponding to the highest peak in the density of states. These conclusions are illustrated by the numerical examples of the following section.

## 7.2. TOTAL ELECTRON ENERGY FOR THE (200) JONES ZONE

The total number  $n(E)$  and total energy  $U(E)$  per unit cell of the electrons for the perturbed and unperturbed problems of the preceding chapter

are shown in Fig. 7.1. The difference between the true curves for the two problems is less than the accuracy of the graph. These functions have discontinuous second derivatives at P and L (see Fig. 6.1 for the location of these points), but this is not detectable in the figure. The number of

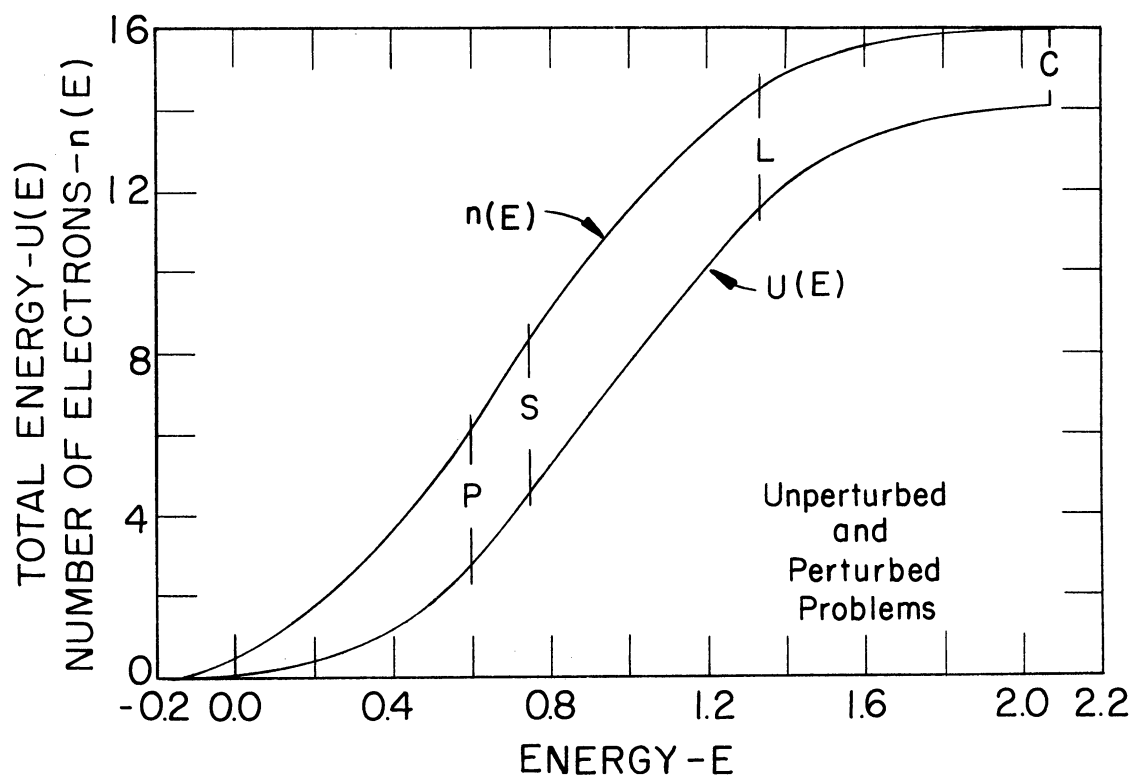


Fig. 7.1. Total electron energy and number of electrons per unit cell as a function of energy.

electrons per unit cell contained within the enclosed sphere of the (200) zone is  $2(4\pi/3) = 8.378$ . For the unperturbed problem this number of electrons is contained within the surface of energy  $E = 0.748$ , as indicated by the point S in the figures. The number of electrons contained within the surface which just touches the zone boundary planes at point P in Fig. 6.1 is 6.110. It is to be noted that, although the critical energy surface is approximately spherical over most of its area, its volume is only about three-fourths that of the enclosed sphere.

Figure 7.2 gives the total energy  $U(n)$  per unit cell of the electrons as a function of the number of electrons per unit cell. The upper curve is for those free electrons with wave vector within the (200) zone, and the lower curve within the accuracy of the figure is for both the unperturbed and perturbed problems. In agreement with the results of the preceding section there is no point on the curves at which one might predict a physical change would occur.

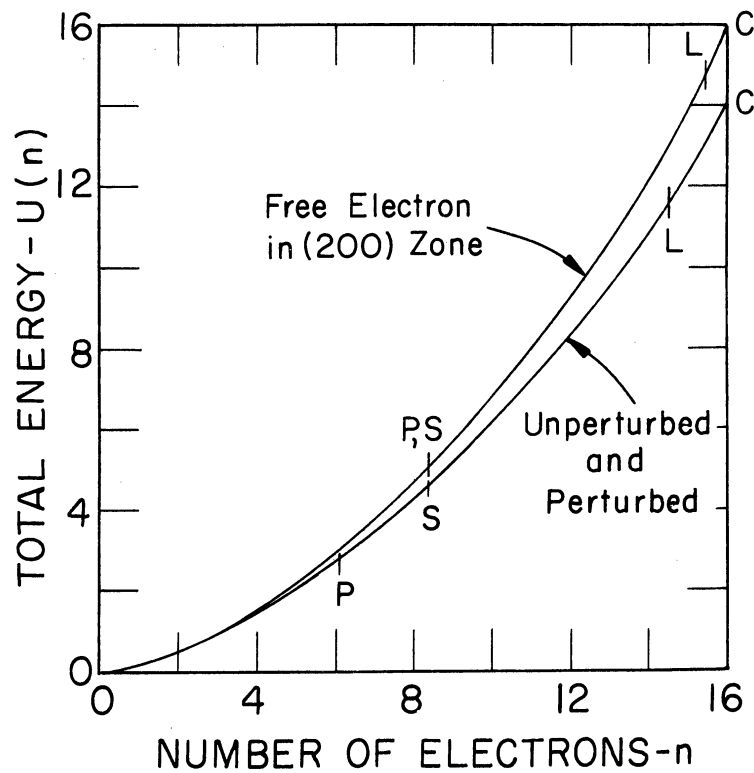


Fig. 7.2. Total electron energy per unit cell as a function of the number of electrons per unit cell.

Further insight into the total energy  $U(n)$  for the unperturbed problem is obtained by comparing it with the total energy  $U_F(n)$  of free electrons in all zones with the same effective mass as the electrons of the unperturbed problem at the center of the zone. The difference  $U(n) - U_F(n)$  is shown in Fig. 7.3. This shows that, instead of increasing at point P,

the total energy of the electrons for the unperturbed problem continues to decrease, relative to the energy of free electrons, almost to the point L.

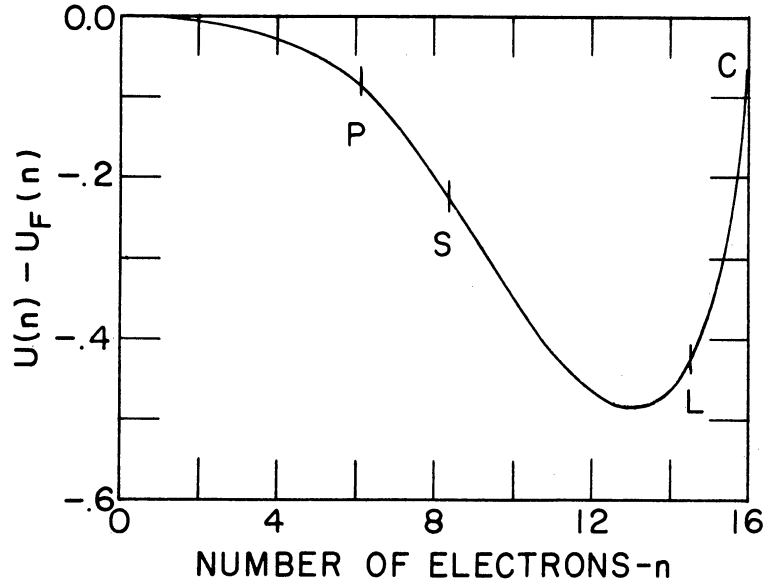


Fig. 7.3. Difference between the total energy  $U$  for the unperturbed problem and the energy  $U_F$  of free electrons with the same effective mass at the center of the zone.

This is a general result for any phase whose density of states  $N_1(E)$  lies above the density of states  $N_2(E)$  of a second phase, as is typical in alloys, because  $U_1(n) - U_2(n)$  is negative in the region, beginning at  $E_m$ , where  $N_1 \geq N_2$  and

$$\left(\frac{d}{dn}\right) (U_1 - U_2) = E_1(n) - E_2(n) \quad (7.7)$$

is also negative. The total energy of the first phase continues to decrease, relative to that of the second phase, until the zones are filled to that energy at which the number of electrons in both phases are equal. Both phase boundaries can only occur beyond this number of electrons.

### 7.3. REMARKS ON THE INTERPRETATION OF THE HUME-ROTHERY RULES

In the approximation that at absolute zero temperature the free energy per unit volume, except for a constant, is just the total energy of the conduction electrons  $U(n)$ , the standard conditions for the equilibrium

of two phases become

$$\left. \frac{dU_1}{dn} \right]_{n_1} = \left. \frac{dU_2}{dn} \right]_{n_2} \quad (7.8a)$$

and

$$U_1(n_1) - n_1 \left. \frac{dU_1}{dn} \right]_{n_1} = U_2(n_2) - n_2 \left. \frac{dU_2}{dn} \right]_{n_2} . \quad (7.8b)$$

The total energy of the electrons for the two phases will be measured relative to the lowest energy  $E_m$  occurring in either of the conduction bands. With this convention and relation (7.5) the equilibrium conditions can be written as

$$E_1(n_1) = E_2(n_2) \quad (7.9a)$$

and

$$U_1(n_1) - n_1[E_1(n_1) - E_m] = U_2(n_2) - n_2[E_2(n_2) - E_m] . \quad (7.9b)$$

Graphically, these conditions are equivalent to the familiar "double tangent" rule on a free energy versus composition diagram. A second graphical interpretation, which is easier to relate to the density-of-states curve, is obtained by combining equations (7.9) [integrate (7.6) by parts] to get

$$\int_{E_m}^E [n_1(E') - n_2(E')] dE' = 0 . \quad (7.10)$$

This has the graphical interpretation that at equilibrium the zones of the two phases are filled to that energy  $E^*$  at which the areas under the  $n(E)$  curves for the two phases are equal. The electron concentrations at the phase boundaries are  $n_1(E^*)$  and  $n_2(E^*)$ . This interpretation is illustrated in Figs. 7.4a and 7.4b for two arbitrary but typical phase boundary problems. Because  $n(E)$  is, except for a factor of 2, the integral of  $N(E)$ , the two  $n(E)$  curves cross at that energy at which the areas under the corresponding density-of-states curves are equal. This is indicated in each of

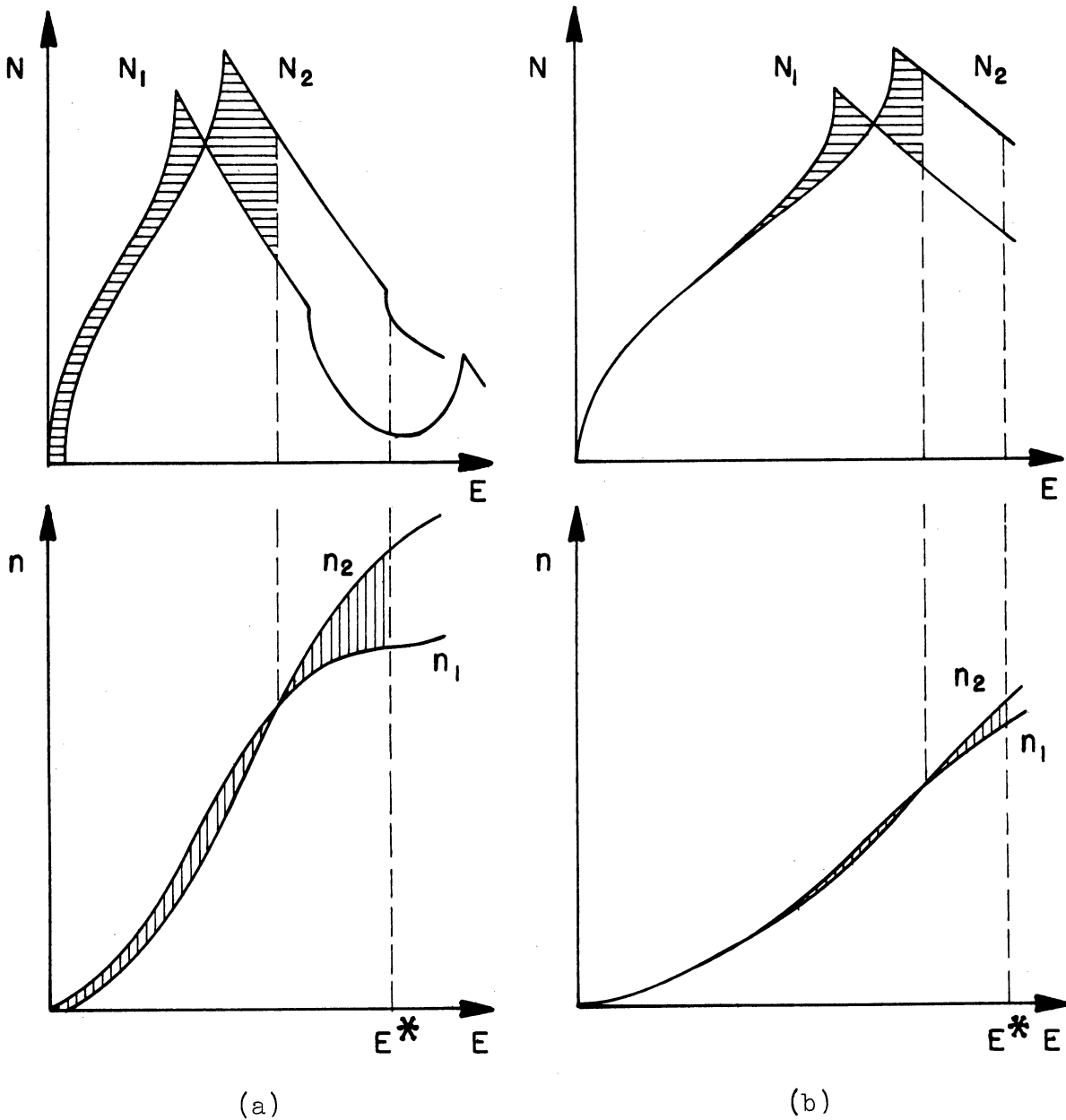


Fig. 7.4 a,b. Typical graphical determinations of the phase boundaries according to equilibrium condition (7.10).

the  $N(E)$  figures by the equality of the shaded areas. The condition of equilibrium is indicated by the equality of the shaded areas in each of the  $n(E)$  figures.

If the density of states is zero or low over an appreciable range of energy, the number of electrons  $n(E)$  will be constant or slowly increasing over this energy range, making a transition to another phase probable at an

approximately predictable electron concentration. This situation is illustrated in Fig. 7.4a. The determination of the  $\gamma\epsilon$  phase boundary of brass should be similar to that shown in this figure because the poor electrical conductivity and the large diamagnetism of  $\gamma$  brass indicate that the density of states of the  $\gamma$  phase at its  $\gamma/\gamma+\epsilon$  phase boundary is relatively low. This dip in the density of states is related to the existence of the Jones zone of the  $\gamma$  phase; but, as discussed in Appendix C, the precise reason for the dip is not known.

The fact that the electrical conductivity of most alloy structures is not low indicates that the density of states is relatively high at the phase boundaries. This type of problem is illustrated in Fig. 7.4b, in which it is evident that the phase boundaries are determined by a close competition between two almost equal functions and cannot be closely related to any singularity in the density-of-states function. This interpretation was already implicit in the work of Jones on the  $\alpha\beta$  phase boundaries of brass; but its generality can be seen more clearly from the results and figures of this chapter. It is worth noting that when the density of states is not low at the phase boundaries, the boundaries are likely to occur "somewhat" beyond the peak in the density of states and that the volume of the sphere enclosed by the Jones zone should also be "somewhat" beyond the peak in the density of states. However, the close correlation, which sometimes exists in practice, between the volume of the enclosed sphere and the position of the phase boundaries appears to be fortuitous.

Further discussion of the interpretation of the Hume-Rothery rules is given at the end of the following chapter.



## CHAPTER VIII

### SUMMARY OF RESULTS

This investigation has touched on several different topics, and many related results were given in different sections in connection with detailed studies of illustrative examples. For the convenience of the reader the significant results are collected here. Reference must be made to the preceding work for the definitions of the technical words.

The first set of results pertains to the existence of an energy gap for a Jones zone of given geometrical shape. The energy gap is the basis of the theoretical importance of Jones zones for the phase boundary and other problems. It is pointed out that the directional, symmetry, and accidental degeneracies which are known to occur between energy bands in the reduced zone scheme must also occur in an extended zone scheme. If these degeneracies occur between energies inside and outside a Jones zone, then an energy gap cannot exist for the zone. Whether or not such degeneracies actually occur for a given Jones zone usually depends on the particular crystal potential and can only be determined by an actual calculation of the electron energies.

Another factor which can prohibit an energy gap from occurring is what is here named a shape degeneracy. The existence of shape degeneracies depends only on the geometrical shape of the zone. Shape degeneracies exist in those Jones zones in which an integral number of fundamental regions cannot be constructed. It follows that shape degeneracies will exist if the volume of the Jones zone is not an integral multiple of the volume of the reduced zone, but shape degeneracies can exist even if the volume

of the Jones zone is an integral multiple of that of the reduced zone. Shape degeneracies will exist if there is a part of the Jones zone boundary which is not connected to any other part of the zone boundary by any reciprocal lattice vector. In all examples studied of Jones zones which are symmetric with respect to inversion in the origin, such an "unconnected" part of a zone boundary face makes the face asymmetric with respect to inversion in the center of the plane forming the face. However, this criterion of asymmetry for a shape degeneracy has not been proven to be rigorously valid. The existence of only parts of Brillouin zones inside the Jones zone does not necessarily imply a shape degeneracy. Examples indicate that in the large alloy Jones zones shape degeneracies may exist in many energy bands. Since shape degeneracies will usually be accompanied by directional degeneracies, it is possible in such cases for the density of states to be relatively high at that number of electron states corresponding to the volume of the Jones zone.

The second set of results relates to the true nature of the energy surfaces in large Jones zones and to the use of the nearly-free-electron approximation to get qualitative information about these surfaces. For problems in which many of the Fourier coefficients of the crystal potential are zero the possibility of simplifying the nearly-free-electron approximation depends on the set  $\vec{B}'$  of reciprocal lattice vectors constructed from those vectors which correspond to the large Fourier coefficients. If the set  $\vec{B}'$  is smaller than the set  $\vec{B}$  of all reciprocal lattice vectors, only the plane waves and zone boundaries corresponding to the set  $\vec{B}'$  need to be used in an approximate calculation of the energy. If the set  $\vec{B}'$  is equal to the set  $\vec{B}$ , no plane waves and zone boundaries can be neglected. The erroneous omission of plane waves in a calculation of the energy

at a particular point of the zone can give both the wrong number of energy levels and the wrong dependence on the strong coefficients. It may be impossible to neglect any plane waves and zone boundaries even if the Jones zone contains an integral number of fundamental regions and hence no shape degeneracy.

For Jones zones which are not the reduced zone of any reciprocal lattice it is not clear at which volume an energy gap is likely to occur. An example for a zone larger than the reduced zone indicates that even for energy surfaces plotted as obtained most naturally by the nearly-free-electron approximation, the Jones zone is not necessarily the same as the zone containing the surfaces of lowest energy. Also, an example shows that the Fourier coefficients corresponding to the Jones zone boundary planes for a zone with a shape degeneracy can cause a gap to occur at a volume greater than that of the Jones zone. It is not known whether these Fourier coefficients can cause a gap at a volume less than that of the Jones zone. These examples suggest for Jones zones which are not the reduced zone of any lattice that the energy surfaces may be much more complicated than the familiar surfaces of the reduced zone and that an energy gap may occur or almost occur at a volume close to but not exactly equal to that of the Jones zone. For any zone energy gaps can only occur at integral multiples of the volume of the true reduced zone.

A third set of results is derived from two three-dimensional numerical problems. For the unperturbed problem the only nonzero Fourier coefficients of the potential are those corresponding to the boundary planes of the Jones zone. For the perturbed problem there are in addition weak coefficients corresponding to Brillouin zone boundary planes which cut inside the Jones zone. Accurate density-of-states curves for these problems illustrate

the results of van Hove on the nature of the singularities in the density-of-states functions. For problems in which the energy surfaces do not deviate too much from spheres it is indicated how a qualitative, occasionally even semi-quantitative, sketch of the density-of-states curve can be made from (1) the density-of-states curve of the zone for free electrons, (2) the type and value of the critical energies occurring in the zone, and (3) the principal effective masses of the electrons with wave vectors at the critical points of the energy surfaces. The theoretical basis of this procedure follows from results of Jones and van Hove. The density of states for the perturbed problem indicates that the effect of interior planes on the density of states should be negligible unless either an entire Seitz zone boundary corresponding to the interior zone planes lies close to a constant energy surface or the ratio of weak to strong coefficients is greater than about one-tenth. Because the density-of-states curve has vertical tangents at its singularities, it is possible for the interior planes to produce a U-shaped dip in the density of states which, if deep, could cause an observable effect on properties which depend on the electrons with energies at the dip.

Jones's approximate analytical method for calculating the density of states, which he used in computing the  $\alpha\beta$  phase boundaries of brass, gives results about three percent low for the unperturbed problem, provided the critical energies and the energy gap are accurately known by some other method. This indicates that even though the energy discontinuity is large for this problem, the nearly-free-electron approximation still represents the energy surfaces satisfactorily.

The final set of results is concerned with obtaining a better physical interpretation of the Hume-Rothery electron concentration rules

for the positions of the phase boundaries in a certain class of alloys. The functions of interest besides the density of states are the number  $n(E)$  of conduction electrons per unit volume of crystal with energies less than or equal to  $E$ , the inverse function  $E(n)$  of this, and the total electron energy  $U(n)$  per unit volume. The energy of the electrons is measured relative to the minimum energy  $E_m$  occurring in the conduction electron bands being considered. Temperature effects are eliminated by considering the problem at absolute zero.

The derivative  $(dU/dn) = E(n) - E_m$  indicates that a sharp increase in the total electron energy and hence in the thermodynamic free energy function can occur only where there is an appreciable energy gap or where the density of states is very small over an appreciable energy range. The  $U(n)$  curve is "straightest" for  $n$  near that corresponding to the highest peak in the density of states. It is assumed that in the typical phase boundary problem the density of states  $N_1$  of the first phase is greater than the density of states  $N_2$  of the second phase until some point beyond the peak in  $N_1$ . For such problems the total electron energy of the first phase, instead of increasing relative to  $U_2$  as the zone is filled beyond the peak in the density of states  $N_1$ , continues to decrease relative to  $U_2$  until that energy is reached at which the total number of electrons are equal in the two phases. Both phase boundaries must occur at still greater electron concentrations. As the volume of the sphere enclosed by the Jones zone should also be greater than the volume corresponding to the peak in the density of states, it is not surprising to find sometimes a correlation between the volume of the enclosed sphere and the positions of the phase boundaries; but any quantitative agreement appears to be fortuitous.

In an energy interval which includes a critical energy of the

type considered by van Hove and which does not include an energy gap in the density of states, the total electron energy function has a continuous second derivative. The smoothness of this function makes it difficult to use in discussing the phase boundary problem. It is shown that at absolute zero and in the approximation that the change in the free energy with composition is due to the change in the total electron energy the equilibrium conditions can be put in the form

$$\int_{E_m}^E [n_1(E') - n_2(E')] dE' = 0, \quad (8.1)$$

which has the advantages that the function  $n(E)$  has more structure than  $U(n)$  has and is more closely related to the density of states than is  $U(n)$ . The discussion of the phase boundary problem in terms of this condition is given in Section 7.3.

Additional results are given in the following appendices.

The results of this investigation suggest some modifications in the usual interpretation of the Hume-Rothery rules. First, it appears both theoretically and in practice that the positions of the phase boundaries are not related to the positions of the singularities in the density of states except when poor electrical conductivity indicates the phase boundary occurs at an energy gap or low dip in the density of states. Second, for the type of problem considered here the density of states and hence the total electron energy is determined primarily by the geometrical shape of the zone. It follows from this that the same phases of the different alloy systems should occur at the same electron concentrations. Moreover, it should be possible to calculate the nominal positions of all phase boundaries which are determined primarily by the total electron energy by a relatively simple calculation. The work of Jones on the  $\alpha\beta$  phase boundaries

is the first step in this program.

Further work is necessary in order to justify the above interpretation. It must be shown either that the positions of the phase boundaries are insensitive to the size of the energy discontinuity at the zone face or else that the energy discontinuity is approximately constant for the different alloy systems. The effect of small differences in the minimum energies of the conduction bands and in the sizes of the energy discontinuities for two neighboring phases should also be investigated.

## APPENDIX A

### SOME BRILLOUIN ZONES OF THE CUBIC LATTICES

This appendix presents some drawings and photographs of the first few Brillouin zones of the face- and body-centered cubic reciprocal lattices.

The shape of the outer surface of each succeeding Brillouin zone is usually more complicated than that of the preceding zone. However, occasionally the shape of a Brillouin zone will be simpler than the shape of one or more preceding zones. For example, the outer surface of the seventh Brillouin zone of the two-dimensional square lattice (see Fig. 5.1) is much simpler than that of the third, fourth, fifth, and sixth zones. Another example is the fourth Brillouin zone of the simple cubic lattice, whose outer surface is simpler than that of the third zone.

One of the early purposes of this study was to see if similar simplifications occurred in the Brillouin zones of the face- and body-centered cubic reciprocal lattices. Drawings of the first four Brillouin zones of these lattices have been given by Nicholas<sup>19</sup> (the first one or two zones were given in the early literature). Brillouin zones five through eight have been worked out here. The work was facilitated by computing an auxiliary table giving for each pair of planes forming zone boundaries the vector to the midpoint of the line of intersection and a vector parallel to this line. From this information the line segments forming the edges of the zone surfaces can be easily constructed.

For purposes of comparison, drawings of the outer surfaces of the first four Brillouin zones as well as of zones five through eight of the face- and body-centered cubic reciprocal lattices are shown in Figs. A.1



through A.10. These figures show only that part of the surface lying in the first octant. A line of intersection of a zone face with the  $k_x k_y$ ,  $k_y k_z$ , or  $k_z k_x$  coordinate plane which is not also a zone boundary edge is shown as a dotted line. "Hidden" zone boundary edges are shown as dashed lines. The numbers within parentheses denote the planes forming the zone faces (as always, a plane is denoted by the components of the lattice vector which is perpendicularly bisected by the plane). The coordinates of the zone corners are denoted by numbers not in parentheses.

Table A.1 gives the number of faces, edges, and corners of the outer surface of the first eight Brillouin zones of the face- and body-centered cubic reciprocal lattices. For the face-centered cubic reciprocal lattice, corresponding to the body-centered cubic direct lattice, a simplification in the outer surface occurs for the third and seventh zones. For the body-centered cubic reciprocal lattice, corresponding to the face-centered cubic direct lattice, a simplification in the outer surface occurs for the fifth zone. However, these simplifications are relatively slight, and the resulting surfaces are still rather complex.

For pedagogic purposes it is useful to have solid models whose surfaces are outer surfaces of Brillouin zones. Several such models have been carved from wood by Mr. Conrade C. Hinds. Because of a general interest shown in these models, photographs of them are shown in Figs. A.11 through A.13.

TABLE A.1

## DATA ON CERTAIN BRILLOUIN ZONES

FACE-CENTERED CUBIC RECIPROCAL LATTICE								
Zone	1	2	3	4	5	6	7	8
Number of Faces	12	48	30	72	216	240	156	288
Number of Edges	24	72	48	120	336	384	264	456
Number of Corners	14	26	20	50	122	146	110	170
BODY-CENTERED CUBIC RECIPROCAL LATTICE								
Zone	1	2	3	4	5	6	7	8
Number of Faces	14	72	96	204	104	576	624	912
Number of Edges	36	132	180	336	228	936	152	1656
Number of Corners	24	62	86	134	126	362	530	746

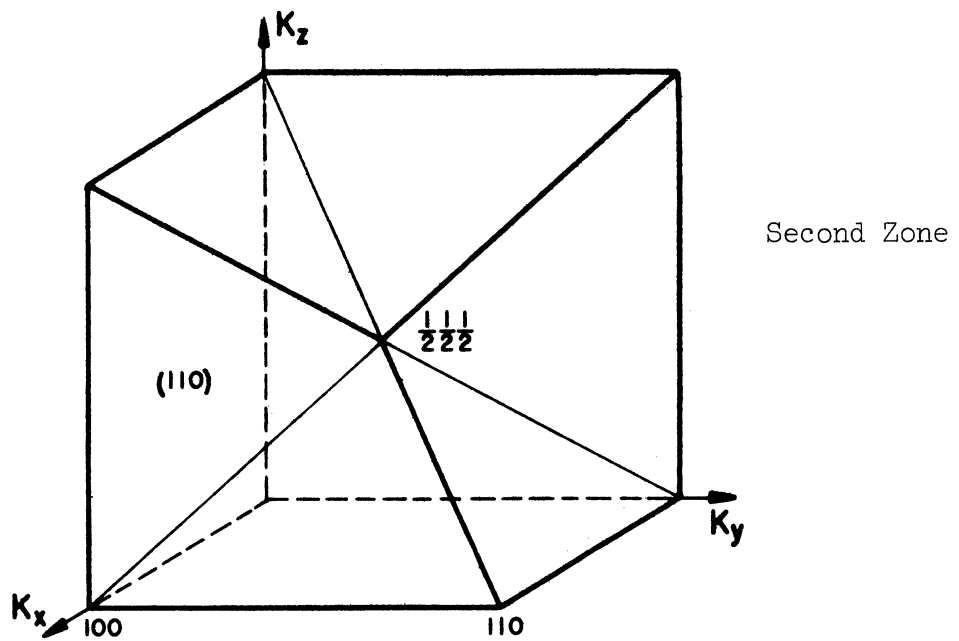
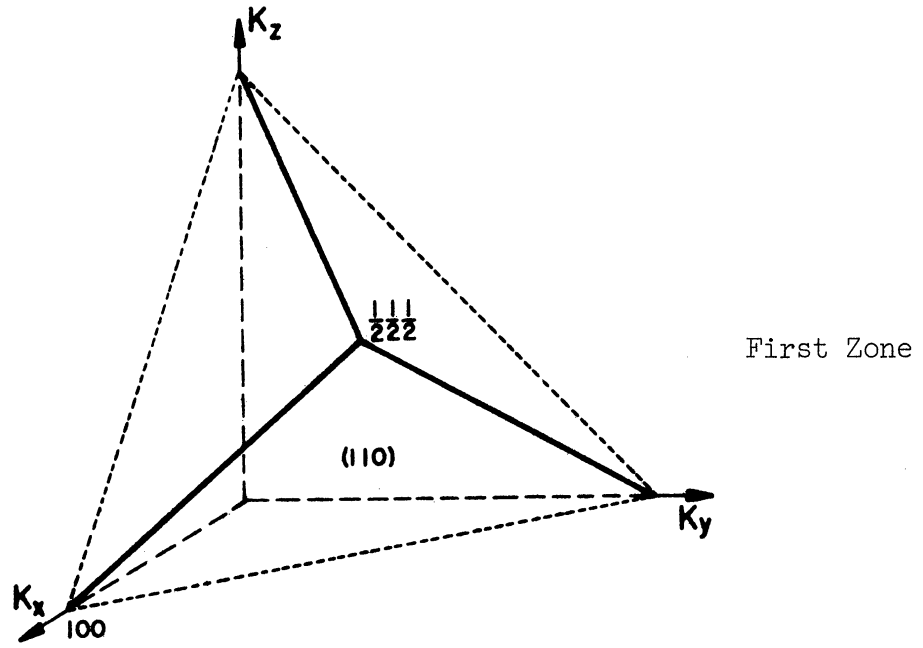


Fig. A.1. Brillouin zones, face-centered cubic reciprocal lattice.

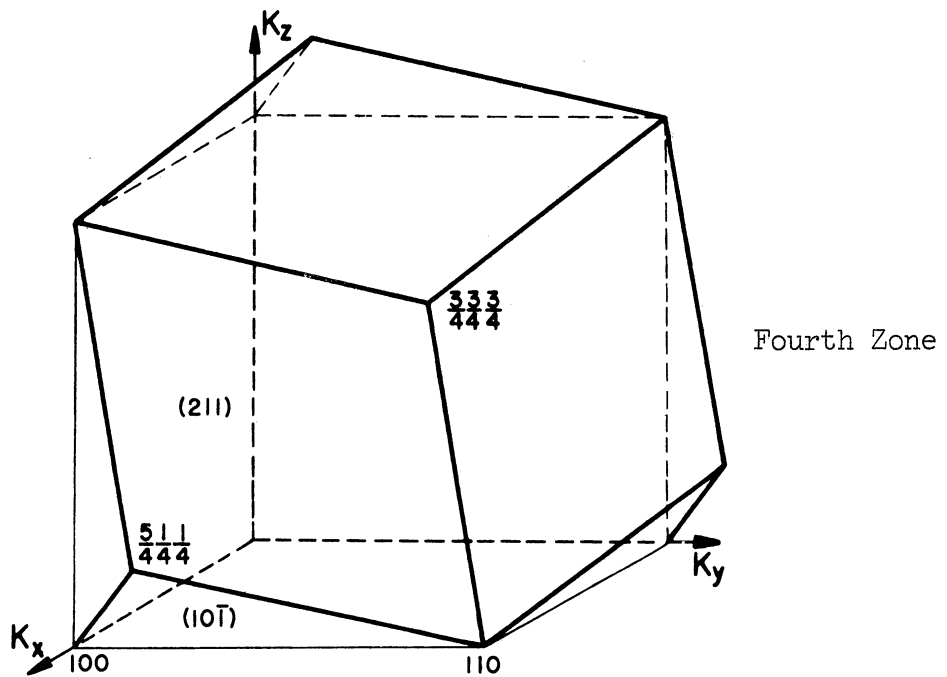
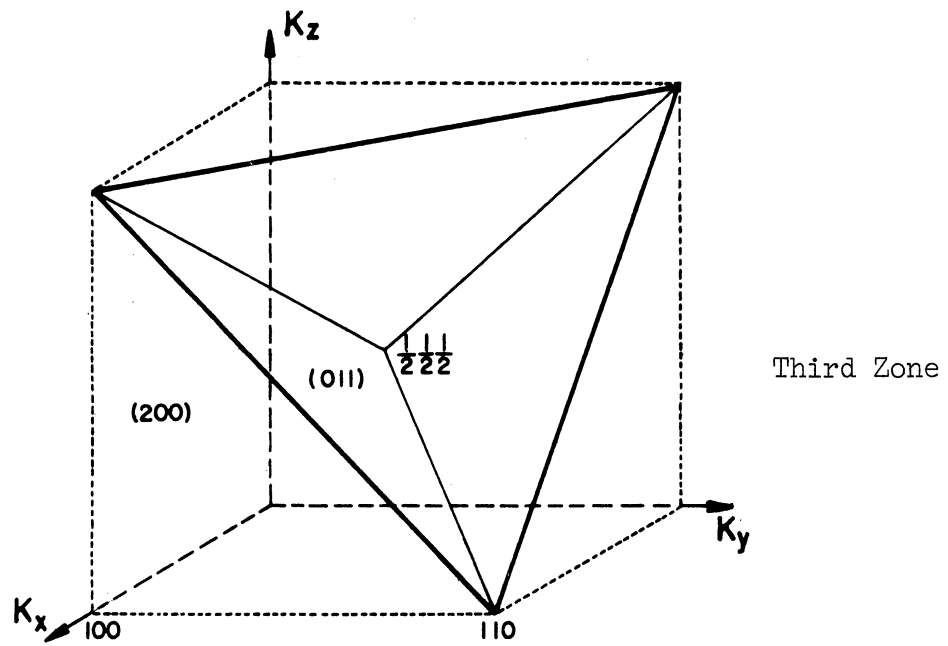


Fig. A.2. Brillouin zones, face-centered cubic reciprocal lattice.

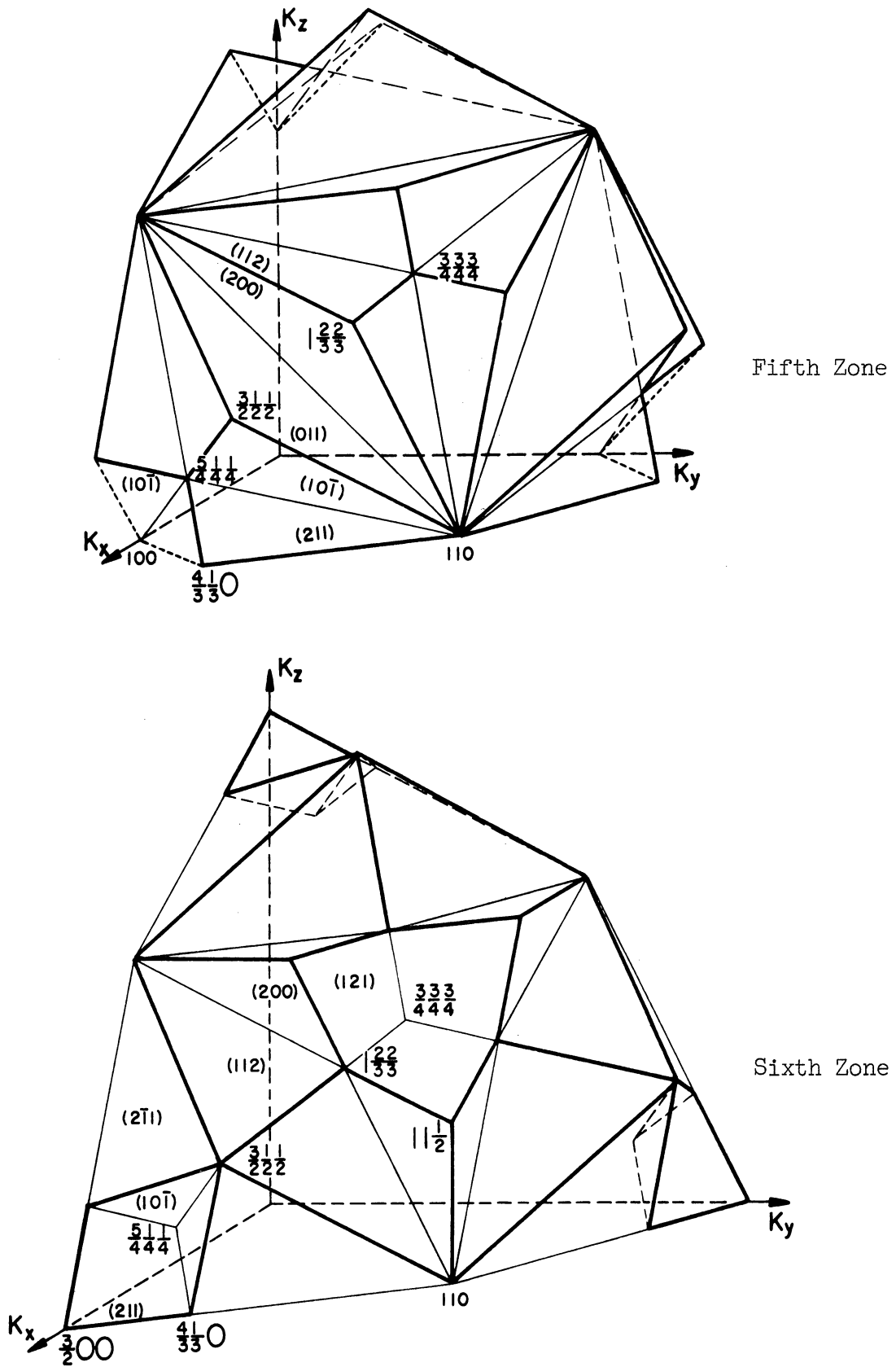


Fig. A.3. Brillouin zones, face-centered cubic reciprocal lattice.

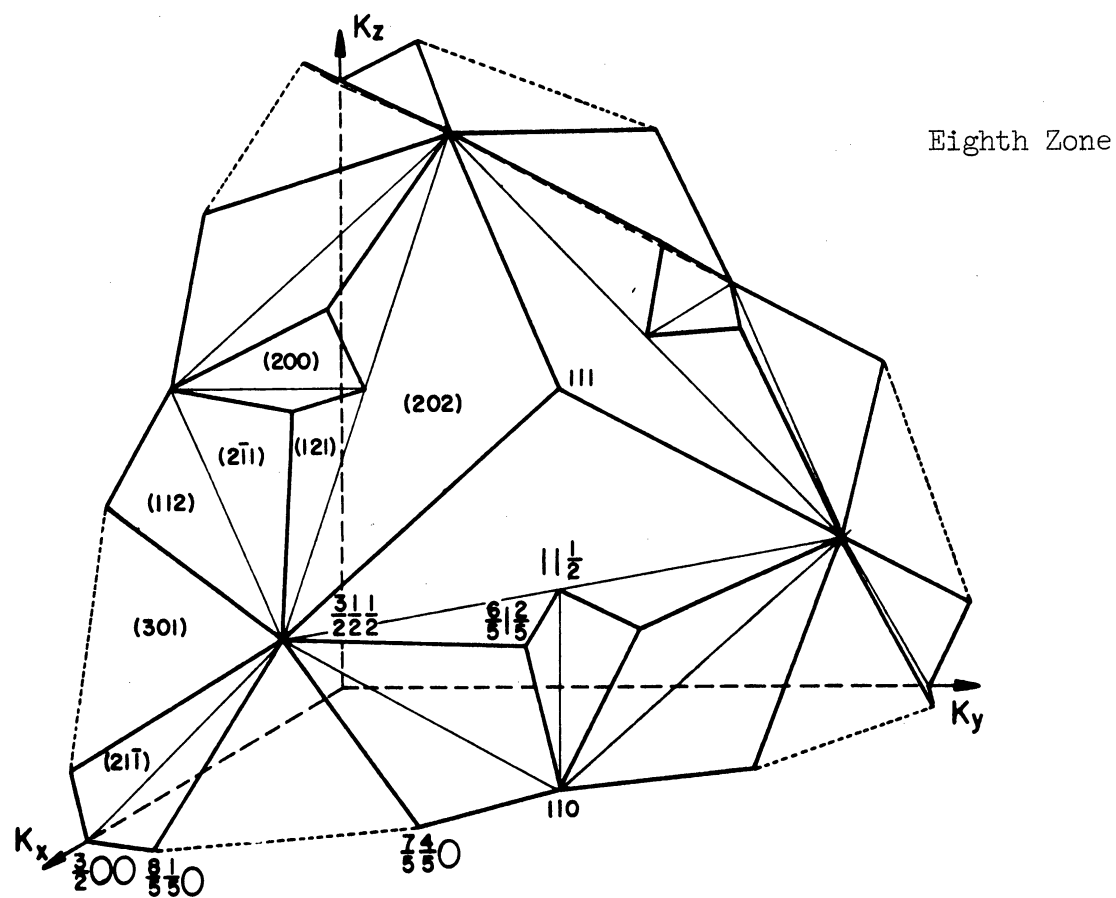
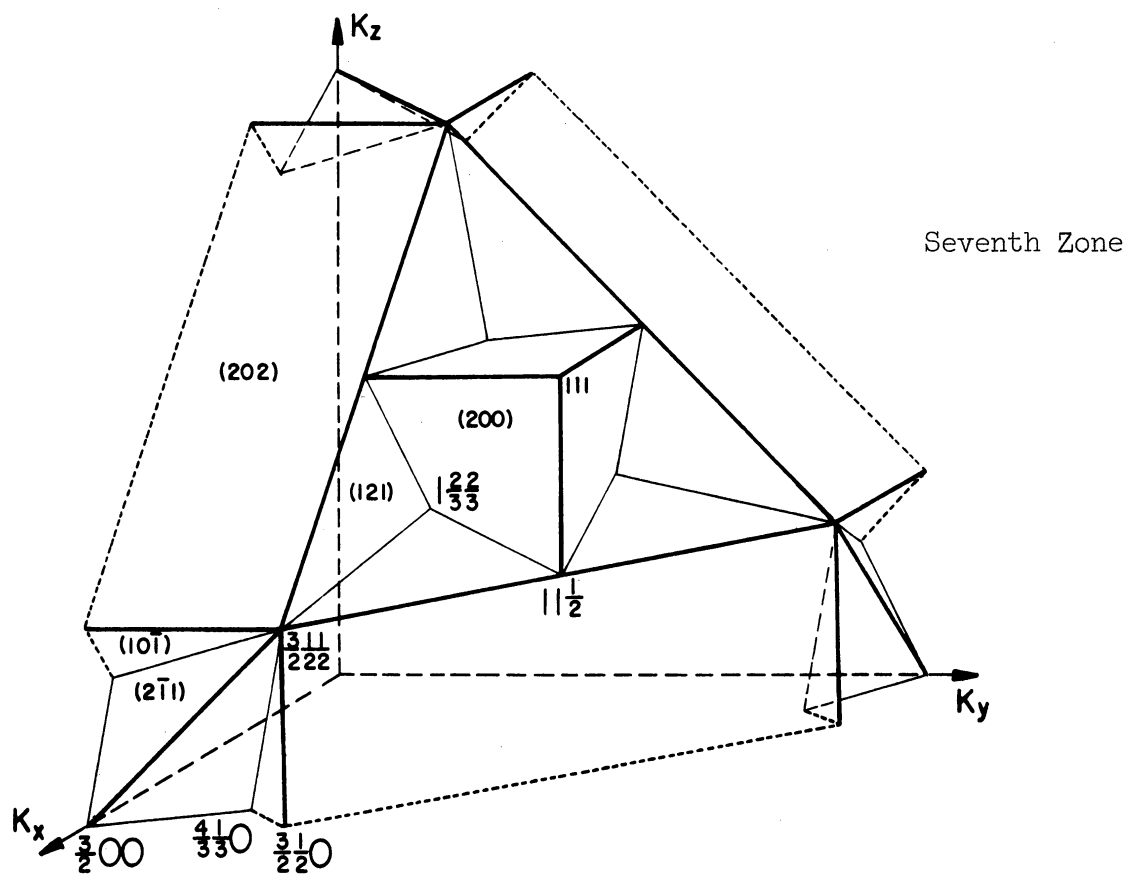


Fig. A.4. Brillouin zones, face-centered cubic reciprocal lattice.

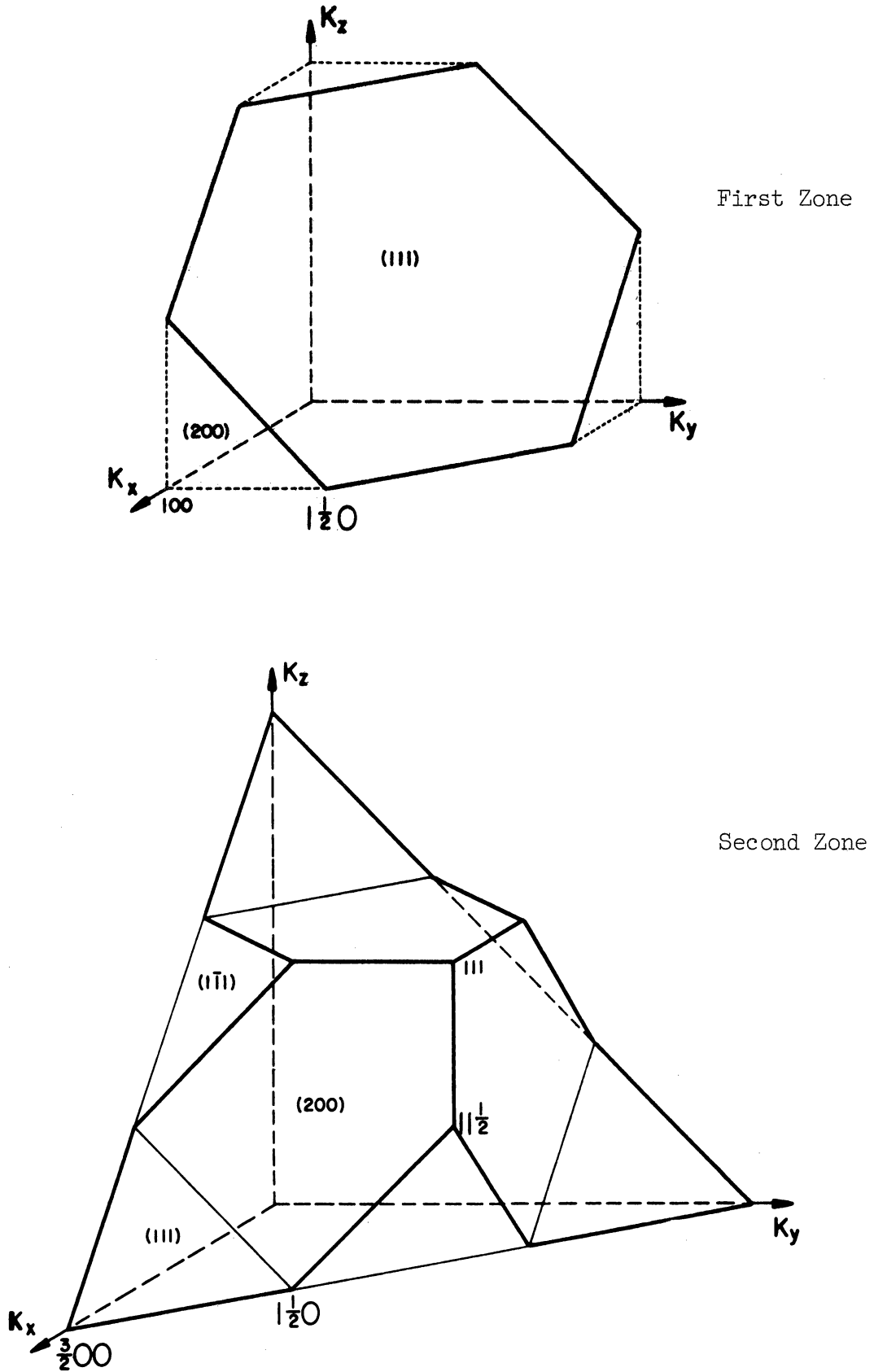


Fig. A.5. Brillouin zones, body-centered cubic reciprocal lattice.

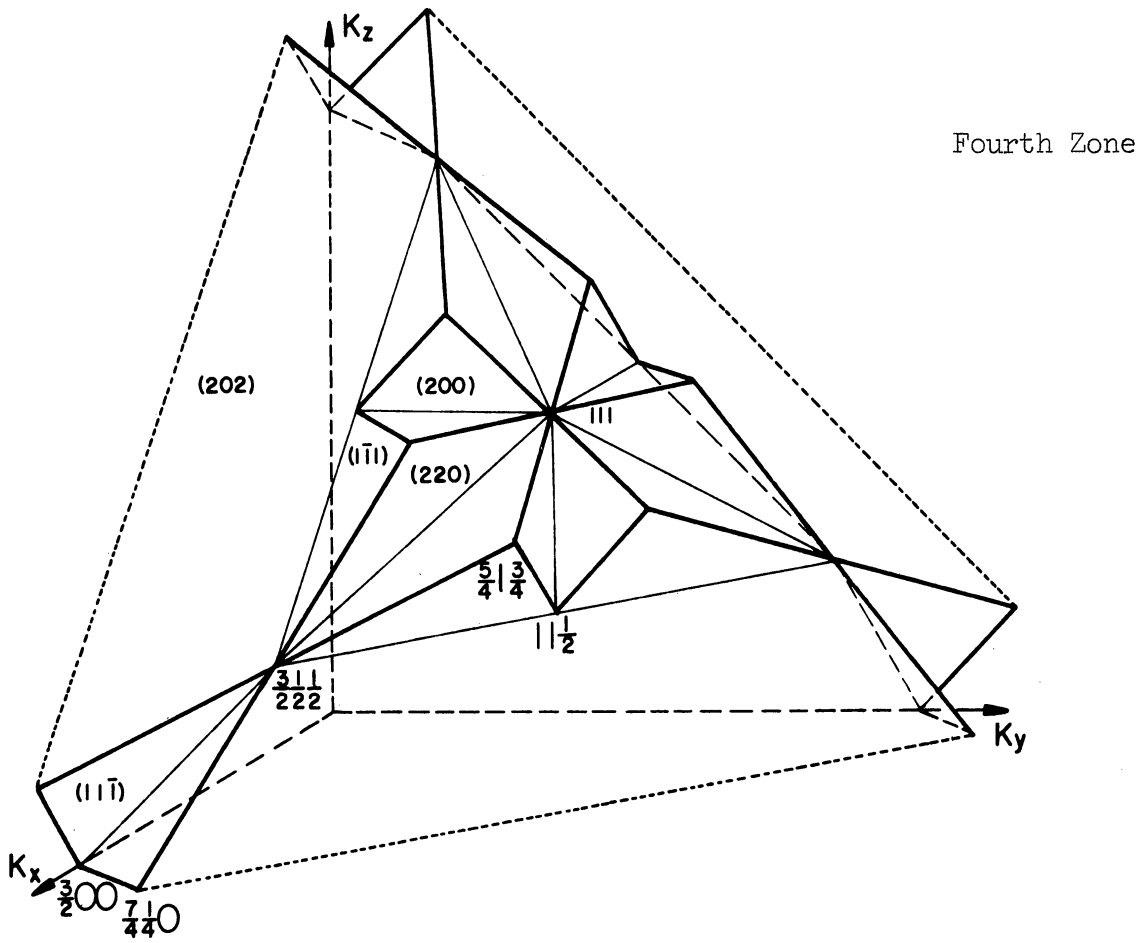
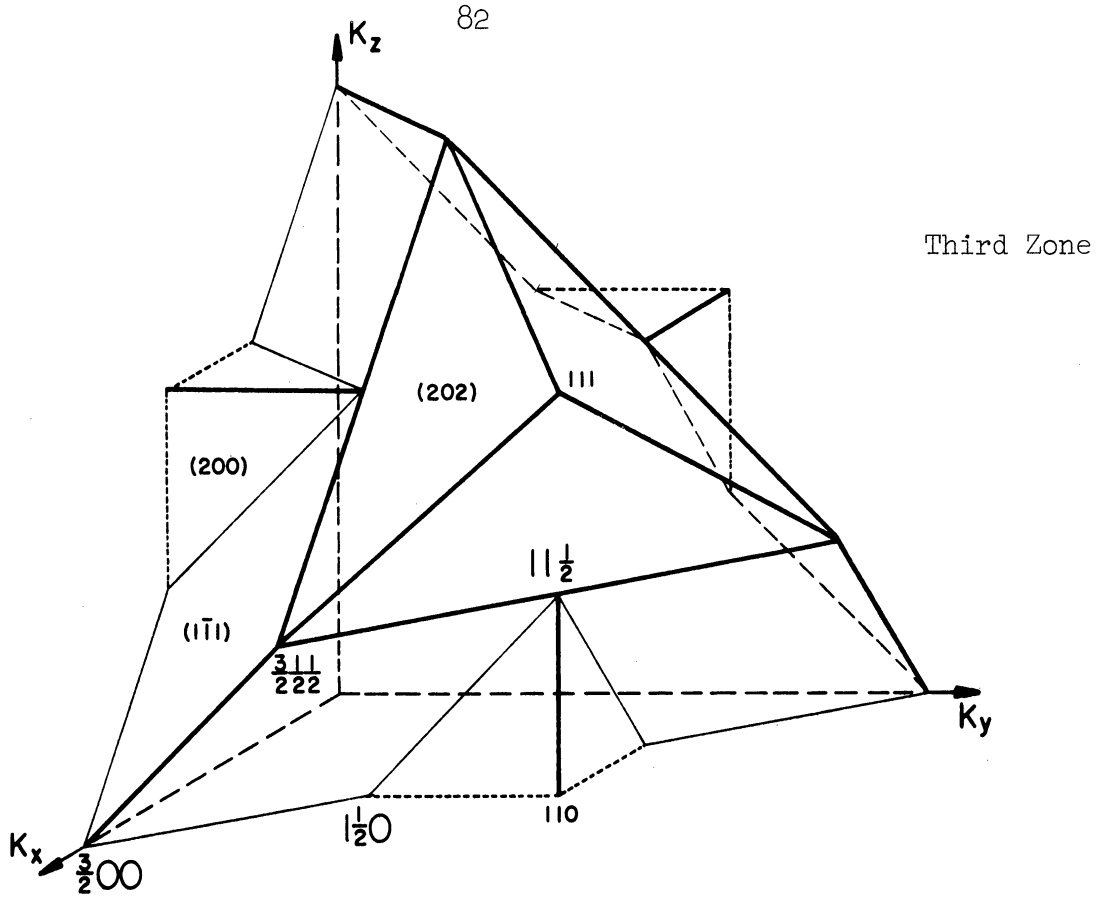
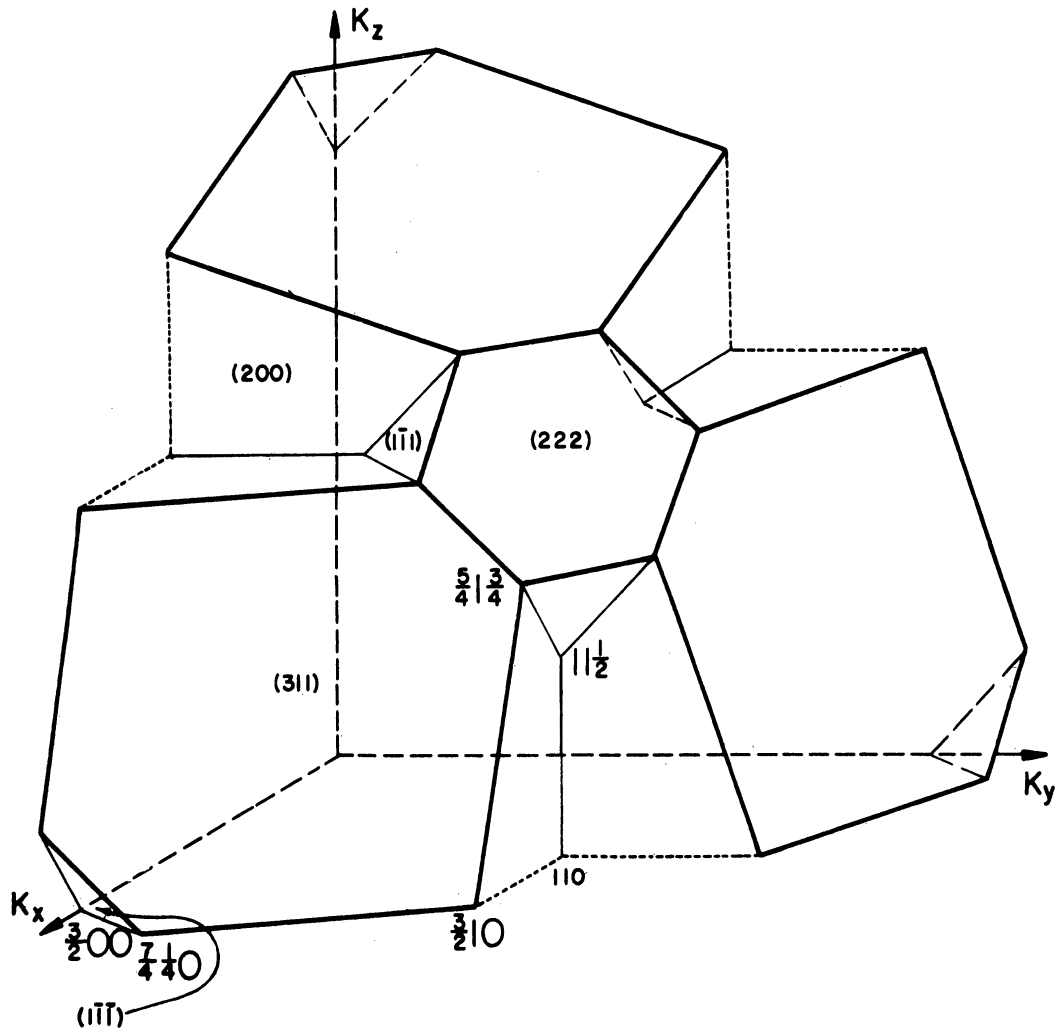


Fig. A.6. Brillouin zones, body-centered cubic reciprocal lattice.

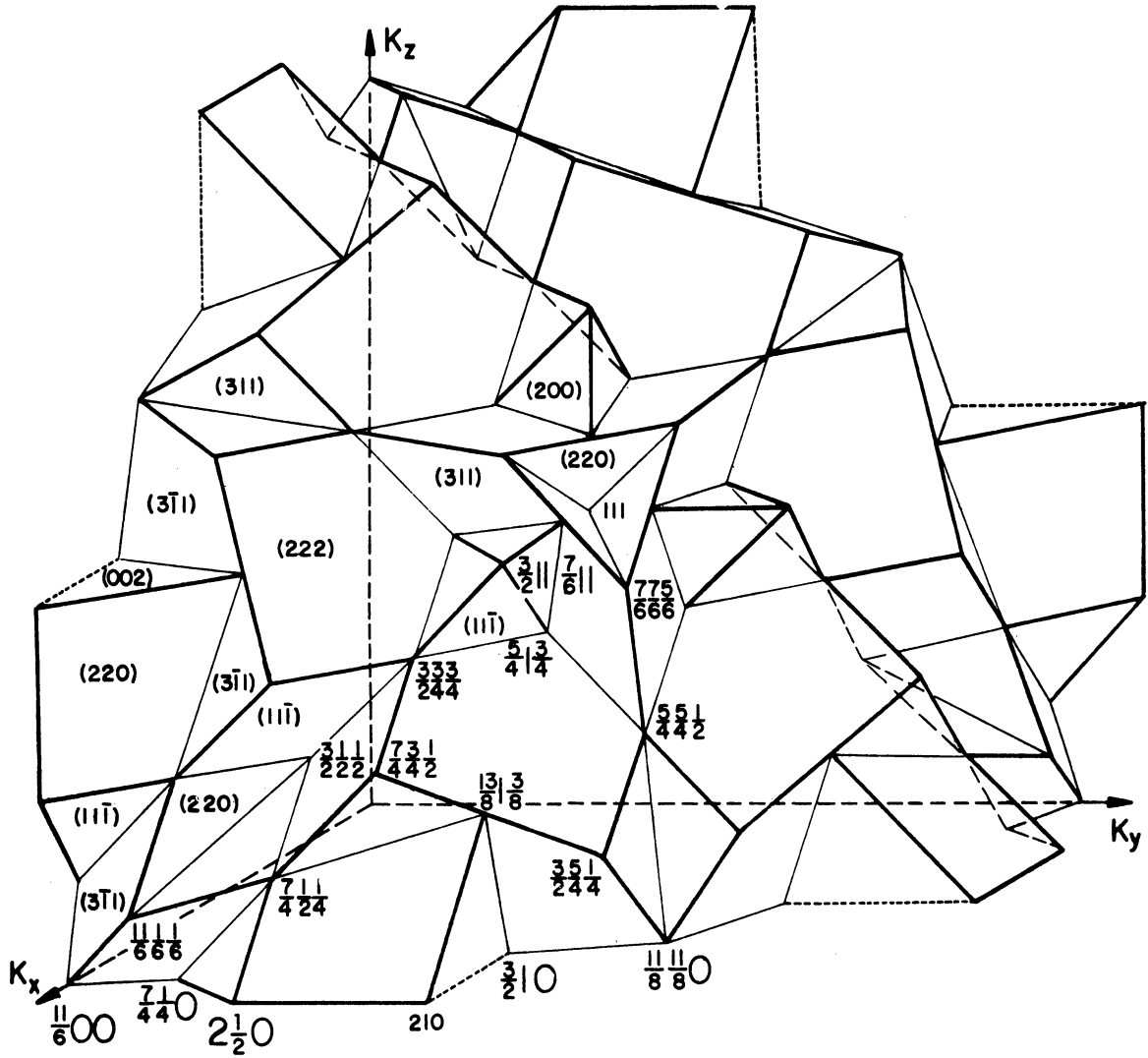




Fifth Zone

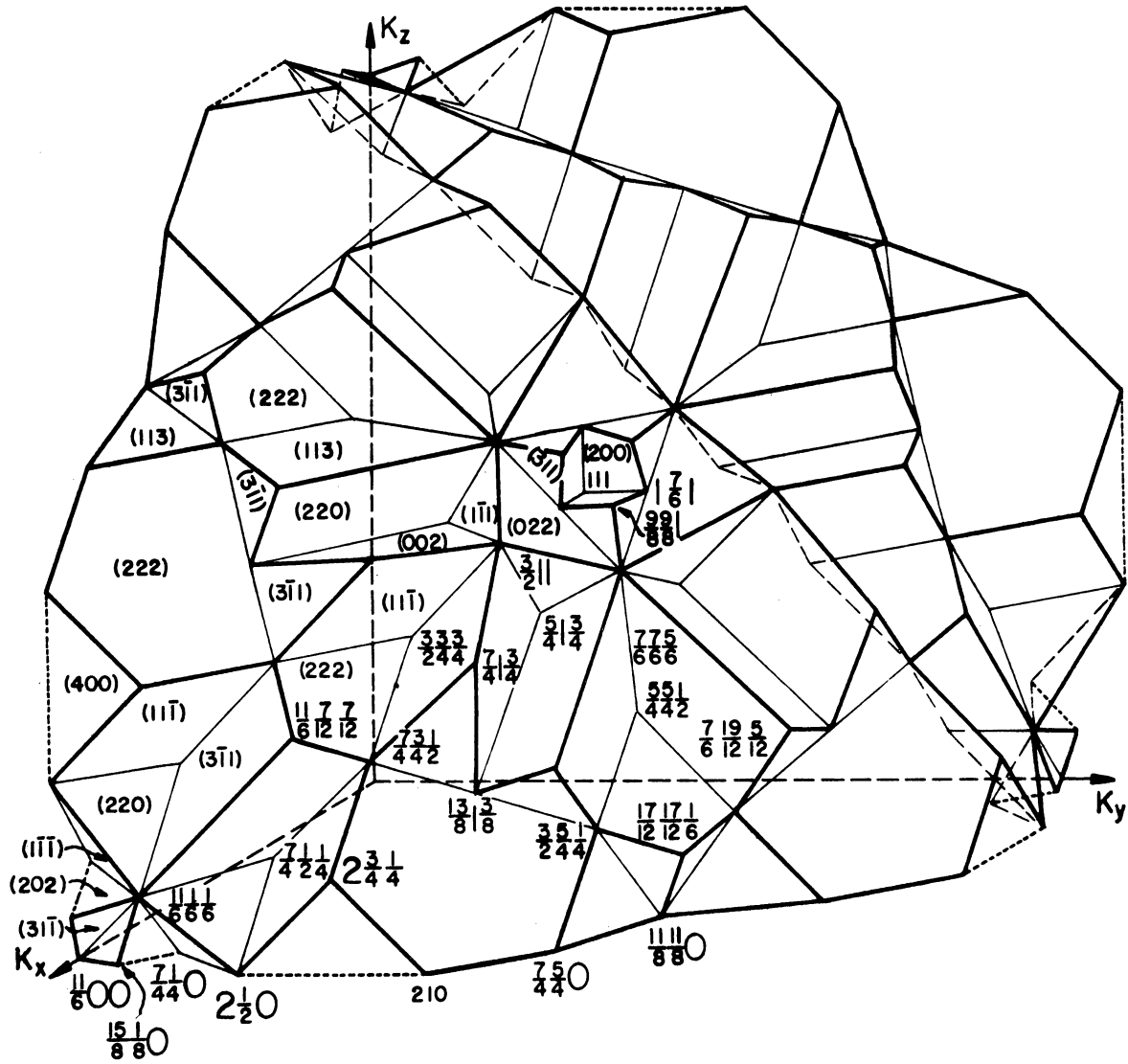
Fig. A.7. Brillouin zone, body-centered cubic reciprocal lattice.





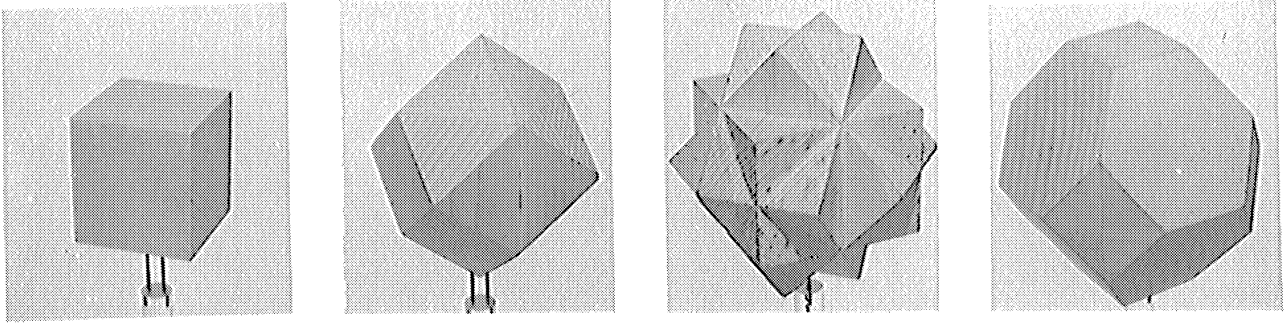
Seventh Zone

Fig. A.9. Brillouin zone, body-centered cubic reciprocal lattice.



Eighth Zone

Fig. A.10. Brillouin zone, body-centered cubic reciprocal lattice.



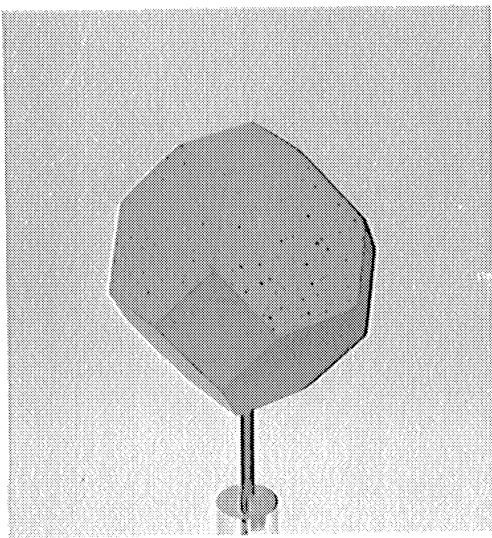
First Zone

Second Zone

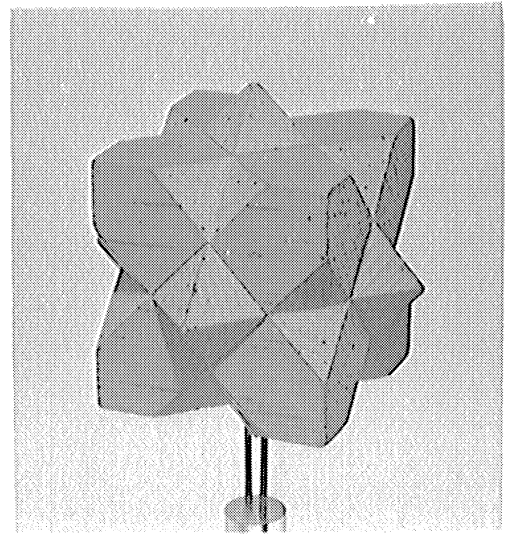
Third Zone

Fourth Zone

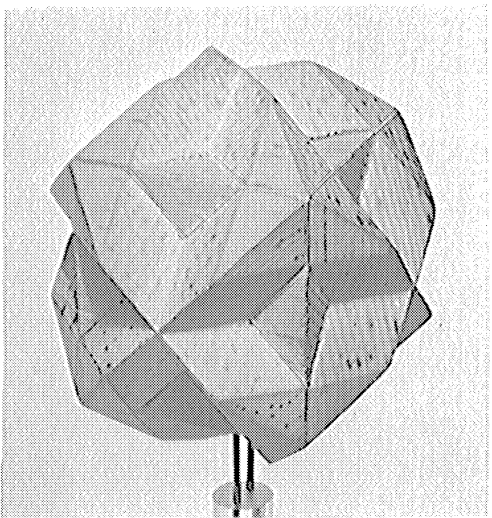
Fig. A.11. Brillouin zones, simple cubic reciprocal lattice.



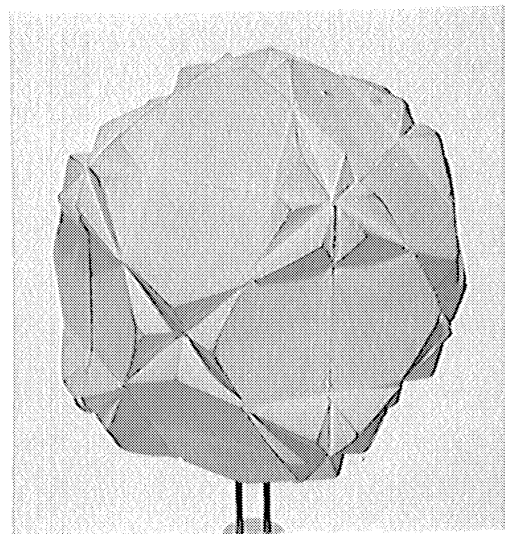
First Zone



Second Zone

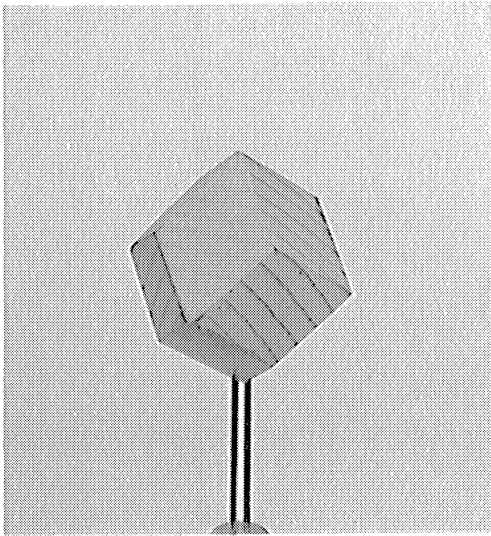


Third Zone

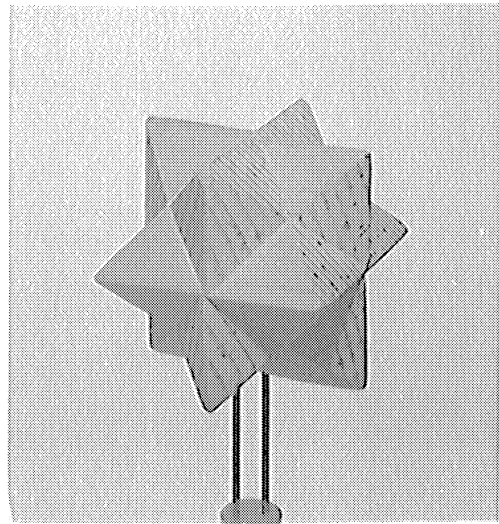


Fourth Zone

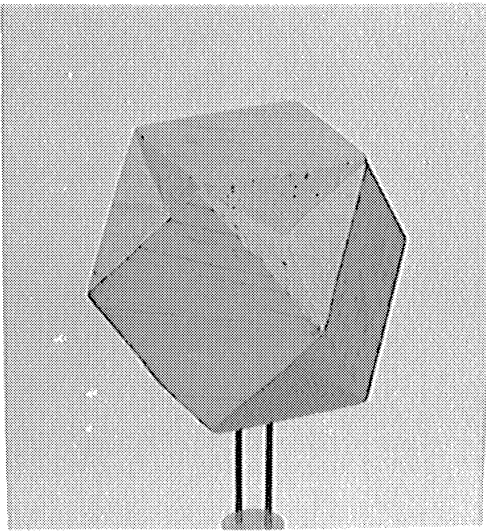
Fig. A.12. Brillouin zones, body-centered cubic reciprocal lattice.



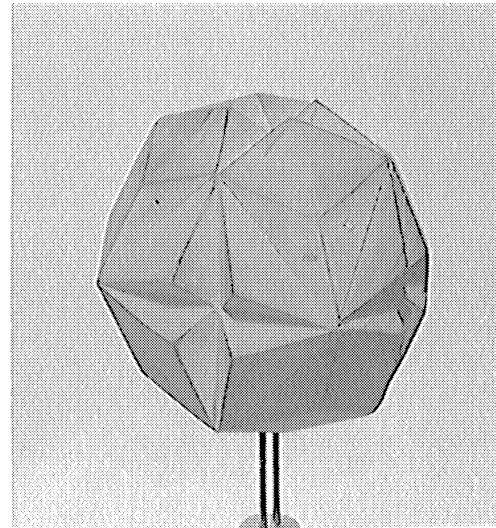
First Zone



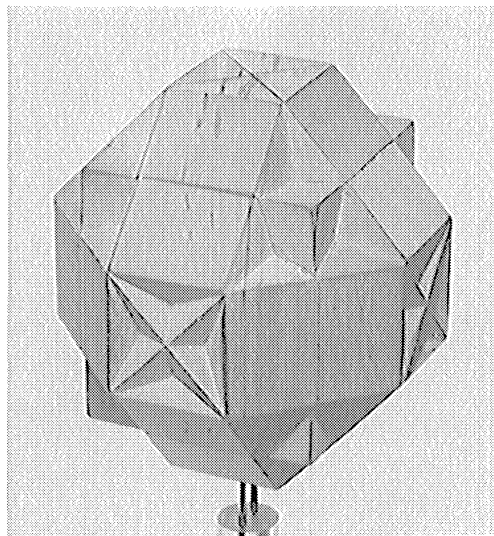
Second Zone



Third Zone



Fourth Zone



Seventh Zone

Fig. A.13. Brillouin zones, face-centered cubic reciprocal lattice.

## APPENDIX B

### WHITTAKER-INCE SOLUTION OF HILL'S EQUATION

The general form of the Whittaker-Ince solution of Hill's equation was discussed in Chapter IV. The motivation for seeking a solution of this form is given in the original articles.<sup>12,13</sup> In this appendix certain additional terms are derived in the power-series solutions of a special case of Hill's equation, namely, equation (4.5) which is repeated here:

$$(\frac{d^2}{dx^2})\psi + 4 (E - 2V_1 \cos 2x - 2V_2 \cos 4x)\psi = 0 \quad . \quad (B.1)$$

Before doing this it was decided to check the pertinent terms in Ince's solution of the general Hill equation. Four errors in Ince's results are indicated in Section B.4.

The essential feature of the Whittaker-Ince method is to expand  $E$  and  $\psi$  as power series in  $V_1^i V_2^j$ . On putting these series into Hill's equation and equating to zero the coefficient of each power of  $V_1^i V_2^j$ , an infinite set of differential equations is obtained for the unknown coefficients in the series for  $\psi$ . These equations are simple to solve in principle; but the equations for the high-degree terms are very long and hence troublesome to handle in practice. This difficulty can be avoided by a recurrence-relation method which breaks up essentially the same calculation into a number of small steps. In addition, this method is more systematic to apply. Consequently, all the derivations reported in this appendix were done by the recurrence-relation method instead of the differential-equation method of Whittaker and Ince. It

should be emphasized, however, that the solutions obtained by the two methods are identical.

The first step in the Whittaker-Ince solution is to set

$$\Psi(x) = \exp(2hx) u(x) \quad , \quad (\text{B.2})$$

in which  $u(x)$  is to have period either  $\pi$  or  $2\pi$ . This form is convenient for analytical work and is easily related to the Bloch form, expression (4.6). The differential equation for  $u(x)$  is

$$(d^2/dx^2)u + 4h(d/dx)u + 4(E + h^2 - 2V_1 \cos 2x - 2V_2 \cos 4x)u = 0. \quad (\text{B.3})$$

In the Whittaker-Ince method this equation is solved by making different expansions of  $u$ ,  $E$ , and sometimes  $h$ . Three such expansions are derived in the following sections.

#### B.1. THE $\kappa$ -EXPANSION

The series solution obtained by the following method is useful only for wave vectors which are not near the Brillouin zone boundaries.

Set

$$u(x) = \sum_{n=-\infty}^{\infty} U_{2n}(\kappa) e^{2nix} \quad \text{with } U_0 = 1 \quad . \quad (\text{B.4})$$

The exponential functions are more suitable for use with the recurrence-relation method than are the trigonometric functions obtained by Ince.

On putting this series into the differential equation (B.3) and equating to zero the coefficient of each exponential, one obtains an infinite set of coupled algebraic equations for the unknown coefficients  $U_{2n}$ . In these equations put

$$E + h^2 = \sum_{i,j=0}^{\infty} E_{ij}(\kappa) V_1^i V_2^j \quad , \quad (\text{B.5a})$$



$$h = i\kappa/2, \quad (\text{B.5b})$$

and for  $n \neq 0$

$$U_{2n} = \sum_{i,j=0}^{\infty} U_{2n}^{ij}(\kappa) V_1^i V_2^j; \quad (\text{B.5c})$$

and equate to zero the coefficient of each power of  $V_1^i V_2^j$ . This gives the following set of recurrence relations (in these  $U_{2n}^{ij}$  is defined to be zero if either  $i$  or  $j$  is negative):

$$E_{ij}(\kappa) = U_{-4}^{ij-1} + U_{-2}^{i-1j} + U_2^{i-1j} + U_4^{ij-1}, \quad (\text{B.6a})$$

$$U_2^{ij}(\kappa) = \frac{1}{1+\kappa} \left[ \sum_{p=0}^i \sum_{q=0}^j E_{i-p, j-q} U_2^{pq} - U_{-2}^{ij-1} - U_4^{i-1j} - U_6^{ij-1} - \delta_{i1} \delta_{j0} \right], \quad (\text{B.6b})$$

$$U_4^{ij}(\kappa) = \frac{1}{4+2\kappa} \left[ \sum_{p=0}^i \sum_{q=0}^j E_{i-p, j-q} U_4^{pq} - U_2^{i-1j} - U_6^{i-1j} - U_8^{ij-1} - \delta_{i0} \delta_{j1} \right], \quad (\text{B.6c})$$

and for  $n \geq 3$

$$U_{2n}^{ij}(\kappa) = \frac{1}{n^2+n\kappa} \left[ \sum_{p=0}^i \sum_{q=0}^j E_{i-p, j-q} U_{2n}^{pq} - U_{2n-4}^{ij-1} - U_{2n-2}^{i-1j} - U_{2n+2}^{i-1j} - U_{2n+4}^{ij-1} \right]. \quad (\text{B.6d})$$

Also, for  $n \geq 1$

$$U_{-2n}^{ij}(\kappa) = U_{2n}^{ij}(-\kappa). \quad (\text{B.6e})$$

These expressions relate  $E_{ij}$  and  $U_{2n}^{ij}$  to coefficients of lower degree. It also follows that  $E_{00} = V_{2n}^{00} = 0$ , so that by successive application of these

relations all coefficients can be determined. The coefficients determined in this study are given in Table B.1. In each section of the table all the nonzero coefficients are given for the range of  $i + j$  indicated.

Since  $u(x)$  has periodicity  $\pi$ , the appropriate relation between  $\kappa$  and the wave vector  $k$  is  $\kappa = 2k$ . Therefore, the energy and wave vector are related by

$$E = k^2 + \sum_{i,j=0}^{\infty} E_{ij}(\kappa) V_1^i V_2^j \quad (\text{B.7a})$$

and

$$k = \kappa/2 \quad . \quad (\text{B.7b})$$

For  $k \ll 1/2$  this becomes

$$\begin{aligned} E = & \left( -2V_1^2 - \frac{1}{2} V_2^2 + 3V_1^2 V_2 + \frac{7}{2} V_1^4 - \frac{20}{9} V_1^2 V_2^2 \right. \\ & \left. + \frac{7}{128} V_2^4 - \frac{136}{9} V_1^4 V_2 + \frac{27}{32} V_1^2 V_2^3 + \dots \right) \\ & + \left( 1 - 8V_1^2 - \frac{1}{2} V_2^2 + 15 V_1^2 V_2 + \frac{111}{2} V_1^4 - \frac{980}{81} V_1^2 V_2^2 \right. \\ & \left. + \frac{111}{512} V_2^4 - \frac{18,472}{81} V_1^4 V_2 + \frac{531}{128} V_1^2 V_2^3 + \dots \right) k^2 \\ & + \dots \quad . \quad (\text{B.7c}) \end{aligned}$$

## B.2. THE $\sigma$ 1/4-EXPANSION

The following solution is useful only near the first Brillouin zone boundary in the extended zone scheme. Set

$$\begin{aligned} u(x) = & \sin(x-\sigma) + \sum_{n=1}^{\infty} \left[ S_{2n+1}(\sigma) \sin[(2n+1)x - \sigma] \right. \\ & \left. + C_{2n+1}(\sigma) \cos[(2n+1)x - \sigma] \right] , \quad (\text{B.8}) \end{aligned}$$

in which  $\sigma$  is a parameter that may be complex. The form of the functions

TABLE B.1

NONZERO COEFFICIENTS IN THE EXPANSIONS (B.5)

$$i + j \leq d$$

	d	ij	
$E_{ij}$	5	20	$-2/(1-\kappa^2)$
		02	$-2/(4-\kappa^2)$
		21	$12/(1-\kappa^2)(4-\kappa^2)$
		40	$2(7+5\kappa^2)/(1-\kappa^2)^3(4-\kappa^2)$
		22	$-80/(1-\kappa^2)(4-\kappa^2)(9-\kappa^2)$
		04	$2(28+5\kappa^2)/(4-\kappa^2)^3(16-\kappa^2)$
		41	$-32(17+7\kappa^2)/(1-\kappa^2)^3(4-\kappa^2)(9-\kappa^2)$
		23	$72(12-7\kappa^2)/(1-\kappa^2)(4-\kappa^2)^3(16-\kappa^2)$
$U_2^{ij}$	4	10	$-1/(1+\kappa)$
		11	$(5+\kappa)/2(1-\kappa^2)(2+\kappa)$
		30	$(7+4\kappa+\kappa^2)/2(1-\kappa^2)(1+\kappa)^2(2+\kappa)$
		12	$-4(8+\kappa)/3(1-\kappa^2)(4-\kappa^2)(3+\kappa)$
		31	$-(252-173\kappa+24\kappa^2+28\kappa^3+12\kappa^4+\kappa^5)/3(1-\kappa^2)^3(4-\kappa^2)(3+\kappa)$
		13	$(3476+2560\kappa+247\kappa^2+14\kappa^3+3\kappa^4)/48(1-\kappa^2)(4-\kappa^2)(2+\kappa)^2(3-\kappa)(4+\kappa)$
$U_4^{ij}$	4	01	$-1/2(2+\kappa)$
		20	$1/2(1+\kappa)(2+\kappa)$
		21	$-4/3(1-\kappa^2)(2+\kappa)(3+\kappa)$
		03	$(28+8\kappa+\kappa^2)/16(4-\kappa^2)(2+\kappa)^2(4+\kappa)$
		40	$-(10+5\kappa+\kappa^2)/3(1-\kappa^2)(1+\kappa)^2(2+\kappa)(3+\kappa)$
		22	$(412+1016\kappa+341\kappa^2+28\kappa^3+3\kappa^4)/48(1-\kappa^2)(4-\kappa^2)(2+\kappa)^2(3+\kappa)(4+\kappa)$
$U_6^{ij}$	3	11	$(5+3\kappa)/6(1+\kappa)(2+\kappa)(3+\kappa)$
		30	$-1/6(1+\kappa)(2+\kappa)(3+\kappa)$
		12	$-(9+\kappa)/8(1-\kappa^2)(2+\kappa)(4+\kappa)$
$U_8^{ij}$	3	02	$1/8(2+\kappa)(4+\kappa)$
		21	$-(7+3\kappa)/12(1+\kappa)(2+\kappa)(3+\kappa)(4+\kappa)$
$U_{2n}^{ij}$ $n \geq 5$	2	None	

used in this series gives the simplest recurrence relations and also affords a direct comparison with the results of Ince. However, if the wave functions themselves were of interest, it might be better to expand in terms of the functions  $\sin(2n+1)x$  and  $\cos(2n+1)x$  or  $\exp[\pm (2n+1)ix]$ . Put the series (B.8) into the differential equation (B.3) and equate to zero the coefficient of each sine and cosine term. This gives an infinite set of coupled algebraic equations for  $S_{2n+1}$  and  $C_{2n+1}$ . In these equations put

$$E = 1/4 + h^2 = \sum_{i,j=0}^{\infty} E_{ij}(\sigma) V_1^i V_2^j, \quad (\text{B.9a})$$

$$h = \sum_{i,j=0}^{\infty} h_{ij}(\sigma) V_1^i V_2^j, \quad (\text{B.9b})$$

$$S_{2n+1} = \sum_{i,j=0}^{\infty} S_{2n+1}^{ij}(\sigma) V_1^i V_2^j, \quad (\text{B.9c})$$

and

$$C_{2n+1} = \sum_{i,j=0}^{\infty} C_{2n+1}^{ij}(\sigma) V_1^i V_2^j; \quad (\text{B.9d})$$

and equate to zero the coefficient of each power of  $V_1^i V_2^j$ . This gives the following recurrence relations (in these  $S_{2n+1}^{ij}$  and  $C_{2n+1}^{ij}$  are defined to be zero if either  $i$  or  $j$  is negative):

$$\begin{aligned} E_{ij}(\sigma) = & -\cos 2\sigma S_3^{ij-1} - \sin 2\sigma C_3^{ij-1} + S_3^{i-1j} \\ & + S_5^{ij-1} - \cos 2\sigma \delta_{i1} \delta_{j0}, \end{aligned} \quad (\text{B.10a})$$

$$\begin{aligned} h_{ij}(\sigma) = & \cos 2\sigma C_3^{ij-1} - \sin 2\sigma S_3^{ij-1} + C_3^{i-1j} \\ & + C_5^{ij-1} - \sin 2\sigma \delta_{i1} \delta_{j0}, \end{aligned} \quad (\text{B.10b})$$

$$S_3^{ij}(\sigma) = \frac{1}{2} \left[ \sum_{p=0}^i \sum_{q=0}^j \left[ E_{i-p} j-q S_3^{pq} - 3h_{i-p} j-q C_3^{pq} \right] - S_5^{i-1j} - S_7^{ij-1} - \delta_{i1} \delta_{j0} + \cos 2\sigma \delta_{i0} \delta_{j1} \right], \quad (\text{B.10c})$$

$$C_3^{ij}(\sigma) = \frac{1}{2} \left[ \sum_{p=0}^i \sum_{q=0}^j \left[ E_{i-p} j-q C_3^{pq} + 3h_{i-p} j-q S_3^{pq} \right] - C_5^{i-1j} - C_7^{ij-1} + \sin 2\sigma \delta_{i0} \delta_{j1} \right], \quad (\text{B.10d})$$

$$S_5^{ij}(\sigma) = \frac{1}{6} \left[ \sum_{p=0}^i \sum_{q=0}^j \left[ E_{i-p} j-q S_5^{pq} - 5h_{i-p} j-q C_5^{pq} \right] - S_3^{i-1j} - S_7^{i-1j} - S_9^{ij-1} - \delta_{i0} \delta_{j1} \right], \quad (\text{B.10e})$$

$$C_5^{ij}(\sigma) = \frac{1}{6} \left[ \sum_{p=0}^i \sum_{q=0}^j \left[ E_{i-p} j-q C_5^{pq} + 5h_{i-p} j-q S_5^{pq} \right] - C_3^{i-1j} - C_7^{i-1j} - C_9^{ij-1} \right], \quad (\text{B.10f})$$

and for  $n \geq 3$

$$S_{2n+1}^{ij}(\sigma) = \frac{1}{n^2+n} \left[ \sum_{p=0}^i \sum_{q=0}^j \left[ E_{i-p} j-q S_{2n+1}^{pq} - (2n+1) h_{i-p} j-q C_{2n+1}^{pq} \right] - S_{2n-3}^{ij-1} - S_{2n-1}^{i-1j} - S_{2n+3}^{i-1j} - S_{2n+5}^{ij-1} \right], \quad (\text{B.10g})$$

and

$$C_{2n+1}^{ij}(\sigma) = \frac{1}{n^2+n} \left[ \sum_{p=0}^i \sum_{q=0}^j \left[ E_{i-p} j-q C_{2n+1}^{pq} + (2n+1) h_{i-p} j-q S_{2n+1}^{pq} \right] - C_{2n-3}^{ij-1} - C_{2n-1}^{i-1j} - C_{2n+3}^{i-1j} - C_{2n+5}^{ij-1} \right]. \quad (\text{B.10h})$$

All coefficients can be determined from these relations. In Table B.2 all nonzero coefficients are given for the range of  $i + j$  indicated.

Since  $u(x)$  has periodicity  $2\pi$ , the appropriate relation between  $h$  and  $k$  is  $2h = i(2k-1)$ . Thus the energy and wave vector are related by

$$E = 1/4 + (k-1/2)^2 + \sum_{i,j=0}^{\infty} E_{ij}(\sigma) V_1^i V_2^j \quad (\text{B.11a})$$

and

$$k - 1/2 = \frac{1}{i} \sum_{i,j=0}^{\infty} h_{ij}(\sigma) V_1^i V_2^j \quad (\text{B.11b})$$

In order to be able to make a comparison with the results of Ince, the following additional expansions must be made:

$$h^2 = \sum_{i,j=0}^{\infty} g_{ij}(\sigma) V_1^i V_2^j, \quad (\text{B.12a})$$

in which

$$g_{ij}(\sigma) = \sum_{p=0}^i \sum_{q=0}^j h_{i-p, j-q} h_{pq}, \quad (\text{B.12b})$$

and

$$E = 1/4 + \sum_{i,j=0}^{\infty} E'_{ij}(\sigma) V_1^i V_2^j, \quad (\text{B.12c})$$

in which

$$E'_{ij}(\sigma) = E_{ij} - g_{ij}. \quad (\text{B.12d})$$

The coefficients  $g_{ij}$  and  $E'_{ij}$  are also given in Table B.2.

Energies in the first and second zones near  $k = 1/2$  are obtained by setting  $\sigma$  equal to either  $i\theta$  or  $i\theta - \pi/2$  and letting  $\theta$  increase from zero (in these cases,  $\theta$  is real,  $h$  is imaginary, and  $k$  is real).

TABLE B.2

NONZERO COEFFICIENTS IN THE EXPANSIONS (B.9) AND (B.12)

$$i + j \leq d$$

Example:  $E_{41} = - (353/432) + (191/108) \cos 4\sigma - (7/16) \cos 8\sigma$

	d	ij	cos 2σ	cos 6σ	ij	1	cos 4σ	cos 8σ
E <sub>ij</sub>	5	10	-1		20	-1/2		
		11	1		02	-2/3		
		30	1/4		21	-1/12	-1/4	
		12	1/9		40	7/12	-5/8	
		31	-65/72	5/8	22	29/27	-41/108	
		13	-5/9		04	22/135		
		50	-37/72	7/16	41	-353/432	191/108	-7/16
		32	145/648	-1361/1296	23	-1115/1080	335/216	
		14	-26/225					
E <sub>ij</sub>	5	10	-1		20	-1	1/2	
		11	1		02	-2/3		
		30	1/4		21	11/12	-5/4	
		12	1/9		40	4/3	-11/8	
		31	-83/72	7/8	22	-11/54	97/108	
		13	-5/9		04	22/135		
		50	-8/9	13/16	41	-1943/432	164/27	-17/16
		32	733/648	-2537/1296	23	17/216	95/216	
		14	-26/225					
g <sub>ij</sub>	5	31	1/4	-1/4	20	1/2	-1/2	
		50	3/8	-3/8	21	-1	1	
		32	-49/54	49/54	40	-3/4	3/4	
					22	23/18	-23/18	
					41	265/72	-155/36	5/8
					23	-10/9	10/9	
S <sub>3</sub> <sup>ij</sup>	4	01	1/2		10	-1/2		
		20	1/4		11	1/3	-1/2	
		21	-55/72	1/2	30	7/12	-5/8	
		03	-7/48		12	-1/9	1/2	
		40	-37/72	7/16	31	-1595/864	599/216	-1/2
		22	97/144	-9/8	13	143/1080	1/144	

TABLE B.2  
(Continued)

	d	ij	cos 2σ	cos 6σ	ij	1	cos 4σ	cos 8σ
$S_5^{ij}$	4	11	-1/18		01	-1/6		
		30	-1/18		20	1/12		
		12	-1/48		21	-5/216	7/108	
		31	475/2592	-85/648	03	37/2160		
		13	257/10800		40	-155/864	41/216	
					22	-89/1440	-1/96	
$S_7^{ij}$	3	02	-1/24		11	1/18		
		21	-1/48		30	-1/144		
					12	-7/180	1/18	
$S_9^{ij}$	3	12	1/225		02	1/120		
					21	-1/144		
$S_{2n+1}^{ij}$ $n \geq 5$	2		None					

	d	ij	sin 2σ	sin 6σ	ij	sin 4σ	sin 8σ
$h_{ij}$	5	10	-1		21	-1/4	
		11	1		40	-3/8	
		30	3/4		22	71/108	
		12	-7/9		41	113/54	-7/16
		31	-211/72	5/8	23	-161/216	
		13	1/3				
		50	-137/72	9/16			
		32	166/27	-2641/1296			
	14	-26/2025					
$C_3^{ij}$	4	01	1/2		11	-1/2	
		20	3/4		30	-3/8	
		21	-119/72	1/2	12	1/2	
		03	-7/48		31	59/27	-1/2
		40	-137/72	9/16	13	1/144	
		22	331/216	-9/8			



TABLE B.2  
(Concluded)

	d	ij	sin 2σ	sin 6σ	ij	sin 4σ	sin 8σ
$C_5^{ij}$	4	11	1/18		21	11/108	
		30	-7/36		40	11/108	
		12	-19/144		22	-49/864	
		31	251/864	-77/648			
		13	3649/32400				
$C_7^{ij}$	3	02	-1/24		12	1/18	
		21	-43/432				
$C_9^{ij}$	3	12	-1/225				
$C_{2n+1}^{ij}$ $n \geq 5$	2		None				

B.3. THE  $\sigma$ 1-EXPANSION

This solution is useful only near the second Brillouin zone boundary in the extended zone scheme. In a manner analogous to the  $\sigma$  1/4-expansion, set

$$u(x) = C_0 + \sin(2x-\sigma) + \sum_{n=2}^{\infty} [S_{2n}(\sigma) \sin(2nx-\sigma) + C_{2n}(\sigma) \cos(2nx-\sigma)] , \quad (\text{B.13})$$

in which  $\sigma$  is a parameter. If this is inserted in the differential equation (B.3) and the coefficient of each sine and cosine term equated to zero, an infinite set of coupled algebraic equations for  $C_0$ ,  $S_{2n}$ , and  $C_{2n}$  is obtained. In these equations put

$$E - 1 + h^2 = \sum_{i,j=0}^{\infty} E_{ij}(\sigma) V_1^i V_2^j , \quad (\text{B.14a})$$

$$h = \sum_{i,j=0}^{\infty} h_{ij}(\sigma) V_1^i V_2^j, \quad (\text{B.14b})$$

$$C_0 = \sum_{i,j=0}^{\infty} C_0^{ij}(\sigma) V_1^i V_2^j, \quad (\text{B.14c})$$

$$S_{2n} = \sum_{i,j=0}^{\infty} S_{2n}^{ij}(\sigma) V_1^i V_2^j, \quad (\text{B.14d})$$

and

$$C_{2n} = \sum_{i,j=0}^{\infty} C_{2n}^{ij}(\sigma) V_1^i V_2^j; \quad (\text{B.14e})$$

and equate to zero the coefficient of each power of  $V_1^i V_2^j$ . This gives the following recurrence relations (in these  $C_0^{ij}$ ,  $S_{2n}^{ij}$ , and  $C_{2n}^{ij}$  are defined to be zero if either  $i$  or  $j$  is negative):

$$E_{ij}(\sigma) = -2 \sin \sigma C_0^{i-1j} + S_4^{i-1j} + S_6^{ij-1} - \cos 2\sigma \delta_{i0} \delta_{j1}, \quad (\text{B.15a})$$

$$h_{ij}(\sigma) = \frac{1}{2} \left[ 2 \cos \sigma C_0^{i-1j} + C_4^{i-1j} + C_6^{ij-1} - \sin 2\sigma \delta_{i0} \delta_{j1} \right], \quad (\text{B.15b})$$

$$C_0^{ij}(\sigma) = - \sum_{p=0}^i \sum_{q=0}^j E_{i-p, j-q} C_0^{pq} - \sin \sigma S_4^{ij-1} + \cos \sigma C_4^{ij-1} \\ - \sin \sigma \delta_{i1} \delta_{j0}, \quad (\text{B.15c})$$

$$S_4^{ij}(\sigma) = \frac{1}{3} \left[ \sum_{p=0}^i \sum_{q=0}^j \left[ E_{i-p, j-q} S_4^{pq} - 4h_{i-p, j-q} C_4^{pq} \right] + 2 \sin \sigma C_0^{ij-1} \right. \\ \left. - S_6^{i-1j} - S_8^{ij-1} - \delta_{i1} \delta_{j0} \right], \quad (\text{B.15d})$$

$$C_4^{ij}(\sigma) = \frac{1}{3} \left[ \sum_{p=0}^i \sum_{q=0}^j \left[ E_{i-p, j-q} C_4^{pq} + 4h_{i-p, j-q} S_4^{pq} \right] - 2 \cos \sigma C_0^{ij-1} \right. \\ \left. - C_6^{i-1j} - C_8^{ij-1} \right], \quad (\text{B.15e})$$

$$S_6^{ij}(\sigma) = \frac{1}{8} \left[ \sum_{p=0}^i \sum_{q=0}^j \left[ E_{i-p, j-q} S_6^{pq} - 6h_{i-p, j-q} C_8^{pq} \right] - S_4^{i-1j} \right. \\ \left. - S_8^{i-1j} - S_{10}^{ij-1} - \delta_{i0} \delta_{j1} \right], \quad (\text{B.15f})$$

$$C_6^{ij}(\sigma) = \frac{1}{8} \left[ \sum_{p=0}^i \sum_{q=0}^j \left[ E_{i-p, j-q} C_6^{pq} + 6h_{i-p, j-q} S_8^{pq} \right] - C_4^{i-1j} \right. \\ \left. - C_8^{i-1j} - C_{10}^{ij-1} \right], \quad (\text{B.15g})$$

and for  $n \geq 4$

$$S_{2n}^{ij}(\sigma) = \frac{1}{n^2-1} \left[ \sum_{p=0}^i \sum_{q=0}^j \left[ E_{i-p, j-q} S_{2n}^{pq} - 2n h_{i-p, j-q} C_{2n}^{pq} \right] \right. \\ \left. - S_{2n-4}^{ij-1} - S_{2n-2}^{i-1j} - S_{2n+2}^{i-1j} - S_{2n+4}^{ij-1} \right], \quad (\text{B.15h})$$

and

$$C_{2n}^{ij}(\sigma) = \frac{1}{n^2-1} \left[ \sum_{p=0}^i \sum_{q=0}^j \left[ E_{i-p, j-q} C_{2n}^{pq} + 2n h_{i-p, j-q} S_{2n}^{pq} \right] \right. \\ \left. - C_{2n-4}^{ij-1} - C_{2n-2}^{i-1j} - C_{2n+2}^{i-1j} - C_{2n+4}^{ij-1} \right]. \quad (\text{B.15i})$$

These relations are sufficient to determine all coefficients. Table B.3 contains all nonzero coefficients for the range of  $i + j$  indicated.

Since  $u(x)$  has periodicity  $\pi$ , the appropriate relation between  $h$  and  $k$  is  $h = i(k-1)$ . Thus the energy and wave vector are related by

$$E = 1 + (k-1)^2 + \sum_{i,j=0}^{\infty} E_{ij}(\sigma) V_1^i V_2^j \quad (\text{B.16a})$$

TABLE B.3

NONZERO COEFFICIENTS IN THE EXPANSIONS (B.14), (B.17), and (B.12)

$$i + \leq d$$

$$\text{Example: } E_{21} = - (13/12) + (16/9) \cos 2\sigma - (1/2) \cos 4\sigma$$

	d	ij	1	$\cos 2\sigma$	$\cos 4\sigma$	$\cos 6\sigma$	$\cos 8\sigma$
$E_{ij}$	5	01		-1			
		20	2/3	-1			
		02	-1/8				
		21	-13/12	16/9	-1/2		
		03		1/64			
		40	-271/216	16/9	-1/2		
		22	56/135	-167/192	17/27	-1/4	
		04	7/768		-5/512		
		41	593/135	-11807/1728	85/27	-3/4	
		23	4397/17280	-497/4050	-553/1152	40/81	-1/8
		05		-37/18432		7/4096	
$E'_{ij}$	5	01		-1			
		20	2/3	-1			
		02	-1/4		1/8		
		21	-4/3	16/9	-1/4		
		03		1/64			
		40	-149/108	16/9	-3/8		
		22	86/135	-191/192	11/27	-1/8	
		04	1/48		-11/512		
		41	653/135	-12239/1728	73/27	-1/2	
		23	6767/17280	-347/4050	-87/128	37/81	-1/16
		05		-1/288		13/4096	
$g_{ij}$	5	02	1/8		-1/8		
		21	1/4		-1/4		
		40	1/8		-1/8		
		22	-2/9	1/8	2/9	-1/8	
		04	-3/256		3/256		
		41	-4/9	1/4	4/9	-1/4	
		23	-79/576	-1/27	115/576	1/27	-1/16
		05		3/2048		-3/2048	

TABLE B.3  
(Continued)

	d	ij	1	$\cos 2\sigma$	$\cos 4\sigma$	$\cos 6\sigma$	$\cos 8\sigma$
$S_4^{ij}$	4	10	-1/3				
		11	-7/24	4/9			
		30	-19/216	1/9			
		12	53/135	-203/576	-5/54		
		31	653/1080	-443/864	-7/54		
		13	581/6912	257/32400	-2783/13824	10/81	
$S_8^{ij}$	4	01	-1/8				
		20	1/24				
		02		1/64			
		21	1/45	-13/288			
		03	7/768		-5/512		
		40	2/135	-11/576			
		22	-1109/34560	17/900	271/13824		
		04		-37/18432		7/4096	
$S_8^{ij}$	3	11	11/360				
		30	-1/360				
		12	11/576	-157/4800			
$S_{10}^{ij}$	3	02	1/192				
		21	-13/4320				
		03		-1/1152			
$S_{2n}^{ij}$ $n \geq 6$	2		None				

	d	ij	$\sin \sigma$	$\sin 3\sigma$	$\sin 5\sigma$	$\sin 7\sigma$
$C_0^{ij}$	4	10	-1			
		11	5/6	-1/2		
		30	7/6	-1/2		
		12		17/36	-1/4	
		31	-815/216	91/36	-3/4	
		13	-3499/17280	-61/1152	53/216	-1/8

TABLE B.3  
(Concluded)

	d	ij	$\sin 2\sigma$	$\sin 4\sigma$	$\sin 6\sigma$	$\sin 8\sigma$
$h_{ij}$	5	01	$-1/2$			
		20	$-1/2$			
		21	$4/9$	$-1/4$		
		03	$3/128$			
		40	$4/9$	$-1/4$		
		22	$289/1152$	$2/27$	$-1/8$	
		04		$-3/1024$		
		41	$-6839/10368$	$47/54$	$-3/8$	
		23	$-4099/10800$	$913/6912$	$10/81$	$-1/16$
		05	$-137/36864$		$9/8192$	
$c_4^{ij}$	4	11	$5/9$			
		30	$2/9$			
		12	$13/192$	$-2/27$		
		31	$-79/2592$	$-1/27$		
		13	$-19661/43200$	$157/4608$	$41/324$	
$c_6^{ij}$	4	02	$3/64$			
		21	$-11/288$			
		03		$-3/512$		
		40	$-25/576$			
		22	$-131/2700$	$521/13824$		
		04	$-137/18432$		$9/4096$	
$c_8^{ij}$	3	12	$-2087/43200$			
$c_{10}^{ij}$	3	03	$-7/2304$			
$c_{2n}^{ij}$	2					
$n \geq 6$			None			

and

$$k - 1 = \frac{1}{i} \sum_{i,j=0}^{\infty} h_{ij}(\sigma) V_1^i V_2^j . \quad (\text{B.16b})$$

As in the  $\sigma 1/4$ -expansion, in order to be able to make a comparison with the results of Ince, the additional expansions (B.12) must be made, except (B.12c) must be replaced by

$$E = 1 + \sum_{i,j=0}^{\infty} E_{ij}'(\sigma) V_1^i V_2^j . \quad (\text{B.17})$$

The coefficients  $g_{ij}$  and  $E_{ij}'$  are also given in Table B.3.

Energies in the second and third zones near  $k = 1$  are obtained by setting  $\sigma$  equal to either  $i\theta$  or  $i\theta - \pi/2$  and letting  $\theta$  increase from zero.

#### B.4. COMPARISON WITH THE RESULTS OF INCE

As the work reported in this appendix both overlaps and extends the results obtained by Ince, it may be helpful to indicate explicitly both some of the differences in notation and the new results given here. To go over to the notation of Ince, set

$$\left. \begin{array}{llll} \psi = y & E = \theta_0/4 & V_1 = -\theta_1/4 & \kappa = -ic \\ x = z & h = \mu/2 & V_2 = -\theta_2/4 & \end{array} \right\} (\text{B.18})$$

The remaining changes are easily obtained by comparison.

The  $\kappa$ -expansion.—The following coefficients are not given by Ince (the exponential functions used here must be suitably combined to give the trigonometric functions used by Ince):

$$\begin{array}{ll} E_{ij}: & 21, 22, 04, 41, 23 & U_6^{ij}: & 11, 30, 12 \\ U_2^{ij}: & 11, 30, 12, 31, 13 & U_3^{ij}: & 21 \\ U_4^{ij}: & 21, 03, 40, 22 & & \end{array}$$

where the pairs of numbers refer to the values of  $ij$ . The remaining coefficients agree with the corresponding ones of Ince.

The  $\sigma$  1/4-expansion.—The following coefficients are not given by Ince:

$$E_{ij}^i: 22, 13, 04, 50, 41, 32, 23, 14$$

$$h_{ij}: 22, 13, 50, 41, 32, 23, 14$$

$$S_3^{ij}, C_3^{ij}, S_5^{ij}, C_5^{ij}: 31, 22, 13$$

The remaining coefficients agree with those of Ince except for the coefficients  $E_{31}^i$  and  $S_3^{21}$ .

The  $\sigma$  1-expansion.—The following coefficients are not given by Ince:

$$E_{ij}^i, h_{ij}: 03, 22, 04, 41, 23, 05 \quad S_8^{ij}, C_8^{ij}: 12$$

$$C_0^{ij}, S_4^{ij}, C_4^{ij}: 12, 31, 13 \quad S_{10}^{ij}: 21, 03$$

$$S_6^{ij}, C_6^{ij}: 21, 03, 40, 22, 04 \quad C_{10}^{ij}: 03$$

The remaining coefficients agree with those of Ince, except for the coefficients  $E_{02}^i$  and  $S_{10}^{02}$ .



## APPENDIX C

### ANALYSIS OF SEVERAL JONES ZONES

In this appendix the results given in the preceding chapters are applied to the Jones zones of the hexagonal close-packed, the  $\gamma$ -brass, and the  $\beta$ -manganese structures. The Hume-Rothery electron concentration rules are known to apply to many alloys with these structures. It will be shown that shape degeneracies exist for these zones and hence that the significance of these zones for the interpretation of the Hume-Rothery rules is less certain than previously supposed.

No shape degeneracy or omission of interior Brillouin zone boundary planes is possible for a Jones zone which is also the first Brillouin zone, as, for example, for the Jones zone of the  $\beta$ -brass phase, which has the body-centered cubic lattice. The  $\beta$ -brass phases (nominal electron/atom ratio of 1.5) occur when the zone is about three-quarters full. It is interesting to note that the calculations of Jones indicate that the electron/atom ratio corresponding to the peak in the density-of-states curve is about 1.0. The electron/atom ratio for a full zone is 2.0. Consequently, for the  $\beta$ -brass phase the electron/atom ratios corresponding to the peak in the density of states and to the total volume of the zone provide no information at all as to the positions of the phase boundaries, because all intermediate phases occur between electron/atom ratios of 1.0 and 2.0.

#### C.1. THE HEXAGONAL CLOSE-PACKED STRUCTURE

The parts in the first octant of the Jones zone and of the second Brillouin zone for the hexagonal close-packed structure are shown in Figs. C.1 and C.2, respectively. The first Brillouin zone is the hexagonal prism  $ABA'B'$ , etc.

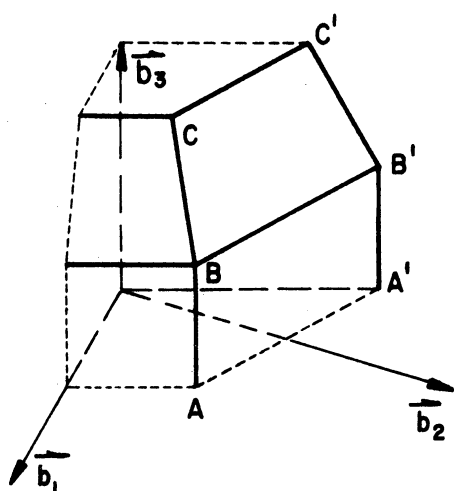


Fig. C.1. The Jones zone of the hexagonal close-packed structure.

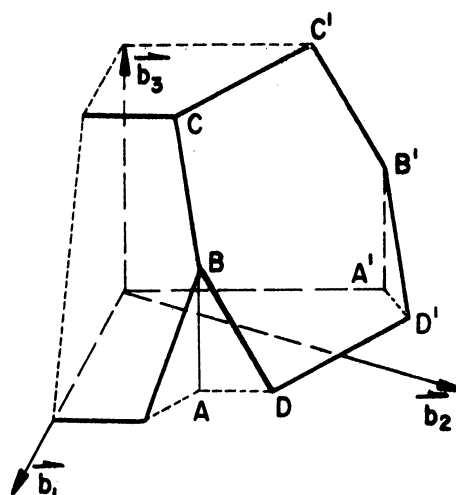


Fig. C.2. The second Brillouin zone of the hexagonal close-packed structure.

The symmetry degeneracies which exist between the first two energy bands are discussed in the papers by Jones and Herring cited in the introduction to Chapter III. On translating the second Brillouin zone back within the first zone it is found that the part of the zone face  $BCC'B'$  joins the face similar but diametrically opposite to the part  $BDD'B'$ . Professor H. Jones pointed out to the author before the present study was begun that the joining of these two faces of the second zone means the energy at each point of the face  $BCC'B'$  of the Jones zone is equal to the energy at some point outside the Jones zone. This simple example of what has here been called a shape degeneracy suggested the general investigation given in Section 3.2.

Some of the lattice vectors associated with the faces of the Jones zone of Fig. C.1 are  $\vec{b}_1$ ,  $-\vec{b}_1$ ,  $\vec{b}_2$ , and  $\vec{b}_1 + \vec{b}_3$ . Therefore, the set  $\vec{B}'$  of lattice vectors constructed from those of the Jones zone contains the vectors  $\vec{b}_1$ ,  $\vec{b}_2$ , and  $\vec{b}_3$  and hence all lattice vectors. It follows from the results of Section 3.3 that no plane waves and Brillouin zone boundary planes can be neglected in computing and plotting the electron energies.

Intermediate, hexagonal close-packed phases of different alloys occur over a wide range of electron/atom ratios, roughly from 1.5 to 1.8. The volume of the Jones zone of Fig. C.1 depends on the  $c/a$  ratio. The corresponding electron/atom ratio is near 1.75 and is necessarily less than 2.0. However, because of degeneracies, the lowest electron/atom ratio at which an energy gap could possibly exist is 2.0. These facts indicate that it is not possible to understand the positions of the hexagonal close-packed phase by considering only the Jones zone of the phase.

### C.2. THE $\gamma$ -BRASS STRUCTURE

Part of the Jones zone of the  $\gamma$ -brass structure is shown in Fig.

C.3. Some  $\gamma$ -brass structures are based on the body-centered cubic space

lattice. Other  $\gamma$ -brass structures are based on a simple cubic lattice; but in the approximation, made in calculating the electron energies, in which the two types of atoms are considered to be identical, these structures should also be considered as based on the body-centered cubic lattice.

The reduced zone of the face-centered cubic lattice, the reciprocal lattice of the body-

centered cubic, will contain four electrons

per unit cell of crystal. Therefore, an

energy gap is to be expected only at electron concentrations such as 84, 88, 92, etc. The Jones zone will contain 90 electrons per unit cell of crystal.

That shape degeneracies exist for the Jones zone follows both from the fact that the volume of the zone is not an integral multiple of the

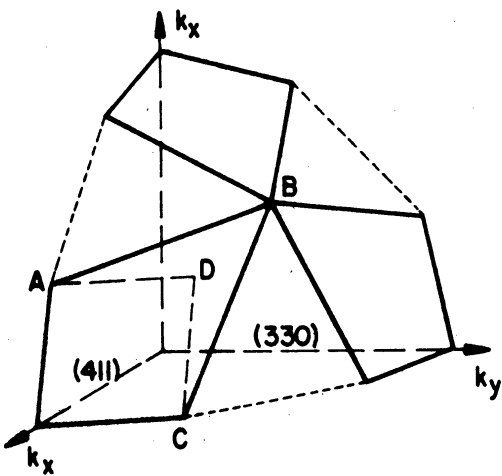


Fig. C.3. The Jones zone of the  $\gamma$ -brass structure.

volume of the reduced zone and also from the fact that parts, such as ABCD in Fig. C.3, of the (411) family of faces are not connected by any reciprocal lattice vectors to any other parts of the zone boundary. A more detailed geometrical investigation shows that shape degeneracies must exist in at least four different energy bands.

The set  $\vec{B}'$  of lattice vectors constructed from those of the Jones zone contains the vector  $2(4\bar{1}1) + 2(\bar{3}30) + (\bar{1}\bar{4}\bar{1}) = (101)$  and, similarly, the other basis vectors of the face-centered cubic reciprocal lattice. Thus, since the set  $\vec{B}'$  contains all the vectors of the reciprocal lattice, no plane waves and Brillouin zone boundary planes can be neglected in calculating and plotting the electron energies.

This investigation is not sufficient to determine the true reason for the empirically indicated dip in the density of states of the  $\gamma$  phase. The density of states may be essentially that of the (330) Jones zone, perturbed in an as yet unknown way by the (411) family of Fourier coefficients of the potential. A true energy gap can exist for the (330) zone at an electron concentration of 108. Presumably, the minimum in the actual density-of-states curve occurs at a smaller electron concentration when overlap starts to take place into the next higher zone. An opposite alternative is that there may be only a weak correlation between the true energy surfaces and those predicted by the nearly-free-electron approximation and that an energy gap almost occurs at, presumably, 88 electrons per unit cell for some reason which is not evident from zone theory.

### C.3. THE $\beta$ -MANGANESE STRUCTURE

The  $\beta$ -manganese structure is based on the simple cubic lattice. The Jones zone of the  $\beta$ -manganese structure is shown in Fig. 72 of the book

by Mott and Jones.<sup>3</sup> The zone is constructed from the (221) and (310) families of planes, and its volume, according to Mott and Jones, is  $971/60 = 16.18$  times that of the reduced zone. This shows that shape degeneracies exist for the zone. The existence of shape degeneracies also follows from the fact that there is a part of every zone boundary face which is not connected to any other part of the zone boundary by any reciprocal lattice vector.

The set  $\vec{B}^0$  of reciprocal lattice vectors formed from the vectors of the Jones zone contains all vectors of the simple cubic reciprocal lattice; so no simplification is possible in calculating and plotting the electron energies. The construction of the density-of-states function for this structure is further complicated by the fact that neither the zone formed by the (221) family of vectors nor the zone formed by the (310) family is a possible reduced zone of a new reciprocal lattice. At this stage zone theory gives essentially no information about the density of states for the  $\beta$ -manganese structure.

## BIBLIOGRAPHY

1. F. Seitz, The Modern Theory of Solids, McGraw-Hill, 1940, Chapter VIII.
2. H. Jones, Proc. Roy. Soc. (London), A144, 225 (1934).
3. N. F. Mott and H. Jones, The Theory of the Properties of Metals and Alloys, Oxford Univ. Press, 1936.
4. H. Jones, Proc. Phys. Soc. (London), 49, 250 (1937).
5. W. Hume-Rothery and G. V. Raynor, The Structure of Metals and Alloys, 3rd ed., The Institute of Metals, 1954.
6. J. R. Reitz, in Solid State Physics, vol. 1, edited by F. Seitz and D. Turnbull, Academic Press, 1955.
7. L. P. Bouckaert, R. Smoluchowski, and E. Wigner, Phys. Rev., 50, 58 (1936).
8. L. Brillouin, Wave Propagation in Periodic Structures, 2nd ed., Dover, 1953, Appendix.
9. H. Jones, Proc. Roy. Soc. (London), A147, 396 (1934).
10. C. Herring, J. Franklin Inst., 233, 525 (1942).
11. C. Herring, Phys. Rev., 52, 361, 365 (1937).
12. E. L. Ince, Mon. Not. of the Roy. Astron. Soc. (London), 75, 436 (1915); 76, 431 (1916).
13. E. T. Whittaker, Proc. Edinburgh Math. Soc., 32, 75 (1914).
14. Tables Relating to Mathieu Functions, U. S. National Bureau of Standards, Columbia Univ. Press, 1951.
15. J. C. Slater, Phys. Rev., 84, 179 (1951).
16. E. Katz, Phys. Rev., 85, 495 (1952).
17. L. van Hove, Phys. Rev., 89, 1189 (1953).
18. E. C. Stoner, Proc. Leeds Phil. Soc., 3, 120 (1936).
19. J. F. Nicholas, Proc. Phys. Soc. (London), B64, 953 (1951).

